

604407

RTD-TDR-63-4021

COPY <u>2</u> OF <u>3</u>	
HARD COPY	\$ . 5.00
MICROFICHE	\$ . 1.00

151p

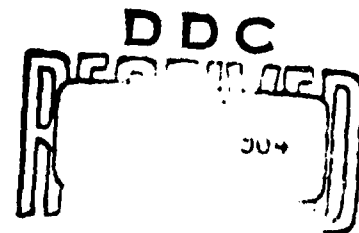
## **SIMULTANEOUS APPLICATION OF STATIC AND DYNAMIC LOADS ON SONIC FATIGUE TEST ARTICLES**

TECHNICAL DOCUMENTARY REPORT No. RTD-TDR-63-4021

JUNE 1964

AIR FORCE FLIGHT DYNAMICS LABORATORY  
RESEARCH AND TECHNOLOGY DIVISION  
AIR FORCE SYSTEMS COMMAND  
WRIGHT-PATTERSON AIR FORCE BASE, OHIO

Project No. 4437, Task No. 443703



(Prepared under Contract No. AF 33(657)-8759 by Northrop Norair  
A Division of Northrop Corporation, Hawthorne, California;  
W. H. Roberts and D. P. Wilhem, co-authors)

**CLEARINGHOUSE FOR FEDERAL SCIENTIFIC AND TECHNICAL INFORMATION CFSTI  
DOCUMENT MANAGEMENT BRANCH 4/L.11**

**LIMITATIONS IN REPRODUCTION QUALITY**

**ACCESSION #**

*HD 604 407*

- ☒ 1. WE REGRET THAT LEGIBILITY OF THIS DOCUMENT IS IN PART UNSATISFACTORY. REPRODUCTION HAS BEEN MADE FROM BEST AVAILABLE COPY.
- ☒ 2. A PORTION OF THE ORIGINAL DOCUMENT CONTAINS FINE DETAIL WHICH MAY MAKE READING OF PHOTOCOPY DIFFICULT.
- ☐ 3. THE ORIGINAL DOCUMENT CONTAINS COLOR, BUT DISTRIBUTION COPIES ARE AVAILABLE IN BLACK-AND-WHITE REPRODUCTION ONLY.
- ☐ 4. THE INITIAL DISTRIBUTION COPIES CONTAIN COLOR WHICH WILL BE SHOWN IN BLACK-AND-WHITE WHEN IT IS NECESSARY TO REPRINT.
- ☐ 5. LIMITED SUPPLY ON HAND: WHEN EXHAUSTED, DOCUMENT WILL BE AVAILABLE IN MICROFICHE ONLY.
- ☐ 6. LIMITED SUPPLY ON HAND: WHEN EXHAUSTED DOCUMENT WILL NOT BE AVAILABLE.
- ☐ 7. DOCUMENT IS AVAILABLE IN MICROFICHE ONLY.
- ☐ 8. DOCUMENT AVAILABLE ON LOAN FROM CFSTI (TY DOCUMENTS ONLY).
- ☐ 9.

**PROCESSOR:** *FA*

## NOTICES

When Government drawings, specifications, or other data are used for any purpose other than in connection with a definitely related Government procurement operation, the United States Government thereby incurs no responsibility nor any obligation whatsoever; and the fact that the Government may have formulated, furnished, or in any way supplied the said drawings, specifications, or other data, is not to be regarded by implication or otherwise as in any manner licensing the holder or any other person or corporation, or conveying any rights or permission to manufacture, use, or sell any patented invention that may in any way be related thereto.

Qualified requesters may obtain copies of this report from the Defense Documentation Center (DDC), (formerly ASTIA), Cameron Station, Bldg. 5, 5010 Duke Street, Alexandria, Virginia, 22314.

This report has been released to the Office of Technical Services, U.S. Department of Commerce, Washington 25, D. C., in stock quantities for sale to the general public.

Copies of this report should not be returned to the Research and Technology Division, Wright-Patterson Air Force Base, Ohio, unless return is required by security considerations, contractual obligations, or notice on a specific document.

## FOREWORD


This report was prepared by Northrop Norair, A Division of Northrop Corporation, Hawthorne, California, under Contract AF 33(657)-8759. The project was initiated by the AF Flight Dynamics Laboratory, Vehicle Dynamics Division, Aero-Acoustics Branch under Project Number 4437, "High Intensity Sound Environment Simulation," Task Number 443703, "Investigation of Methods for Simultaneous Application of Static and Dynamic Loads on Sonic Fatigue Test Articles," with D. N. Wolf as project engineer. This report covers work performed during the period from June 1962 to June 1963, and has been assigned Report No. NOR 63-196 for internal control.

The authors express their appreciation for the contributions of the numerous aerospace companies and government agencies for reports, discussions and data. In addition, acknowledgement must be given to the valuable contribution of Dr. S. R. Vailuri. The comments of and helpful discussions with, the consultants to this study, E. K. Walker and K. E. Eldred who provided Appendices A and B are greatly appreciated. Contributions to the overall task by project personnel, J. D. Labor, Designer, F. A. Grabowy, Test Engineer, P. E. Holligan (Appendix C), D. K. Skilling, along with the capable direction of Dr. C. M. Wong and administration of F. V. Lindquist are also gratefully acknowledged.

## ABSTRACT

With the existence of the RTD sonic test facility, it becomes necessary to investigate the requirements for reliability fatigue testing during the simulated application of static, dynamic, and acoustic service loadings. This report includes the findings of an extensive investigation of previous combined load failures, documents the existence of such failures and suggests possible future problems based on an industry-wide survey of actual case histories. Analytical substantiation of the increased probability of failure and theoretical acoustic considerations are presented to indicate that combined loads do present a particular problem area. The simulation of static, dynamic, and acoustic loads is discussed in terms of general principles which must be taken into consideration, and general testing methods applicable to difficult and costly vehicle fatigue problems. Limitations and possible future extensions to the RTD sonic test facility are discussed and recommendations presented. Seven specific testing arrangements which have been developed for combined loads simulation of several selected cases are described and illustrated. The following conclusions have been determined as applicable to any type of structural combined loads testing. The superposition of loads on a test article during sonic excitation requires the accurate simulation of many loading parameters without affecting structural response to the acoustic forcing function. Where practicable actual time-mission history loading must be employed to prevent erroneous results and conclusions from the testing data.

This technical documentary report has been reviewed and is approved.

  
HOWARD A. MAGRATH  
Chief, Vehicle Dynamics Division

# TABLE OF CONTENTS

	<u>PAGE</u>
I INTRODUCTION . . . . .	1
II DEFINITION OF COMBINED LOADS . . . . .	2
ACOUSTIC LOADS . . . . .	6
AERODYNAMIC LOADS . . . . .	6
STATIC LOADS . . . . .	7
DYNAMIC LOADS . . . . .	7
THERMAL LOADS . . . . .	9
III GENERAL DISCUSSION . . . . .	10
BACKGROUND . . . . .	10
INVESTIGATION OF PREVIOUS COMBINED LOADS	
FAILURES AND POSSIBLE PROBLEM AREAS . . . . .	10
B-58 AIRCRAFT . . . . .	10
T-38 SUPERSONIC JET TRAINER . . . . .	11
MERCURY CAPSULE . . . . .	11
CENTAUR VEHICLE . . . . .	11
CAVITY RESONANCE B-52, X15 COMBINATION . . . . .	13
VERTICAL TAKEOFF AND LANDING (VTOL) AIRCRAFT . . . . .	14
NAVAL AIRCRAFT OPERATIONS . . . . .	14
AIR LAUNCHED MISSILE . . . . .	14
SPACECRAFT - MISSILE COMBINATIONS . . . . .	16
UNUSUAL AERODYNAMIC LOADINGS . . . . .	16
FURTHER DISCUSSION ON ACOUSTIC LOADING . . . . .	19
IMPORTANCE OF COMBINED LOADS . . . . .	19

TABLE OF CONTENTS (continued)

	<u>PAGE</u>
FATIGUE . . . . .	19
THE IMPORTANCE OF COMBINED LOADS TO THE CUMULATIVE DAMAGE PROCESS . . . . .	20
EXPLANATION OF THE CUMULATIVE DAMAGE FRACTION DIAGRAM . . . . .	23
SUBSTANTIATION OF THE GRIFFITH-IRWIN THEORY . . . . .	25
HIGH PROBABILITY OF FAILURE IN THE EARLY LIFE . . . . .	25
OTHER STRUCTURAL CONSIDERATIONS . . . . .	28
LIQUID LOADING . . . . .	28
NATURAL LOADING . . . . .	28
COMBINED FAILURE MODES . . . . .	30
DYNAMICALLY SIMILAR STRUCTURAL MODEL . . . . .	32
COMPOUND PROBABILITIES . . . . .	32
IV GENERAL TESTING METHODS . . . . .	33
ENGINE AIR INLET DUCT . . . . .	34
AFTERBURNER TRANSIENT AND MECHANICALLY TRANSMITTED THRUST OSCILLATIONS . . . . .	37
PRIMARY STRUCTURAL QUALIFICATION . . . . .	45
STATIC FIRING OF MISSILE BOOSTER . . . . .	50
LARGE SCALE TURBULENCE . . . . .	54
SYSTEMS VIBRATION TEST . . . . .	62
COMPONENT TEST . . . . .	65
ALTERNATE TEST METHODS AND COMMENTS ON TEST PROCEDURES . . .	69
V CONCLUSIONS . . . . .	71
VI RECOMMENDATIONS . . . . .	72
REFERENCES . . . . .	73

## LIST OF APPENDICES

		<u>PAGE</u>
APPENDIX A	LIMITING PHENOMENA FOR FATIGUE CRACK FAILURES . . . .	75
APPENDIX B	EFFECTS OF LIQUID LOADING . . . . .	86
APPENDIX C	PROBABILITY DENSITY FUNCTION OF THE SUM OF TWO RAYLEIGH VARIABLES . . . . .	97

## LIST OF ILLUSTRATIONS

<u>FIGURE</u>		<u>PAGE</u>
1	T-38A DUCT REQUIREMENTS . . . . .	12
2	VERTICAL TAIL IN B-52 WING CUTOUT . . . . .	13
3	CALCULATED AND EXPERIMENTAL LOADS AND ACCELERATIONS DURING NOSE TOW CATAPULTING . . . . .	15
4	RELATIVE PRESSURE FLUCTUATIONS . . . . .	17
5	TURBULENT BOUNDARY LAYER NOISE . . . . .	18
6	FATIGUE PROPAGATION AND DAMAGE DENSITY - LOSS IN RESIDUAL STRENGTH . . . . .	21
7	CUMULATIVE DAMAGE . . . . .	24
8	PROBABILITY OF FAILURE RATE OF TRANSPORT AIRCRAFT UNDER MANEUVER AND ACOUSTIC LOADS . . . . .	26
9	PROBABILITY OF FAILURE RATE OF TRANSPORT AIRCRAFT UNDER MANEUVER AND ACOUSTIC LOADS . . . . .	27
10	LONGITUDINAL COMPARED TO LATERAL BUCKLING . . . . .	29
11	COMBINED FAILURE MODES . . . . .	31
12	ENGINE AIR INTAKE DUCT . . . . .	35
13	AFTERBURNER TRANSIENTS AND MECHANICALLY TRANSMITTED THRUST OSCILLATIONS . . . . .	39
14a	AFTERBURNER TRANSIENT AND MECHANICALLY TRANSMITTED THRUST OSCILLATION CURVE . . . . .	40
14b	ACOUSTIC LOADING SPECTRUM . . . . .	40
15	OVERALL SOUND PRESSURE LEVEL CONTOURS - B58 WING . . . .	42



# LIST OF ILLUSTRATIONS (continued)

<u>FIGURE</u>		<u>PAGE</u>
16	PRIMARY STRUCTURAL QUALIFICATION - PRESSURE CELL METHOD . . . . .	47
17	STATIC FIRING OF MISSILE BOOSTER . . . . .	51
18	T-38A SPEED BRAKE MEASUREMENTS . . . . .	55
19	LARGE SCALE TURBULENCE . . . . .	56
20	TURBULENCE BEHIND THE DIVE BRAKES OF AN AIRCRAFT IN FLIGHT . . . . .	58
21	COMPARISON OF (A) TURBULENCE AND (B) ACOUSTIC FORCING FUNCTIONS . . . . .	59
22	INCREASING SOUND PROPAGATION VELOCITY OVER A SURFACE BY VARYING ANGLE OF INCIDENCE . . . . .	61
23	VEHICLE SYSTEMS VIBRATION TEST IN A REVERBERANT SOUND FIELD . . . . .	63
24	COMPONENT TEST . . . . .	66
25	STRESS ENVIRONMENT . . . . .	77
26	COLUMN THEORY . . . . .	78
27	CRACK THEORY . . . . .	78
28	NET STRESS . . . . .	79
29	CRITICAL CRACK THEORY . . . . .	79
30	FATIGUE CRACK STABILITY CURVE - 2024-T3 ALUMINUM . . . . .	81
31	FATIGUE CRACK STABILITY CURVE - 7075-T6 ALUMINUM . . . . .	82
32	FATIGUE CRACK STABILITY CURVE 7075-T6 & DTD687 ALUMINUM . . . . .	83
33	FATIGUE CRACK STABILITY CURVE - 2024-T3 ALUMINUM . . . . .	84
34	LIQUID LOADING ON A PISTON IN AN INFINITE WALL .	87
35	EQUIVALENT CIRCUIT OF PISTON IN INFINITE WALL .	89

LIST OF ILLUSTRATIONS (continued)

<u>FIGURE</u>		<u>PAGE</u>
36	RADIUS TO THICKNESS RATIO VERSUS RATIO OF EQUIVALENT SYSTEM MASS TO MASS OF PISTON . . .	92
37	RADIUS TO THICKNESS RATIO VERSUS RATIO OF LOADED NATURAL FREQUENCY OF EQUIVALENT SYSTEM TO UNLOADED NATURAL FREQUENCY OF PISTON . . . . .	93
38	RADIUS TO THICKNESS RATIO VERSUS ACOUSTIC EFFICIENCY RATIO OF LOADED EQUIVALENT SYSTEM TO UNLOADED PISTON . . . . .	94
39	RADIUS TO THICKNESS RATIO VERSUS ACOUSTIC EFFICIENCY RATIO OF LOADED EQUIVALENT SYSTEM TO UNLOADED PISTON . . . . .	95
40	RADIUS TO THICKNESS RATIO VERSUS RATIO OF MEAN SQUARES OF EQUIVALENT LOADED SYSTEM TO UNLOADED SYSTEM . . . . .	96

LIST OF TABLES

<u>TABLE</u>		<u>PAGE</u>
I	COMBINED LOADS . . . . .	3
II	COMBINED LOADS ON CASE HISTORIES - DRAWING CASES . . . . .	4
III	COMBINED LOADS ON CASE HISTORIES - ENGINEERING CASES . . . . .	5

## I INTRODUCTION

The application of static loads has been the principal method of qualifying aircraft and missile structures for many years. As the result of difficulties in the area of vehicle fatigue, leading in turn to costly engineering changes, large maintenance burdens, and loss of weapon effectiveness, it has been deemed a necessity to perform fatigue testing and thereby provide structural integrity. The present fatigue testing procedures may either be similar to static testing or include the dynamic loads.

To provide satisfactory designs, a radical shift in emphasis may be required due to recent evolutions in the engineering picture:

- Improved structural design and stress analysis allow smaller margins for static loads.
- Radical new vehicle design and missions.
- Accurate design criteria for vehicles is unavailable when these are not part of the evolutionary chain of vehicle development.

These shifts in the background of new vehicle design result in a group of static and dynamic loads each tending to use a large fraction of the available structural strength or fatigue load carrying capabilities. Certain of the new vehicle designs have been pushed to 30,000 - 50,000 hour lifetimes. Contrasting missile designs for use on a one shot basis have also proved to be vulnerable to their new static and dynamic load environment.

The work presented here has been an investigation to determine whether the existence of several loading types, none of which are sufficiently dominant to cause strength failures, may be the cause of structural failures through fatigue or other failure modes. The fatigue failure categories may be either low cycle repeated load failures or endurance limit failures. Other general or discrete categories of fatigue failure may also be involved. Survey work conducted in conjunction with this study has demonstrated a rather complete failure of the existing state of the art to encompass this phase of design.

Contributing significantly to the importance of combined loads are the new dynamic loadings arising from separation and reattachment of the external flow field, oscillating shock waves, base pressure fluctuation or cavity resonance. Where these unusually high loadings appear, failures have also appeared. In most cases the high dynamic loads have a principal component arising from the high noise levels. A large sonic test facility is presently nearing completion at RTD that will have the capability of subjecting full scale aircraft, missiles and components to high intensity noise levels. In many cases the realistic simulation of the loading of the structure will require the super-position of static, quasi-static and the various dynamic loads in combination with high intensity noise. A system for applying static and dynamic loads to structure undergoing sonic testing has never been developed.

The purpose of this investigation is to suggest methods for accurate reproduction of these loads in an acoustic environment, specifying the particular problem areas for investigation, and stating the limitations which may be encountered in applying these loads in a sonic environment.

The investigation has accomplished the following tasks:

- Determined whether cases exist that require testing under combined static and dynamic loads simultaneously with high intensity sound.
- Determined and defined in general terms the combined load conditions that are present in particular cases.
- Determined in general terms how the combined loads may best be simulated on acoustic fatigue test articles in the RTD sonic fatigue facility.

## II DEFINITION OF COMBINED LOADS

A thorough investigation was made of all available sources to provide substantiating evidence of combined loads failures. The first question that arises is a definition of combined loads.

Taking any individual load or combination of loads into consideration, failure, and in particular fatigue failure, will be the end result. Therefore, proof testing on high reliability items is a must. This necessitates a definite requirement that as many loads as the vehicle or component may undergo during actual operating conditions should be simulated to the best state of the art available. The elimination of one of many loads during qualification may lead to an undesirable condition of the "missing" load being the most influential factor contributing to catastrophic failure. There is also the possibility that this particular load is likely to occur singly or in combination with other insignificant loads thereby accelerating its contribution to eventual failure.

Simulating the exact loads that will occur during a typical mission profile in the proper sequence is the most desirable method of proof testing any article. A general classification of these loads can be grouped into five areas; static, aerodynamic, acoustic, dynamic, and thermal. A more complete breakdown is shown in Tables I, II and III. Some vehicles during their life history will encounter parts of all of these groups; others may encompass only a few.

TABLE I  
COMBINED LOADS

ACOUSTIC	AERODYNAMIC (PSEUDO-NOISE)	STATIC	DYNAMIC	TEMPERATURE
Engine Noise	Buffet	Maneuver	Wind	Aerospace Heat
Cavity Resonance	Separation	Inertia	Wind Shear	Engine Heat
Internal Vehicle Noise	Convected Turbulence	Steady Air Loads	Gust	Hot Spots due to Turbulence
	Base Pressure Fluctuation	Ground-Air -Ground Cycles	Launch or Take-off	Cryogenic Fuels
	Oscillating Shock	Pressure	Ground Handling	Space Temperature Differential
	Wakes From Drag Devices		Landing	
	Boundary Layer		Gross Vehicle Motion During Engine Run-up	
			Mechanically Transmitted Thrust Oscillation	
			Engine Vibration	
			Transient Afterburner	
			Shock	
			Vibration Due To Internal Equipment	
			Fuel Slosh	
			Flutter	
			Engine Gimbaling	

**TABLE II**  
**COMBINED LOADS ON CASE HISTORIES**  
**DRAWING CASES**

<div> <div>LOADS</div> <div>DRAWING CASES</div> </div>	ENGINE AIR INTAKE DUCT						
	AFTERBURNER TRANSIENT AND MECHANICAL TRANSMITTED THRUST OSCILLATION						
	PRIMARY STRUCTURAL QUALIFICATION						
	STATIC FIRING						
	LARGE SCALE TURBULENCE						
	SYSTEMS VIBRATION						
							COMPONENT TEST
<b>ACOUSTIC</b>							
1. Engine Noise	X	X	X	X		X	X
a. Cavity Resonance		X				X	
b. Internal Vehicle Noise						X	
<b>AERODYNAMIC (PSEUDO-NOISE)</b>							
1. Buffet							
2. Separation	X						
3. Convected Turbulence					X	W	
4. Base Pressure Fluctuation						I	
5. Oscillating Shock						T	
6. Wake from Drag Devices					X	H	
7. Boundary Layer							
<b>STATIC</b>						S	
1. Maneuver			X			Y	X
2. Inertia						S	
3. Steady Air Loads			X			T	
4. Ground-Air-Ground Cycles			X			E	
5. Pressure				X		M	
<b>DYNAMIC</b>						S	
1. Wind							X
2. Wind Shear						O	X
3. Gust						P	X
4. Launch or Takeoff			X			R	
5. Ground Handling						R	
6. Landing			X			A	
7. Gross Vehicle Motion at Rump						T	X
						I	
8. Mechanically Transmitter Thrust Oscillation		X				N	
						G	
9. Engine Vibration	X	X		X			X
10. Afterburner Transient		X					
11. Shock							X
12. Vibration due to Internal Equipment				X			X
13. Fuel Slosh				X			
14. Flutter							
15. Engine Gimballing							
<b>THERMAL</b>							
1. Aerospace Heat							X
2. Engine Heat							X
3. Hot Spots due to Turbulence							X
4. Cryogenic Fuels				X			
5. Space Temperature Differential							

TABLE III  
COMBINED LOADS ON CASE HISTORIES  
ENGINEERING CASES

LOADS	AIR LAUNCHED MISSILE						
	MISSILE-SPACECRAFT COMBINATIONS						
	MERCURY CAPSULE						
	NAVAL AIRCRAFT OPERATIONS						
	CAVITY RESONANCE B-52, X-15						
	VTOL AIRCRAFT						
							CENTAUR
<b>ACOUSTIC</b>							
1. Engine Noise	X	X		X	X	X	X
a. Cavity Resonance					X		
b. Internal Vehicle Noise							
<b>AERODYNAMIC (PSEUDO-NOISE)</b>							
1. Buffet					X		
2. Separation		X					X
3. Convected Turbulence		X					
4. Base Pressure Fluctuation		X					
5. Oscillating Shock		X	X				
6. Wake from Drag Devices		X					
7. Boundary Layer	X	X					
<b>STATIC</b>							
1. Maneuver	X	X				X	
2. Inertia	X	X	X	X		X	
3. Steady Air Loads	X	X				X	
4. Ground-Air-Ground Cycles	X	X		X		X	
5. Pressure		X	X			X	
<b>DYNAMIC</b>							
1. Wind		X	X	X		X	
2. Wind Shear		X	X			X	
3. Gust	X	X	X	X	X	X	
4. Launch or Takeoff		X	X	X	X	X	X
5. Ground Handling		X		X		X	
6. Landing				X		X	
7. Gross Vehicle Motion at Runup				X		X	
8. Mechanically Transmitted Thrust Oscillation		X		X		X	
9. Engine Vibration		X		X		X	
10. Afterburner Transient				X			
11. Shock		X					
12. Vibration due to Internal Equipment	X	X	X	X			
13. Fuel Slosh		X		X		X	
14. Flutter							
15. Engine Gimballing		X					
<b>THE MAL</b>							
1. Aerospace Heat		X					
2. Engine Heat		X		X			
3. Hot Spots due to Turbulence		X					
4. Cryogenic Fuels		X					
5. Space Temperature Differential		X					

The following is a list of definitions of combined loads as used in this study and shown in Tables II and III:

#### ACOUSTIC LOADS

##### Engine Noise:

The acoustic energy radiated from the power source of the vehicle, i.e., from a jet engine, rocket engine, etc. This energy is propagated through air, causing a random pressure fluctuation on the surfaces it strikes, i.e., a sound pressure level (SPL), a frequency spectrum, velocity of propagation, direction, and correlation in time and space.

##### Cavity Resonance:

Pressure oscillations in a cavity arising from sloshing of the air mass at one of its natural frequencies. An infinite spectrum of such modes exists so that turbulence over the mouth of a cavity has the capability of excitation modes over a wide frequency band. The pulsating pressure may resonate at values near free stream dynamic pressure in exceptional cases.

##### Internal Vehicle Noise:

The acoustic environment existing inside a vehicle from any external acoustic source transmitted through the walls of the vehicle can also be noise originating from equipment located inside the vehicle.

#### AERODYNAMIC LOADS

##### Buffet:

A randomly varying pressure applied over an aerodynamic surface of an aircraft wing by the phenomenon of air flow separation and turbulence.

##### Separation:

The separation of air flow from an external or internal surface causing a randomly varying pressure over the surface. Adverse pressure gradients or flow angularity are possible reasons.

##### Convected Turbulence:

Randomly varying pressure pulses where the pressure pattern moves with characteristic velocity and direction across the surface.

##### Base Pressure Fluctuation:

For a body with a blunt base, the base pressures are characterized by pressure oscillation covering a frequency spectrum not unlike that of the other large scale turbulent phenomena presented under aerodynamic loads. The excitation comes from turbulent flow at the edges of the blunt base, and is the result of turbulent mixing of the free stream flow with the dead air moving along the blunt base.



### Oscillating Shock:

In a wide Mach number band in the transonic region, shock waves may oscillate at high frequency traveling over one or two panel widths. The phenomenon can only occur when the structure has reentrant angles or as a result of shock wave-boundary layer interaction.

### Wake from Drag Devices:

A randomly varying pressure over a surface as a result of turbulent wake behind a projection into the air flow.

### Boundary Layer:

A randomly varying pressure due to the relatively thin layer of turbulence caused by friction between high speed flow and the skin of the vehicle.

## STATIC LOADS

### Maneuver:

Sum total of the static loads imposed on the vehicle under steady or maneuvering flight. These static loads vary slowly in time.

### Inertia:

Forces resulting from acceleration of a vehicle, either through change of magnitude or direction of its velocity.

### Steady Air Loads:

The unvarying aerodynamic force imposed on a moving airfoil applied as a pressure over a surface.

### Ground-Air-Ground Cycles:

The cycle of aerodynamic loads on the airfoil of a vehicle as it lifts off from, and returns to land on the ground, as in the flexure of a wing as it goes from zero lift to lift for normal flight and back to zero lift, but not including other loads during flight such as maneuver, gust, etc.

## DYNAMIC LOADS

### Wind:

Forces applied to a vehicle by ground winds with the vehicle tied down or stationary.

### Wind Shear:

Forces caused by gradients in the wind velocity during forward or upward flight at high speeds causes an angle of attachment variation of the incoming air.

#### **Quat:**

The load imposed upon a flight vehicle by atmospheric turbulence, suddenly encountered and of short duration, applied as a pressure over an area, and normally affecting the vehicle as a whole rather than acting on portions of the vehicle.

#### **Launch Environment:**

Severe acoustic loads occur during launch resulting from the very high pressure fluctuation surrounding the vehicle. The acoustic field is strongly dependent on the pod configuration and the handling of the exhaust products. The moving pressure field is characterized by magnitude, frequency spectrum, velocity, direction, and correlation in time and space.

#### **Takeoff:**

Loads applied to an aircraft during its takeoff roll, including vertical vibration due to runway roughness and horizontal forces of slowly varying magnitude applied to the tire by the runway.

#### **Ground Handling:**

Those specific forces applied to a given vehicle when it is handled on the ground not under its own power, such as towing an aircraft or hoisting a missile.

#### **Landing:**

Loads applied to an aircraft by contact with the runway, primarily the sudden vertical and aft loads associated with ground contact.

#### **Gross Vehicle Motion and Runup:**

Landing gear fluctuation and variation in engine thrust causing the vehicle to lurch about.

#### **Mechanically Transmitted Thrust Oscillation:**

Random forces from engine combustion which are mechanically transmitted to structure, through the engine mounts.

#### **Engine Vibration:**

The transverse sinusoidal vibration caused by the slight out-of-balance of rotating parts of a turbojet engine, transmitted by the engine case to the engine mounts of the vehicle.

#### **Afterburner Transient:**

The variation in thrust resulting from ignition of the afterburner of a jet engine (also resulting from some conditions of afterburner shutdown), applied longitudinally and transmitted by the engine case to the engine mounts of the vehicle. It is characterized by a rapid rise time pulse load decaying slowly with several plus and minus peaks.

**Shock:**

Any condition which creates a single pulse load with relatively rapid rise time.

**Vibration Due to Internal Equipment:**

Mechanical transmission loads and forces acting on structure and equipment resulting from operation of internal items of equipment.

**Fuel Slosh:**

The variation in pressure on the inside surface of a fuel tank due to relative motion of the fuel.

**Flutter:**

Primary structural instability due to passage of a flexible vehicle through an atmosphere at high speed. Aerodynamic, structural, and inertial forces couple the motion in the primary vehicle modes in such a way as to supply energy from the air stream.

**Engine Gimballing:**

The reaction on a missile structure to the forces applied to the engine case to change the angle between the centerline of the missile and the centerline of thrust, together with the transverse component of thrust.

**THERMAL LOADS**

**Aerospace Heat:**

Heat gain over a surface due to friction with the atmosphere.

**Engine Heat:**

Combustion heat from vehicle's propulsion plant.

**Hot Spots:**

Intense turbulence generates heat transfer rates an order of magnitude greater than heat transfer associated with normal flow in the Mach number band where aerodynamic heat is significant.

**Cryogenic Fuels:**

Low temperature fluid (oxygen, hydrogen, etc.) which influence material fatigue properties.

**Space Temperature Differential:**

The differential temperature with resulting heat flow and heat loss caused by a vehicle existing in a low temperature space environment. Internal and external heat sources may contribute.

### III GENERAL DISCUSSION

#### BACKGROUND

Significant engineering failures occurring in new vehicles have led to lengthy experiments to uncover the reasons for failure. In many cases these failures have been satisfactorily explained. A review of many recent cases was undertaken in this study to determine whether combined loads were a significant contributor to the overall damage.

An industry survey was conducted to determine the present state of the art in combined loads studies. This survey is easily summarized. With one exception, the contractors stated either that combined loads were not important or that no case of combined loads failures had come to their attention. Prevailing opinion from structures personnel and those concerned with fatigue studies was that the static loads alone were damaging, and in almost every case the importance was represented by a single load component. NASA and one aerospace contractor were exceptions and provided definite cases.

Acoustic fatigue damage to Air Force, airline and other vehicles has proven tremendously damaging. During a five year period \$100,000,000 was spent on engineering change proposals for prevention of acoustic fatigue by the Air Force. Further costs included maintenance and loss of weapon effectiveness. Because no reasonable method appeared to provide an analytic attack to the problem, a decision was made to proceed with the establishment of the present RTD sonic facility for testing of full scale vehicles and components.

As pointed out in the introduction, the change in the engineering background: small margins, new vehicles and missions, less accurate design criteria; occurred simultaneously with heterogeneous failures in a wide class of vehicles. A natural tie existed, therefore, between determining whether combined loads were important and a comprehensive review of recent structural failures. Parallel efforts were carried out to develop suitable test procedures and to conduct analytical studies for the determination of significant causes or explanations.

A series of case histories will be documented later in the report giving somewhat greater detail in each case. Engineering studies concerned the question of the importance of combined loads while the test simulation cases call out cases representing best use of the RTD sonic facility.

#### INVESTIGATION OF PREVIOUS COMBINED LOADS FAILURES AND POSSIBLE PROBLEM AREAS

##### B-58 Aircraft

An ample number of cases were available for study. Perhaps of greatest technical interest was a case which occurred on the early model B-58. A low frequency wing motion, less than 20 cps, in one of the wing natural modes of vibration was driven by mechanically transmitted thrust oscillation from afterburner operation. In addition, the high sound field (reaching 168 db overall on the wing) and transients occurring during afterburner light-up were contributing. A series of studies were required to extract the essential dynamic definitions of the loadings. A ten hour sonic fatigue test during full afterburner operation was initially performed. A number of failures were uncovered and repaired. In production, however, further extensive failures in wing spar webs appeared with the necessity for additional investigations.

### T-38 Supersonic Jet Trainer

The Northrop twin engined supersonic jet trainer exhibited early engine inlet duct failures due to separated flow inside the inlet. The investigation included discussions with other contractors and the finding was that inlet air duct failures were present on practically every jet aircraft built to that date. The phenomena is limited to ground operation in which air enters the duct from the sides and the rear of the nacelle. Turbulence and separation of the incoming air resulted inside the inlet. Panels approximately 30 inches behind the lip failed as a result of the loads imposed by separated flow and negative pressure condition. As a corrective remedy, panel sizes of 7 x 14 x .025 inches were backed up by aluminum honeycomb to stiffen the structures. Figure 1 shows the 154 db overall environment during ground operation as contrasted to a maximum 141.5 db overall occurring in flight where smooth entry of the incoming air occurs. Two separate phenomena are illustrated. The high excitations resulted from separated flow while the turbulent boundary layer excitation occurred at a significantly lower level. An interesting item of information was tallied to define the phenomena when a bell mouth was fashioned and attached to the intake and used for ground runup. Smooth air flow resulted in a return to the lower excitation level. Engineering fixes for a completed duct installed in a vehicle are complex. Also, the duct design conditions are severe due to both high positive and negative static pressures during various portions of the flight profile.

### Mercury Capsule

On the Mercury capsule the aerodynamics of the nose of the vehicle was heavily compromised by the open trusswork on the retro rocket tower. The straight line changes from cylinder to conical mold lines and back again on the Mercury Atlas vehicle combined with the heavy turbulent flow from the tower caused an intense oscillating shock in the transonic band of flight. Equivalent oscillating pressures reached 166 db with the oscillation occurring at high frequencies. One of the early test vehicles was lost and the adapter between the capsule and the booster came under intense study. The adapter was heavily reinforced and the Mercury program continued. The reinforced adapter was subjected to analytical and experimental studies, combining shock, acoustic and longitudinal compressive loading, without obtaining positive evidence that the high loadings were responsible for the failure in the adapter.

### Centaur Vehicle

The Centaur vehicle exhibited a panel failure near the nose of the vehicle, resulting in loss of fuel and loss of the vehicle. Aerodynamic separation of the flow occurs subsonically as a result of the sharp cone cylinder intersection at the nose. Supersonically, however, an expansion fan at the intersection establishes potential flow, i.e., a relatively smooth transition around the abrupt change in mold line. The transition is abrupt resulting in a 1q pressure step, (5 psi at 20,000 feet altitude). Studies on this vehicle and on Saturn show the transition occurs between 0.75 and 0.94 Mach number depending on the cone angle and the local flow conditions upstream of the critical point.

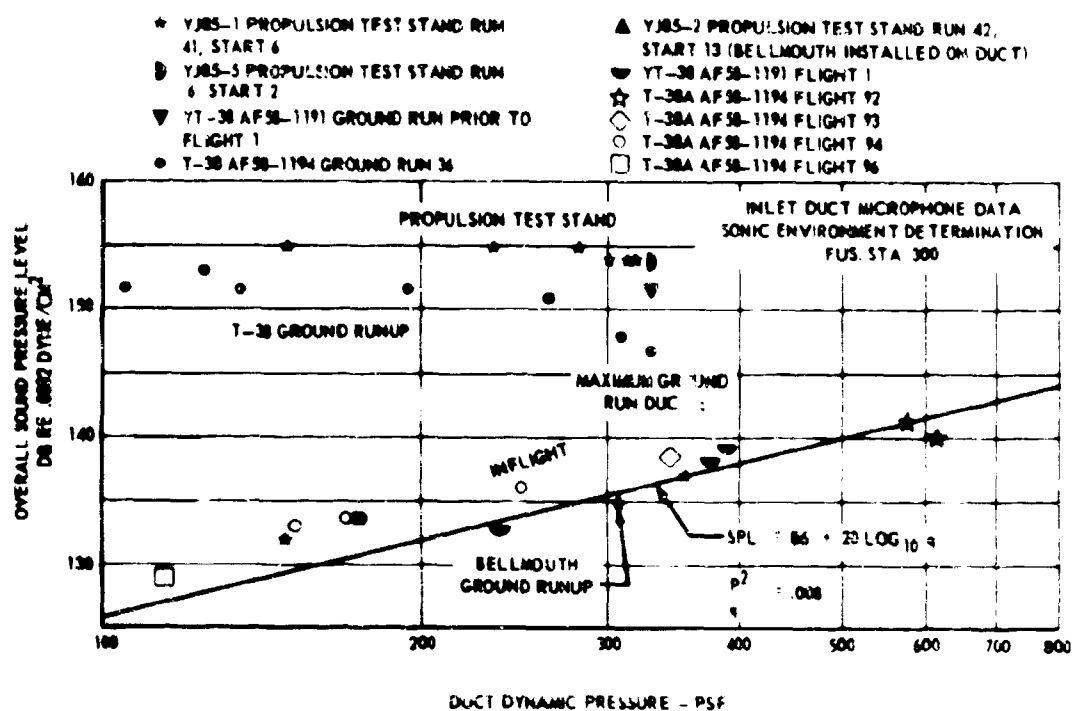


FIGURE 1 T-38A DUCT REQUIREMENTS



FIGURE 2 VERTICAL TAIL IN B-52 WING CUTOUT <sup>1</sup>

#### Cavity Resonance B-52,X-15 Combination

An unusual loading appearing on the X-15 research vehicle concerned cavity resonance in the open area created by the cutout in the wing trailing edge of the B-52 designed to accept the vertical stabilizer of the X-15 (Figure 2)<sup>1</sup>. The large blunt base and the sides of the vertical stabilizer combine to define a cavity open at both ends. Excitation is provided to the fluid in the cavity by turbulence flowing over the bottom surface originating with the thick pylon supporting the entire vehicle, which is mounted forward and in line with the cavity. Structural failures were found in the upper vertical tail after the third captive flight. An 18 inch separation of a rib and its flange occurred. Pressure measurements made on the side of the B-52 wing cutout showed  $\Delta p/q$  of 0.4 and a predominant frequency of 100 cps. These pressures converted to equivalent noise values are as follows:

<u>q, psf</u>	<u>db</u>
150 .....	154
300 .....	160
600 .....	166

Structural modifications were necessary to the vertical stabilizer.

Throughout the flight program, the vehicle experienced vibration from various sources. These include: 1) aerodynamic buffeting; 2) panel flutter; 3) structural feedback from the horizontal stabilizer acting through the stability augmentation control system; and 4) horizontal and vertical stabilizing motions at their fundamental frequencies. The vehicle penetrates its buffet boundary during pullup after launch and usually encounters mild buffet after completing the supersonic portion of the flight.<sup>1</sup>

## Vertical Takeoff & Landing (VTOL) Aircraft

The present design of VTOL aircraft utilizes directional jet exhaust nozzle techniques to control angular thrust direction. Other prototypes suggest variable fan or fixed/variable fan combinations. All of these techniques will produce an atmosphere of severe acoustic, static and quasi-static combined loads problems. Serious ground reflections will occur during the transition stages of flight. Reflected acoustic energy will produce noise levels on the order of 150-180 db overall on the undersurface of the aircraft. Rough landings are a characteristic of this type of aircraft and when combined with the high noise levels associated with ground reflection, a combined loads problem exists.

The transition phase of the flight program can best be simulated by setting the aircraft on edge or on its tail with the bottom of the fuselage facing the main bank of sirens. The noise levels on the bottom of the fuselage can be simulated in the RTD sonic facility by a jet and/or propeller type spectrum reproduced by the main siren bank. Any masking required for gradient purposes can be accomplished by curtaining off the particular areas involved.

The inertial loads will of course be different from those in the actual case but a sacrifice must be made to realistically reconstruct the acoustic loads which substantially contribute to the damage process.

Gear shock action due to rough landing characteristics can be simulated by hydraulic cylinders programmed to produce the shock action and connected to the gear struts. Movement in three planes will be required for accurate simulation.

It is possible that the method described in Figure 16 for Primary Structural Qualification can be applied to the wing and fuselage section to reproduce the dynamic pressure loadings as a further extension to this testing case.

## Naval Aircraft Operations

During catapulting procedure of a carrier based type aircraft many dynamic loads are introduced into the structure via the catapult mechanism. Typical response curves taken at the drag strut and engine for a modified North American Aviation XAJ-1 during nose tow catapult are shown in Figure 3, as reproduced from Reference 2. These dynamic loads transmitted to the structure will be combined with acoustic loads due to jet and/or propeller noise reflection off the deck. Reinforcement of the acoustic energy will occur and effect certain areas (undersurface of wing, fuselage, tail section, etc.) of the aircraft and accelerate the damage process.

Simulation of the acoustic reflection will be rather simple in the RTD sonic facility; however, the application of the dynamic shock loading will tend to be more difficult. The rise time associated with this acceleration might possibly be obtained by use of programmed hydraulic cylinders although the magnitude of some of the loads involved may be impossible to reach and trade-offs will be necessary.

## Air Launched Missile

There are two possible damage conditions that can occur to the missile carrier aircraft which must be taken into account during combined loads testing. When a vehicle carries a missile, be it large or small, conditions can exist for combined loads damage to the aircraft structure. Aerodynamic noise coupled to the natural vibratory modes of the missile will contribute to the overall aircraft wing damage process. This type of loading will differ from that which occurs during the actual firing process in that the firing sequence involves the addition of acoustic energy



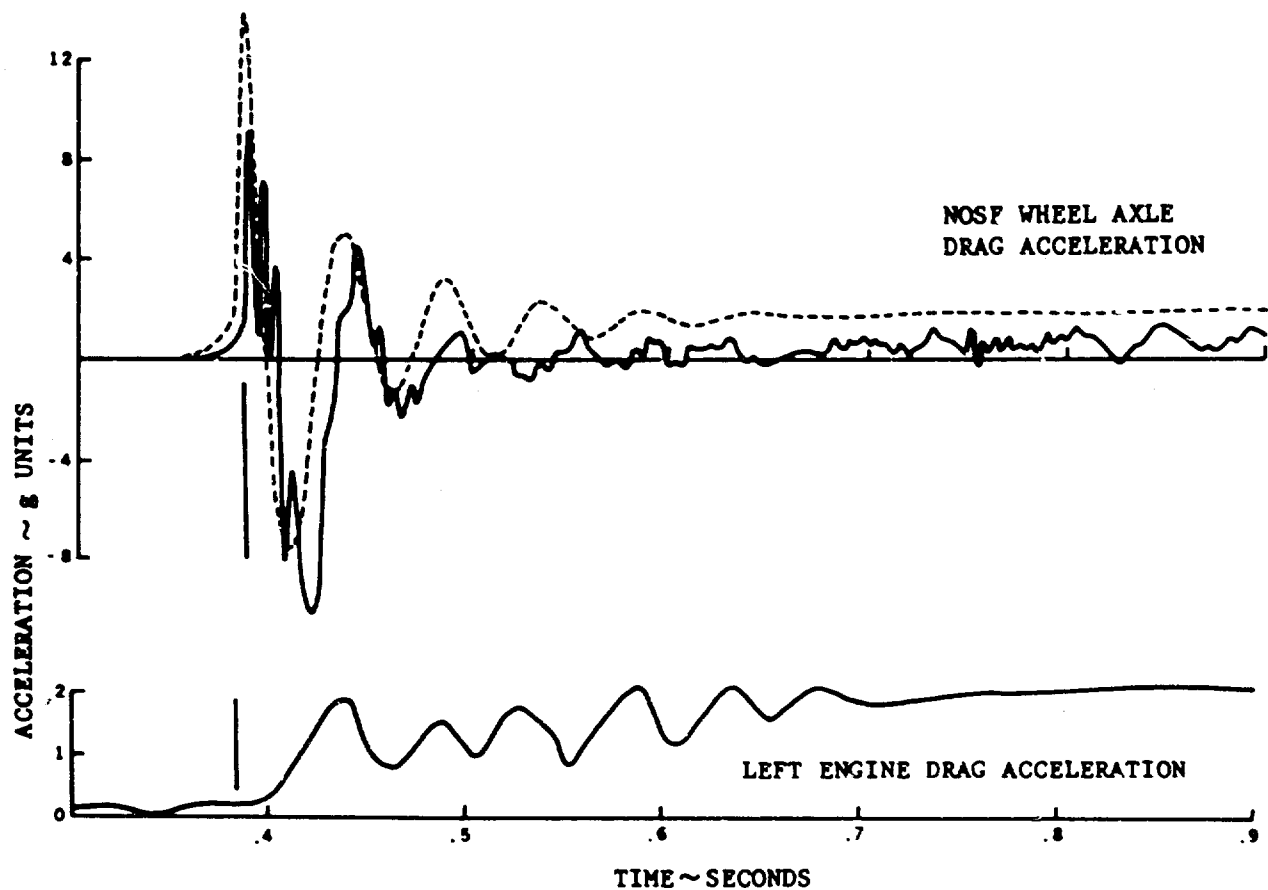
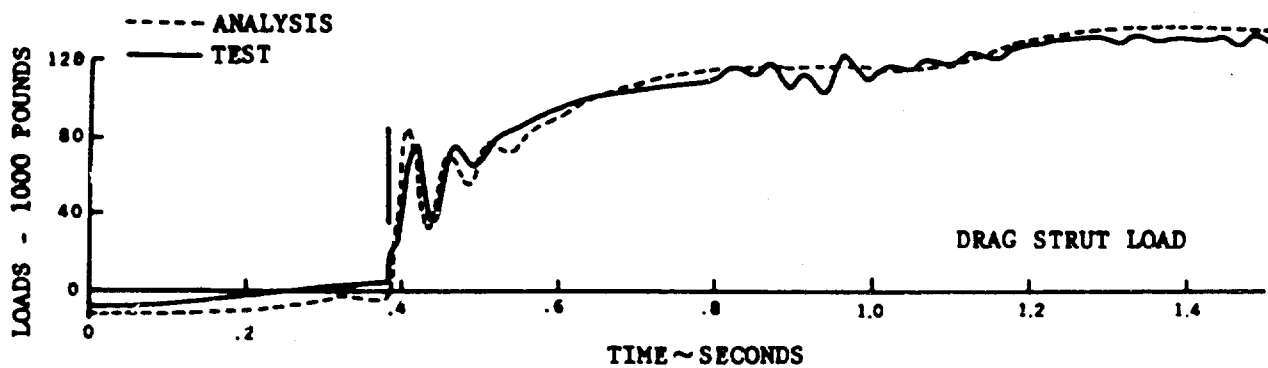


FIGURE 3 CALCULATED AND EXPERIMENTAL LOADS AND ACCELERATIONS  
DURING NOSE TOW CATAPULTING <sup>2</sup>

to the wing undersurface and the typical mission profile must be followed for proper simulation purposes. This, of course, is dependent on type of launch condition.

The loads taking place during the mission can be those associated with turbulence, boundary layer noise, proximity to jet exhaust noise, and induced noise during missile firing. It will not necessarily be true that the firing noise will occur during each mission; therefore, this load should appear only as a programmed periodic occurrence.

The simulation can be accomplished in the same manner as the afterburner transient case utilizing the main siren bank for jet noise reproduction using the noise spectrum associated with aircraft engine settings without afterburner. The aerodynamic noise associated with turbulence will no doubt be of primary interest and simulation can be attempted in the same manner as large scale turbulence shown in Figure 19. The missile firing can best be attempted by a short duration, small area blast of random low frequency noise in that vicinity of the wing affected by the rocket noise. Flexure of the missile itself can be accomplished by attaching shakers to hard structural points in the wing or missile itself to produce bending and torsional modes similar to those encountered during an actual mission.

#### Spacecraft - Missile Combinations

Typical mission profiles for spacecraft, aerospace plane, and missile combinations provide the test engineer with problems to which a solution is generally limited by the state of the art. The contemplated mission which these craft undergo from launch or take-off to impact or landing make it mandatory that the testing procedure follow as closely as possible the combined loads sequencing contemplated. In no other case selected are so many loading combinations likely during the vehicle service history. The general categories of acoustic, aerodynamic, static, dynamic and thermal loads are shown to exist by breaking the mission profile into its loading sequences as shown in Reference 3. In the temperature realm cryogenic fuels, space temperature differential, and aerospace heat provide thermal loadings of a complex nature. Dynamic loadings due to combustion instability, shocks, system interaction, aerodynamics and maneuvers are also present. The static loadings are caused by pressurization, both internal and external, mass flow, impact and long period maneuver loads. The acoustic loads are always present due to the engine noise and aerodynamic forcing modes.

#### UNUSUAL AERODYNAMIC LOADINGS

Unusual aerodynamic loadings are catalogued in Figures 4 and 5 showing a rank ordering of a variety of these loadings. The scale of turbulence is estimated also and shows variations of significance in that response of local structure such as panels, stringers, longerons and substructure is dependent on the size of the forcing function. Size in the sense of the correlated area is represented by a like positive or negative pressure. When the scale of turbulence is small, relative to the model shape of structure, very little response occurs. The turbulent boundary layer is an example where the scale of turbulence is so small as to prevent response in the fundamental structural modes, where greatest damage potential can develop. The unusual aerodynamic loadings range up to sixty times the magnitudes associated with the turbulent boundary layer. Their damage potential is doubly increased by the large scale of turbulence characterizing these loadings.

SOURCE	$\Delta P/q$ RMS	APPROXIMATE MAGNITUDE (IN DECIBELS)	RELATIVE MAGNITUDE
Rocket Noise		160-166 (max recorded 172)	Large
Cavity Resonance	to 0.4	to 177	Smallest Dimension
Oscillating Shock	to 0.1	165	Variable
Separated Flow	to 0.1	165	Dimensions of Flow Separation
Wakes	to 0.037	155	Dimensions of Wake
Base Pressure Fluctuations	0.015	149	Large
Turbulent Boundary Layer	0.006	141	Very Small

FIGURE 4 RELATIVE PRESSURE FLUCTUATIONS

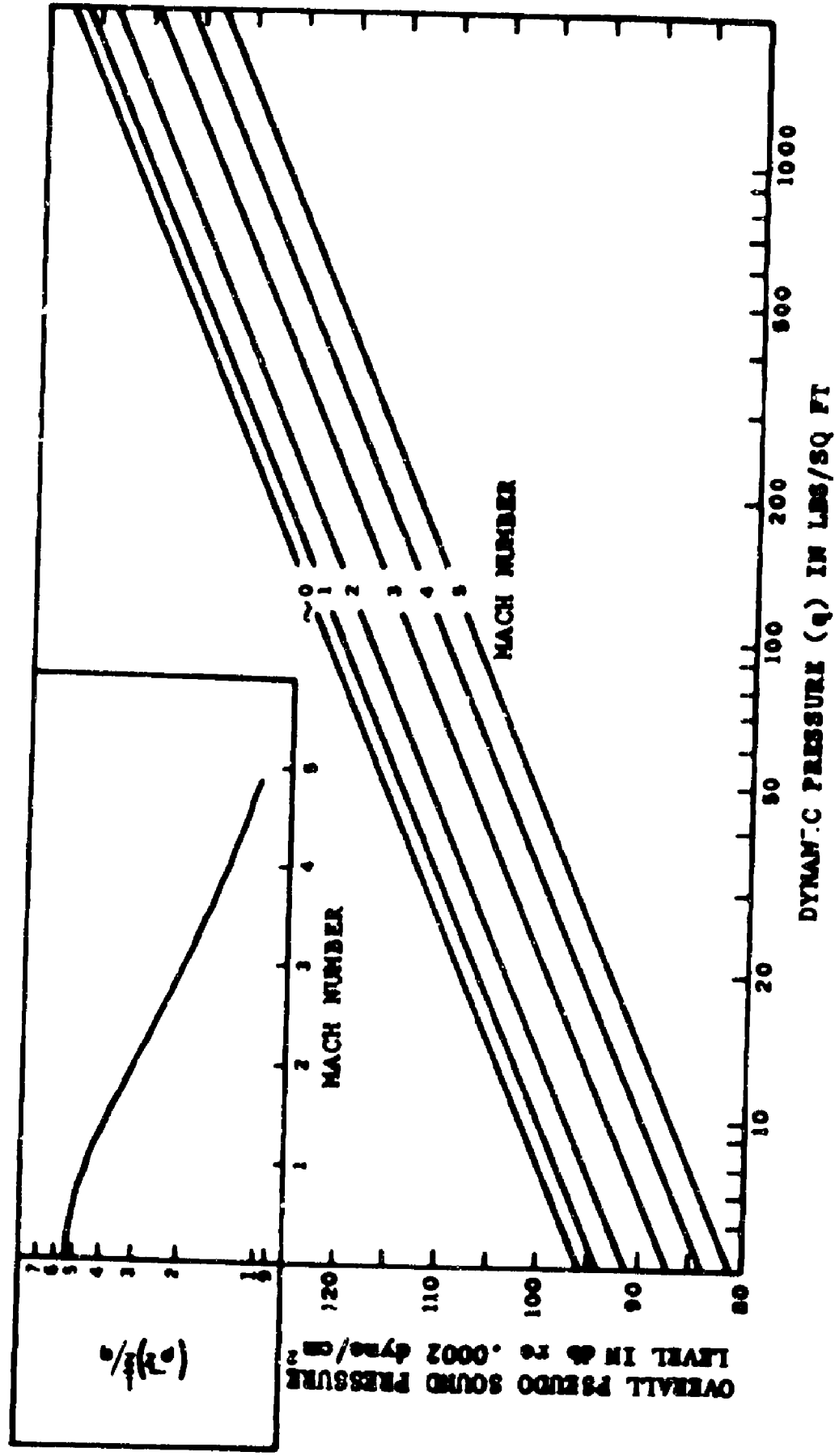


FIGURE 5 TURBULENT BOUNDARY LAYER NOISE

## FURTHER DISCUSSION ON ACOUSTIC LOADING

Five parameters are needed to define an acoustic load. These are magnitude, velocity, and direction of propagation, frequency distribution of the energy, and correlation in time or space. An acoustic load is a random loading in that amplitudes and phase angles are randomly occurring events. A model of random acoustic loading of some value may be constructed as follows: Let an acoustic field be generated downstream of a cylindrical vehicle by a line distribution of noise sources along the axis of the vehicle. The random pressure pulses are propagated upstream along this axis. Imagine a plastic film in the form of a cylinder surrounding the structure deformed so that the plastic is bulged out by negative pressure proportionate to the pressure, which in turn covers an area having the pressure. Positive pressures deform the film inward so that the film is alternately covered by waves inward or outward, of different depth and different area. Imagine these pressures as held constant with time, "frozen turbulence," and allow the film to be drawn over the structure at the speed of sound, say 1000 feet/sec. in the forward direction along the axis of the vehicle, deforming the structure as it moves.

The model is incomplete in that the turbulence does not stay frozen but changes with time. On the other hand the field is stationary in the statistical sense in that parameters describing its level and statistical characteristics such as correlation in time and space, instantaneous distribution of pressure at the pressure peaks, are all constant in time.

## IMPORTANCE OF COMBINED LOADS

The structural cases presented previously were considered by the contractor. In addition, a number of secondary engineering study cases are also presented. The serious nature of the vehicle failures and the costs in time and money were determined. The tentative conclusion was reached that combined load studies are of the utmost importance where any of the loadings listed in Table I occur simultaneously. The most common example of combined load failures has been the engine inlet air duct with extensive damage on a great number of jet aircraft. Another convincing example may follow from acoustic fatigue cases in general, where stresses measured near the failure points occur in the band 1000 to 2000 psi stress, whereas the endurance limit is listed as 4000 psi (rms). This possibly is indicative of the presence of other significant load components. Partial substantiation for this conclusion depends on the fatigue studies carried out in this document.

## FATIGUE

Experimental<sup>4</sup> and theoretical<sup>5</sup> studies completed recently show the occurrence of fatigue damage due to random loading which is an order of magnitude greater than that used in existing analytical practice in structural and fatigue analysis.

The purpose of the fatigue studies has been to show possible explanations for widespread occurrence of unsatisfactory performance of vehicle structure due to the fatigue aspects of the problem. Random damage, high probability of failure in the early life, and loss in strength provide these explanations.

The study presented by Dr. Valluri, (RTD-TDR-63-4021, Supplement 1), is based on defining the rate of crack growth and the use of the Griffith-Irwin instability boundary. The important outcome of the Valluri engineering theory is the loss in residual strength accompanying the cyclic stressing. This finding is directly opposed to the commonly held view that a part undergoes no loss in strength up to final failure. Typical loss in residual strength curves are presented in Figure 6. Both the Freudenthal and Valluri results are somewhat at odds with experience on real structures, until the important differences in conditions are better understood. Some of the differences are dispelled by work presented in this study. The experimental and theoretical results apply to unnotched specimens, whereas reasonably high stress concentrations always accompany real structure. An important secondary difference in material performance appears in the experimental results where steel showed a minimum cumulative damage fraction of 0.1, while aluminum showed approximately 0.2. This variation should be expected to be much greater when space age materials and different fabrication techniques are considered. An important conclusion then is that materials show considerable difference in their ability to withstand random loading and in other aspects of their fatigue performance.

#### The Importance of Combined Loads to the Cumulative Damage Process

The development of valid testing procedures for structural qualification of aerospace vehicles is contingent upon development of a synthetic environment which contains all elements significant to the cumulative damage process. This could ideally be accomplished by subjecting the test vehicle to a test environment identical to the anticipated service environment. There are, however, limitations to this approach in terms of analytic technique and physical facilities.

A study of probable vehicle environment utilizing the present state of the art techniques will lead to a reasonable definition of the gross environment components. These gross environment components can then be sequenced on a mission basis. However, arbitrary sequencing of individual loads such as gust and maneuver loads within the gross environment will be necessary. The sequencing of superimposed vibratory response, corrosion and temperature, when included, will also be arbitrary.

It is well known that the sequencing of environment components can have considerable effect upon the cumulative damage process. As an example, recent studies made by Schijve<sup>6</sup> indicate that such simple features of combined loads as the interchange of the negative and positive halves of one high load cycle could alter the fatigue life by a factor of 7.

It is evident that even a faithful reproduction of an arbitrarily selected complete service environment for the qualification test of a vehicle will not necessarily result in a positive determination of vehicle reliability for other equally probable environmental histories. This, however, is a difficulty whose solution is beyond the present state of the art. Considerable work needs to be done in determining the effect of environment sequencing on the cumulative damage process. Only after the effect of environment sequencing on cumulative damage is determined will it be possible to knowledgeably extrapolate the performance of the test vehicle to determine the probable range of performance of an identical vehicle subject to expected variances in environment. The problem stated is of course further complicated by the statistical nature of the strength properties of the vehicles.

The development of a test environment is, however, not reducible, in a practical sense, to inclusion of all environment parameters in their true form. The omission or modification of environmental parameters is often necessary to accommodate limitations on testing facilities, limitations in definition of environment, or limitations

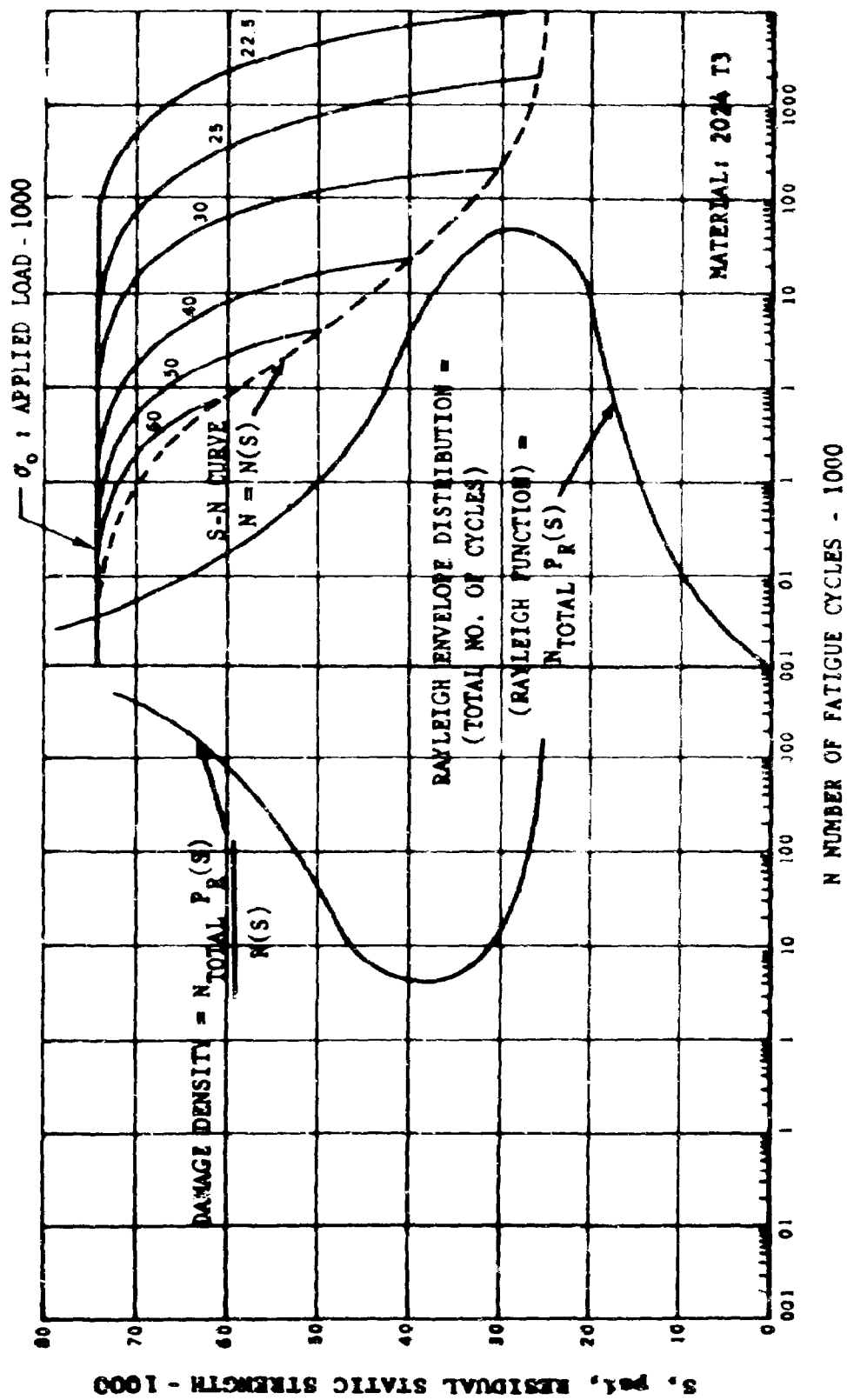


FIGURE 6 FATIGUE PROPAGATION AND DAMAGE DENSITY-LOSS IN RESIDUAL STRENGTH

in time. When omissions or modifications of environment components are made, their effect on the cumulative damage process should be understood. It is only through this understanding that the performance of the test vehicle be justifiably extrapolated to vehicles of the same type under service environments. The present level of understanding of the cumulative damage process does not permit omission or modification of any of the parameters of environment which contribute significantly to the cumulative damage process. There are, however, reasonable justifications for omission or modification of some environmental parameters which, in a particular case, may be qualitatively evaluated as making only minor contributions to the cumulative damage process. There is no justification, however, in generalizing regarding the omission of parameters as each environment, vehicle response history is unique. It is probable that most serious errors in testing technique result from failure to reassess applicable parameters as the environment-vehicle relationship alters.

The first step in establishing test procedure for a particular environment-vehicle condition is that of reviewing the parameters which are known to be generally contributory to the cumulative damage process to determine what omissions or modifications, if any, are justifiable for the particular case in question.

The various components of vehicle environment can be loosely classified as loads. This definition of loads includes environmental factors such as temperature, corrosive environment and high frequency vibrations as well as the quasi-static loads generally considered. Each has its own particular significance to the vehicle response and the cumulative damage process. The complete exploration of the significance of particular load types or combinations of load types does not need to be developed here. A qualitative appraisal and the establishment of fundamental ground rules is, however, a necessary step prior to the development of vehicle qualification tests utilizing the combined loading concepts.

The magnitude of a load can be a misleading standard to use in the evaluation of its contribution to the cumulative damage process. The stress inducing potential of a load is a function of a load magnitude and the geometry of the structure. Geometric considerations are particularly important when appraising the importance of the stress inducing potential of vibratory acoustic loads which cause bending and membrane stresses in sheet or shell structures. Localized stress concentrations above the nominal endurance limit of the material are frequently possible.

The number of cycles of load, or the number of times it will be applied during the expected vehicle life are as significant as the magnitude of the load to the cumulative damage process. Here again the importance of acoustically induced vibrations can be particularly significant. The current practice of appraising acoustic loads in terms of RMS stress levels needs some qualification as it fails to identify what could be a significant number of peaks well above the endurance limit of the material.

An equally important factor to consider when evaluating the effect of a load is its relationships to loads from other sources. The possibility of superposition should be given serious consideration as stresses which, when considered independently, might appear to be below the endurance limit, might after superposition upon a base quasi-static load, become an alternating tensile or compressive stress well beyond the endurance limit.

The loading rate and the length of time the load remains on the structure must also be considered. It is not particularly significant in the low stress range, but can be of considerable significance when the induced stress is high. The accumulation of plastic strain during a load cycle is dependent upon the duration of the load. The accumulation of plastic strain is not only of fundamental significance to the cumu-



lative damage process, but is also important to the stress distribution during subsequent loadings.

The temperature history during the application of loads must also be given consideration if extremes of high or low temperatures are part of the vehicle environment. Extremes in temperature greatly influence the accumulation of plastic strain during the vehicle life and thus have a direct influence upon the cumulative damage process. Extremes in temperature also result in modification of the residual strength of damaged materials by altering the stress level at which rapid or catastrophic cracking will occur. The possibility of changes in material properties and strength resulting from long periods of exposure to temperature extremes must also be given consideration.

Corrosion coupled with the fatigue process can greatly accelerate the cumulative damage process and should be included as a load component particularly if the surface environment during the vehicle service life is expected to be particularly severe. In this latter case, any attempt to accelerate the service life by omitting periods of non-operation in a corrosive environment might lead to considerable error in life prediction. At the other extreme, in the absence of surface environment (vacuum) there are indications that cumulative damage near the surface will be considerably lessened as a result of rebonding of particles along the slip planes, a process normally inhibited by the presence of surface environment and temperature consideration.

In summary it can be stated that all the components of vehicle environment (loads) can be significant to the cumulative damage process. It is not possible to generalize regarding the justifications for eliminating or modifying vehicle environment when tests for vehicle reliability are being developed. Fortunately the current state of the art will permit at least a qualitative appraisal of the significance of components of environment. A thorough study of each environment-vehicle relationship is desirable prior to any modifications. Failure to make this appraisal can severely limit the validity of vehicle qualification based upon the test results in modified environment.

When appraising the value of vehicle reliability tests, it must be remembered that positive determination of vehicle or component life cannot be expected. What can be expected, however, is a positive identification of fatigue sensitive areas or parts. It is believed that this fatigue sensitivity can be adequately determined when testing procedures are based on an understanding of the importance of combined loads.

#### Explanation of the Cumulative Damage Fraction Diagram

Figure 7 contains a curve of peculiar shape, an evaluation of which gives much better definition of the usability of the S-N curve. Bearing in mind the manner in which the S-N curve is developed; a constant set of loads of same maximum and minimum stress values is endlessly repeated to failure. This leads to the conclusion that any load history made up of loads within a few percent of any given reference point on the stress axis should conform to a cumulative damage fraction of 1.0. That is, applying one-third of the loads at 31 ksi required for failure at that stress, one-half of the required loads at 32 ksi, and one-third at 33 ksi would be expected to cause failure because the load history used is very like the loads used to generate points on the S-N curve. It would be reasonable to conclude that any load history or damage density curve which is compactly distributed along the stress axis would be described by a cumulative damage fraction of 1.0.

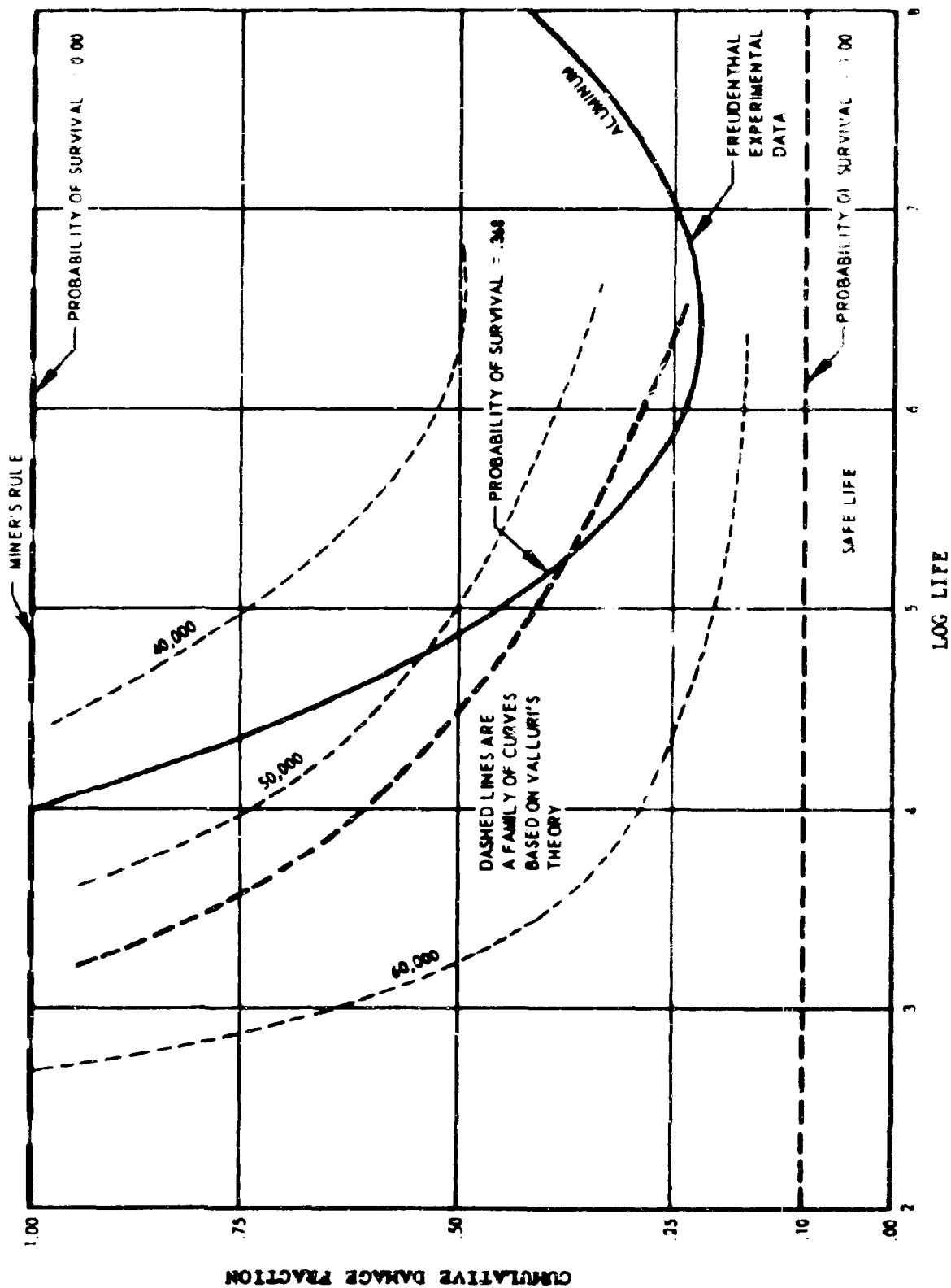


FIGURE 7 CUMULATIVE DAMAGE

The experimental data approaches cumulative damage fractions of 1.0 at very low cycle fatigue and then turns up and heads for higher cumulative damage fractions at unusually high numbers of cycles. A reasonable explanation is that the damage density is compactly distributed along the stress axis (damage density is the curve obtained by dividing the number of applied loads at any stress by the number required to cause failure).

Minimum cumulative damage fraction was obtained when the load history covered an extensive range of stress with randomly applied loads, leading to extensive coverage or fullness in the damage density curve.

The more critical effects of random damage may be defined as follows:

- Cumulative damage is an order of magnitude less than 1.0.
- The random endurance limit is less than the normal endurance limit.
- The strength remaining continuously decreases during damage accumulation.

#### Substantiation of the Griffith-Irwin Theory

Appendix A contains further substantiation of the Griffith-Irwin instability theory for recent measured data on the strength of partially cracked panels<sup>7</sup>. Presentation of the data is of considerable value to an understanding of the Valluri supplement (RTD-TDR-63-4021). The data is given as net stress versus crack length. A particular crack may begin at any given stress level and follow any given path, up, down, or sidewise on the plot. In all probability the bulk of all fatigue failures, especially small parts and test specimens, are concerned with loci which bound quickly upward and the part undergoes yielding and rupture without ever reaching the instability boundary. The diagram serves to divide, with great clarity, the two cases. Crack growth continued at low stress levels will eventually reach the instability boundary.

#### High Probability of Failure in the Early Life

Starting with assumed static and dynamic stress histories, and the ability to specify the probability of occurrence at each different stress level, a calculation of the probability of failure is possible using Valluri's loss in residual strength concept. A remarkable gradient in the early life is obtained which is quite different from the commonly held view of the integrity of a part undergoing fatigue loading. Normally one might expect the probability of failure to hold constant at a very low value and then rise near the end of the life producing a curve convex downward. The opposite appears to be the actual case. Although the stress history chosen was considered normal, it must have been descriptive of a poorly designed or highly stressed part. The probability of failure rises in the early life. A single component stress history was used with a stress distribution defined by gust loads.

A dynamic component was added simultaneously with the result shown in Figures 8 and 9. A further increase of one order in the probability of failure was obtained at 4 ksi dynamic load and correspondingly higher orders at 8 ksi. Dividing the load components into static and dynamic, implies a high and low frequency component. This a combination assists in obtaining the joint probability of occurrence of a high dynamic and high static load which is necessary to obtain the damaging high stress. A Rayleigh peak distribution was used for the dynamic component.

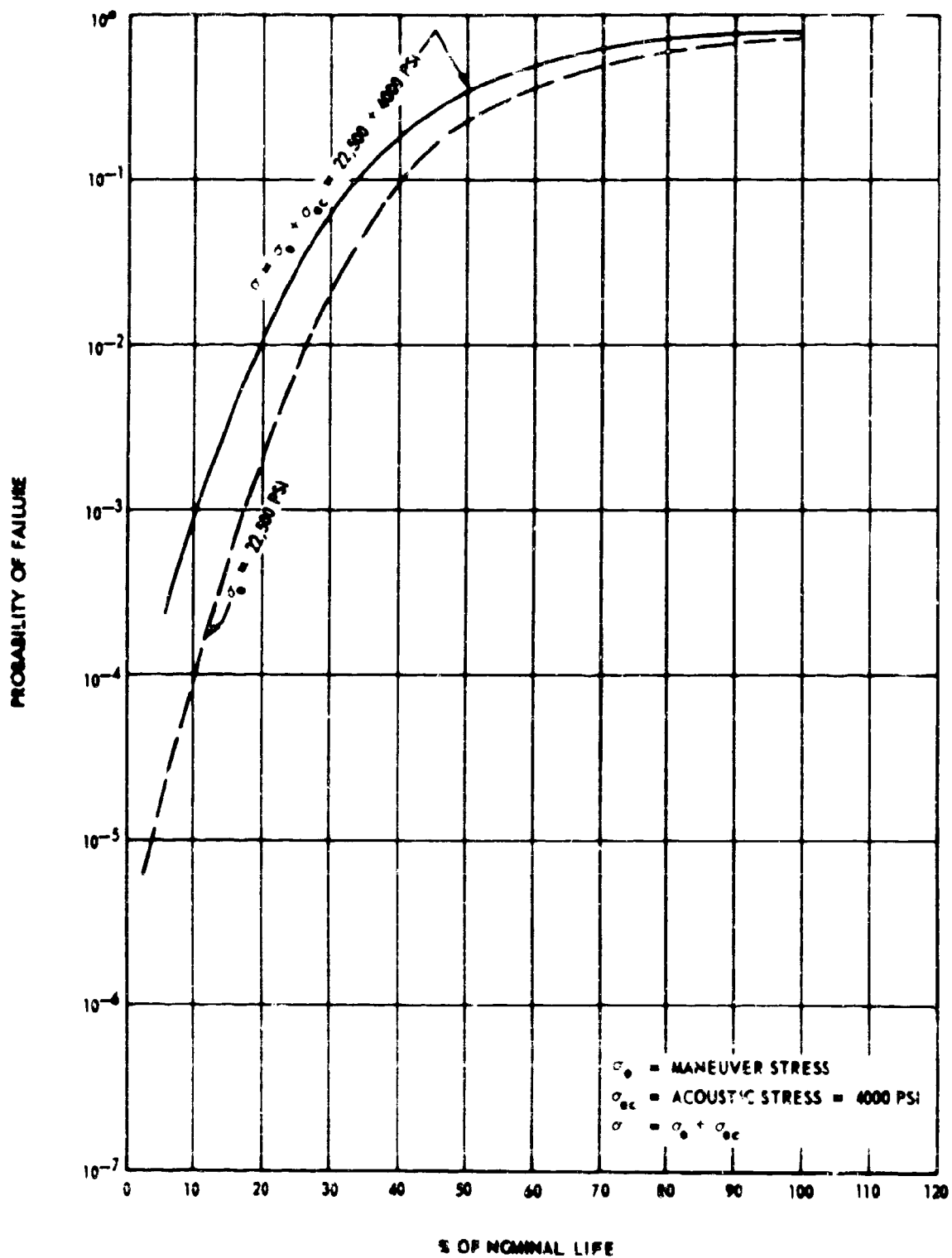


FIGURE 8 PROBABILITY OF FAILURE RATE OF TRANSPORT AIRCRAFT  
UNDER MANEUVER AND ACOUSTIC LOADS (MIL-F-8866)

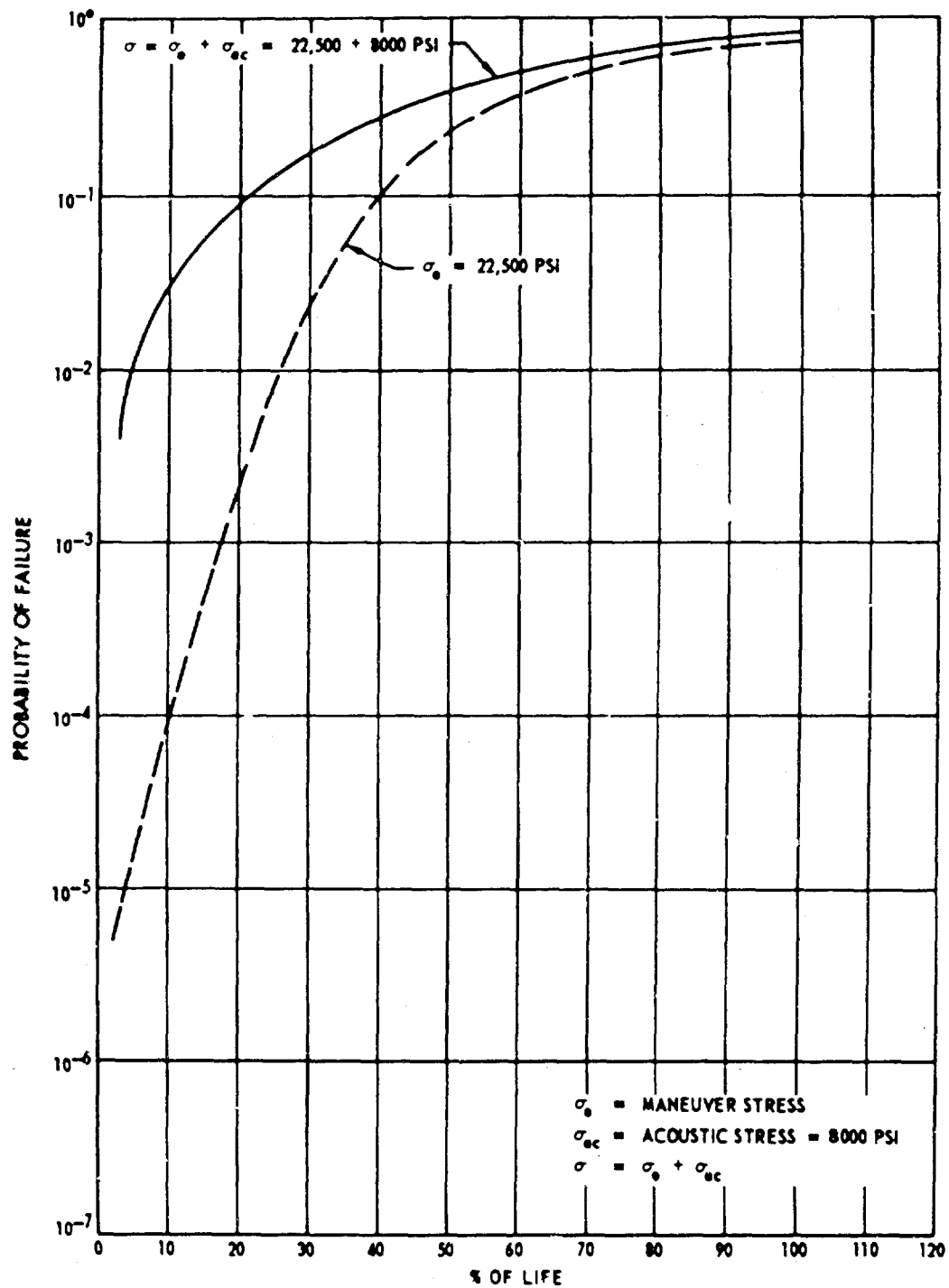


FIGURE 9 PROBABILITY OF FAILURE RATE OF TRANSPORT AIRCRAFT UNDER MANEUVER AND ACOUSTIC LOADS (MIL-A-8866)

## OTHER STRUCTURAL CONSIDERATIONS

The large missile and booster systems undergo longitudinal acceleration which varies from quite low values at launch to high values approaching 8 "g" near burnout for each stage. The compressive loads occurring in structure has resulted in reported cases of loss in frequency at the natural bending modes of the vehicle. These changes in frequency can be damaging since the guidance control systems are tailored to provide either frequency separation or frequency mismatch between the guidance control and that of the structure. The loss in frequency is due to a loss in stiffness resulting from a close approach to buckling. Loss in panel stiffness due to compressive loads has been studied extensively and represents a classical problem. Lateral stiffness of the panel drops to zero. A test method to define closeness to buckling, and buckling point is to measure the fundamental mode of the panel and determine its approach to zero.

Longitudinal stiffness of the panels is the governing parameter in this case, however, and it will not follow the same pattern or depend on similar parameters. For example, with no panel eccentricity, the longitudinal stiffness does not change up to the buckling point. Eccentricity therefore appears as the governing parameter. Structures of high eccentricity such as single thickness panels with joints introducing eccentric loads or moments, or those with poor manufacturing quality would contribute to loss of longitudinal stiffness. Pressurization also contributes while curvature would lessen the effective eccentricity. Sandwich panels or other designs in which the radius of gyration of the panels were large would minimize the effect. A qualitative plot is shown in Figure 10.

## LIQUID LOADING

Early Saturn data showed the vibration attenuation resulting from liquid loading in the booster was only 2:1. Since approximately ninety percent of the vehicle weight is liquid fuel it might be expected that liquid loading would have the ability to attenuate the vibratory motion by a much higher percentage. Appendix B is an analysis of a flat panel with liquid lying along one side of an infinite baffle. The analysis shows that the odd numbered modes 1, 3, 5, etc. which include the fundamental modes, are greatly attenuated, while the even numbered modes are affected to only a slight degree. The odd numbered modes attempt to move fluid perpendicular to the face of the panel while the even numbered modes only need displace fluid parallel to the face of the panel. Since the even numbered modes are affected to only a slight degree, this accounts for the large fraction of the remaining vibratory motion. While the remaining motion with liquid loading is a high percentage of the motion without liquid, the damage fraction may be significantly different from the motion fraction. Using an accelerometer to measure "g" (rms) the transducer is a device more sensitive to motion in the high frequency modes. Damage is measured by displacement which is proportional to stress in any given mode and the criterion to compare different modes in terms of their stress production, while not directly measured by displacement, is damaged by this effect. Thus cancellation of motion in the fundamental mode with liquid loading may prevent a very large fraction of the total damage done without liquid, leading to less damage by a ratio such as 4:1 for example.

## NATURAL LOADING

Certain combinations of structural loads are often generated which are natural combinations. The combinations listed below illustrate this point.

- Panel flutter, compressive panel loads, acoustic or aerodynamic panel loads.

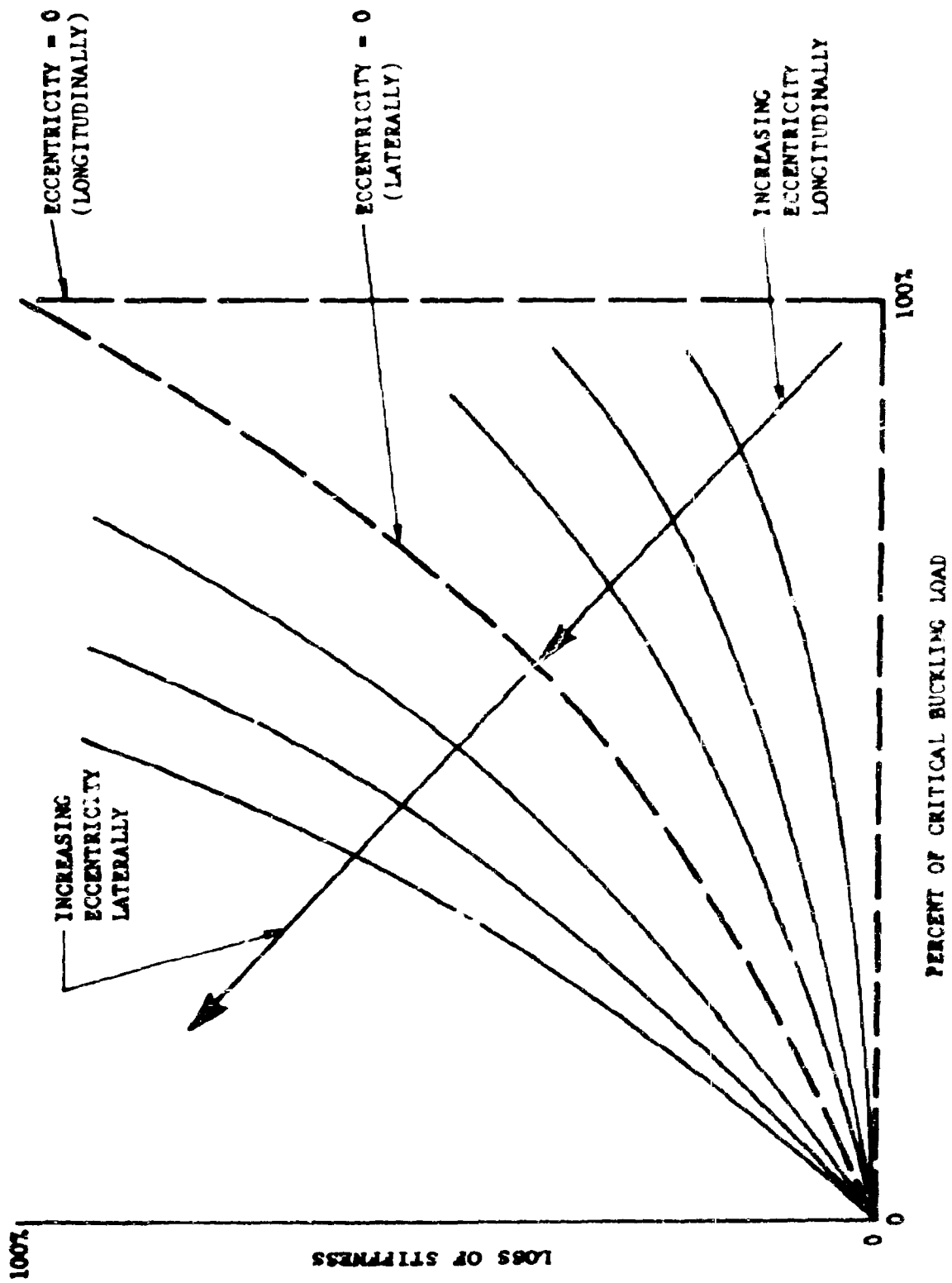


FIGURE 10 LONGITUDINAL COMPARED TO LATERAL BUCKLING

- Mechanically transmitted thrust oscillation, and the near field acoustic loads for rocket engines. For jet engines; mechanically transmitted thrust oscillation, afterburner transients at lightup, engine vibration.
- Separation, static pressure loads, sudden flow reattachment.
- High Mach number flight yields aerodynamic heating, hot spots due to local turbulence (can increase heat transfer by factor of  $12^6$ ).
- Space temperature, cryogenic temperature, engine heat, wakes, separation or base pressure fluctuation. Space temperature fluctuations may occur in a brief period following the occurrence of the high Mach number loads.
- Gross vehicle motion at runup, afterburner excitation via thrust fluctuation of the fundamental modes of the vehicle, acoustic loads, heat from engine wake, cavity resonance in open wheel wells or other cavities, ground reflection.
- Runway roughness, acoustic loads (maximum acoustic loads from jet exhaust occur at take-off), ground reflection, cavity resonance between wing, ground, and separate engine pylons.
- Silo launch or launch under conditions which redirect the engine exhaust close to vehicle.
- Missile nose flexure leading to divergence instability, compressive load from gross vehicle acceleration, oscillating shock, front end turbulence from compromised aerodynamics, hammerhead configuration leading to structural instability of the nose of the vehicle from phase lag in aerodynamic loads.

The list is endless and all components need not necessarily be present simultaneously. One of the conclusions to the structural portion of the study is that a large number of load components using a high percentage of the available strength combined with a second group of instability parameters each using a high percentage of whatever parameter defines the stability boundaries, are not likely to indicate long life or high structural reliability.

#### COMBINED FAILURE MODES

In the same way that a number of loads may coalesce to cause failure in one mode, a single load may act on a number of failure modes to generate failures; no one mode generating sufficient damage to cause failure by itself. More generally a number of loads will act on a number of failure modes. See Figure 11.

$$\{\text{Damage } (i)\} = [A_{ij}] \{\text{Load } J\} \quad (1)$$

Total damage is the summation of damage in each failure mode. The  $A_{ij}$  express the damage in the  $(i^{\text{th}})$  failure mode due to the  $(j^{\text{th}})$  load component. If interaction between the loads or damage mechanisms exist the problem is probably intractable. Even in its linear form very little work is available.



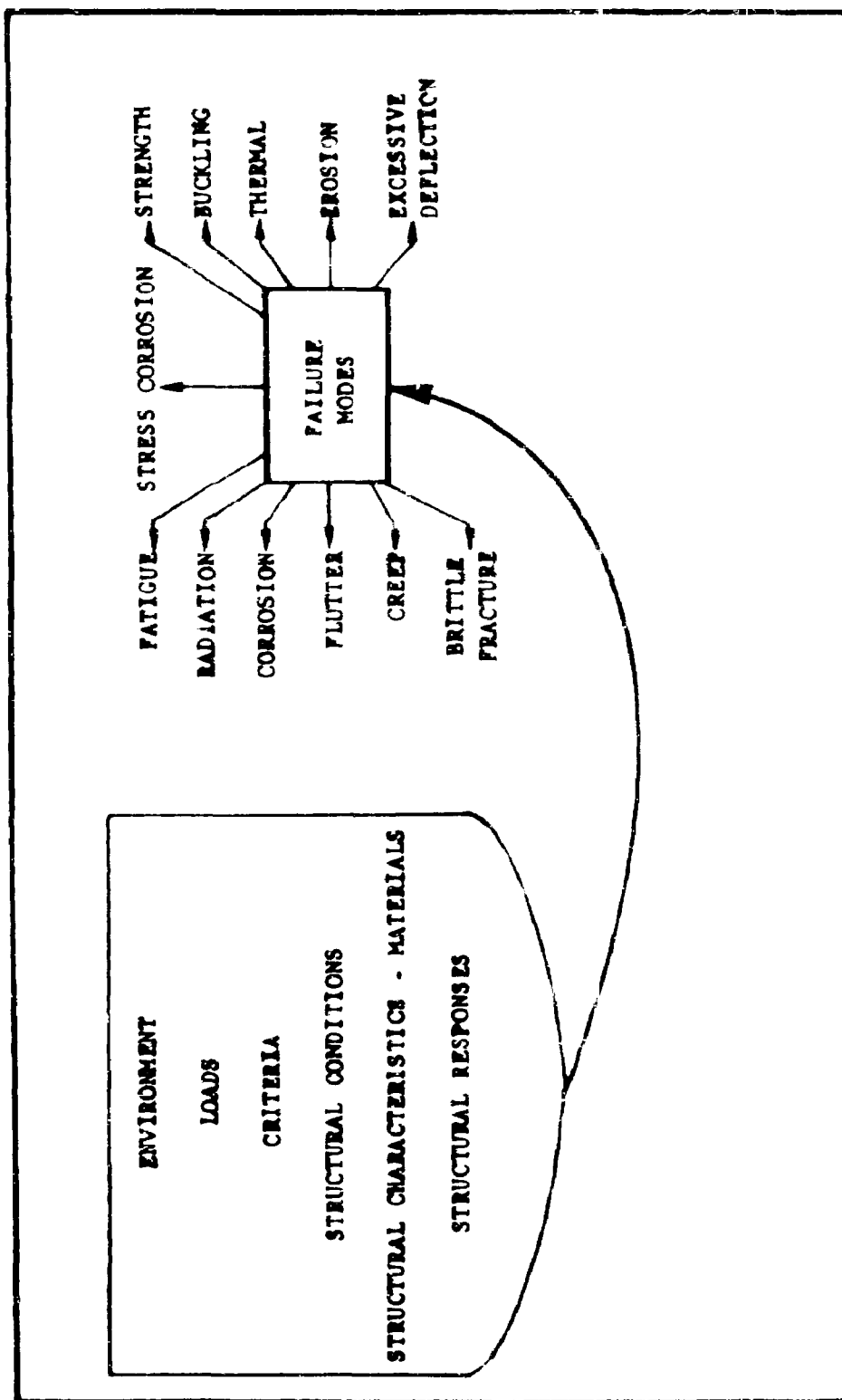


FIGURE 11 COMBINED FAILURE MODES

## DYNAMICALLY SIMILAR STRUCTURAL MODEL

A design tool has been under development for many years which should plug a gap for many systems. This is the dynamically similar structural model whose high frequency capabilities are presently being substantiated in two Northrop-RTD contracts, one of which is complete.<sup>10</sup> The program will compare model response to rocket engine excitation and full scale vehicle response. Complex structure was simulated item-by-item. The scaling laws show no limitation for load, structural characteristics, structural response, and damage, and in addition, thermal, fatigue, engine excitation, and high frequency responses are accurately handled. The advantage of the structural model is its ability to move structural dynamic studies back into the design period and to integrate the whole phenomena of loads, structural characteristics in detail, and damage into a final answer of unusual accuracy. Its consideration for combined load problems is merited.

## COMPOUND PROBABILITIES

The form of a particular quantity of interest (such as stress) may be found to be the sum or the product of two or more independently distributed random variables. The probability density functions (or distribution functions) of such combinations are not in general easy to obtain. For the case of two or more normal (Gaussian) random variables, it is well known that the distribution of a sum is normal and is characterized by a mean which is the sum of the means of the component normal variables and by a variance which is the sum of the component variances. The analogue is true for log-normal random variables. Another well known result is that for the case of a sum of squares of standardized (zero mean, unit variance) normal variables; namely, the Chi-square distribution. The well known Student's -t and Fisher's -F distributions are also compound functions.

Mixtures of random variables with different distributions may present analytical and computational problems of great complexity. For example, the density function for the sum of a Rayleigh random variable, A, and a normal random variable, B, is given in Reference 11 by the function

$$P_{A+B}(Q) = \frac{Q\sigma_a \exp\left[-\frac{Q^2}{2(\sigma_a^2 + \sigma_b^2)}\right]}{2(\sigma_a^2 + \sigma_b^2)^{3/2}} \left[ 1 + \operatorname{erf}\left[\frac{Q\sigma_a}{\sigma_b\sqrt{2(\sigma_a^2 + \sigma_b^2)}}\right] \right] + \frac{\sigma_b \exp\left[-\frac{Q^2}{2\sigma_b^2}\right]}{\sqrt{2\pi}(\sigma_a^2 + \sigma_b^2)} \quad (2)$$

Additional interesting examples of compound probabilities are available in this reference.

An illustration and discussion of the complexity involved in the analytical development of compound probability functions may be found in Appendix C where the case of the sum of two Rayleigh variables is considered. The density function developed there is typical of many compound probability problems in that it cannot be determined in a mathematically closed form.

#### IV GENERAL TESTING METHODS

Limitations in the present state of the art make it necessary to spell out certain cases which are available now or loom as particular problem areas which fall into categories that are desirable to test in a combined loads atmosphere at the RTD sonic test facility.

The suggestions that are put forth for testing methods in the following combined loads cases are ideas and techniques advanced as practical solutions to some difficult combined loading situations. Each case must be studied, analyzed, and experimented individually before testing is attempted. It should be pointed out at this time that although some of the cases selected for drawing presentation are suited to specific aircraft; they can be applicable to any type of aircraft or aerospace vehicle.

The following cases were chosen as the most representative and challenging of the numerous failure problems uncovered during the course of an extensive industry and government agency survey. Seven cases have been selected for presentation; engine air intake duct, afterburner transient and mechanically transmitted thrust oscillation, primary structural qualification, missile static firing, large scale turbulence, systems vibration and component test. Each case is taken to show its particular application to the combined loads picture. Background, problem definition, and suggestion for simulation are presented for the seven cases, and references to specific cases are made where applicable. Stress conditions and types of failures are also given for these case histories. A drawing is presented for each case as a pictorial presentation for case simulation in the RTD sonic facility.

##### ENGINE AIR INLET DUCT

###### Background

On the original configuration of the Northrop T-38 supersonic jet trainer inlet duct panel, failures occurred approximately two to three feet aft of the intake plane inside the duct proper. The most severe operational condition found to be contributing to these fatigue failures was that of engine ground operations. A series of tests were run on the duct to determine the optimum design changes necessary to prevent a reoccurrence of this failure. The new design configuration of honeycomb panels was selected as a final corrective remedy.

## Problem Definition

It had been determined from previous tests that the acoustic environment reached an overall level of approximately 170 db at the location of the detected panel failures. The high intensity compressor whine propagated upstream in combination with intake turbulence caused by separated flow around the mouth of the duct caused panel failures a few diameters within the duct.

The static differential pressure existing within the duct varies from 0 to 3.3 psi collapsing and 5.0 psi bursting. This pressure is dependent on engine setting and duct configuration. The compressor whine is also dependent on engine type and setting and will contain one fundamental frequency and several less pronounced modes. Another type of reaction load occurring within the duct, although it is usually not considered a problem, is that of transmitted engine vibration into the duct panels. However, during actual engine operation this can approach five mils and must be considered as contributing to the overall combined loads problem.

## Simulation

In any case of a failure occurring due to load interaction an accurate simulation of actual conditions should be observed. The unique application of this case as shown in Figure 12 is that of actual engine simulation without the need for engine operation. The operational conditions of the various components, i.e., mass flow, compressor whine frequency spectrum, and vibrational limits can be obtained from the engine manufacturer and may be applied to any aircraft duct configuration once these operational conditions are determined.

## Case History

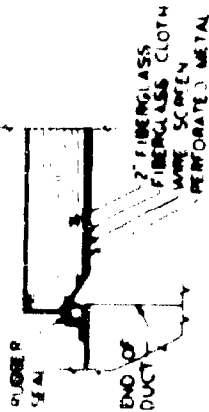
### Description

The structure being tested consists of the intake air duct for a turbojet engine and the adjacent structure of the aircraft.

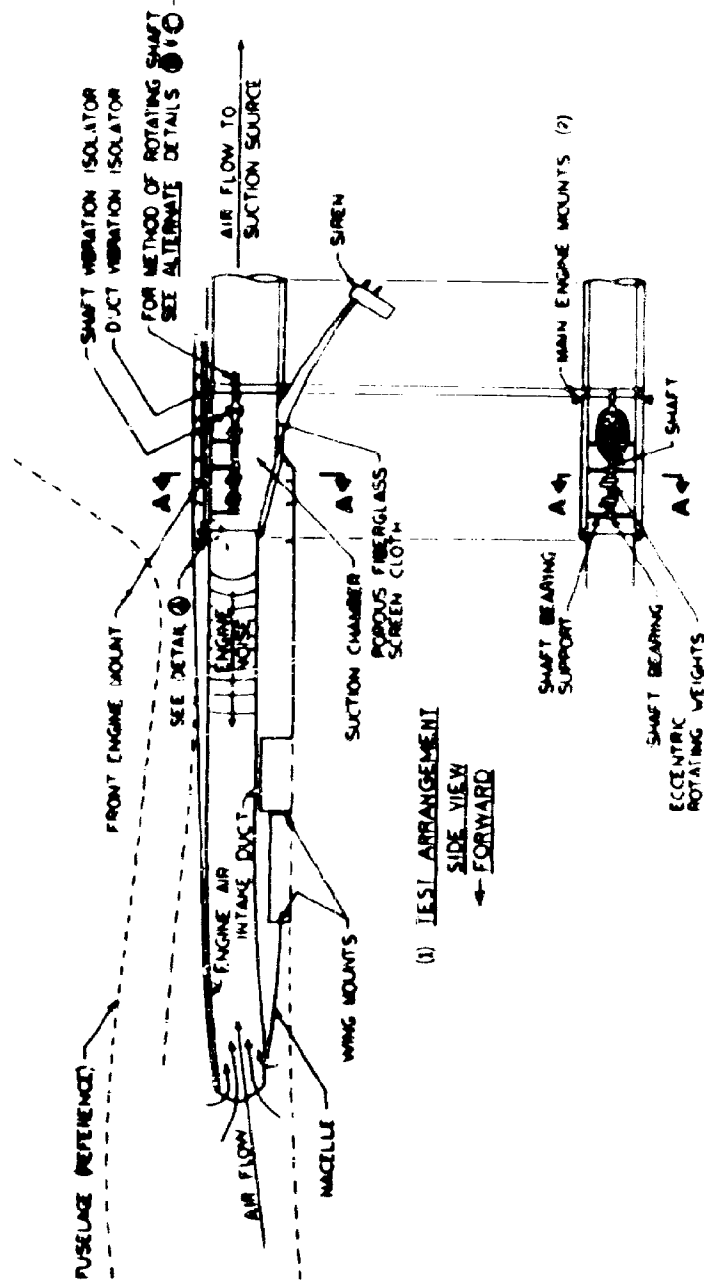
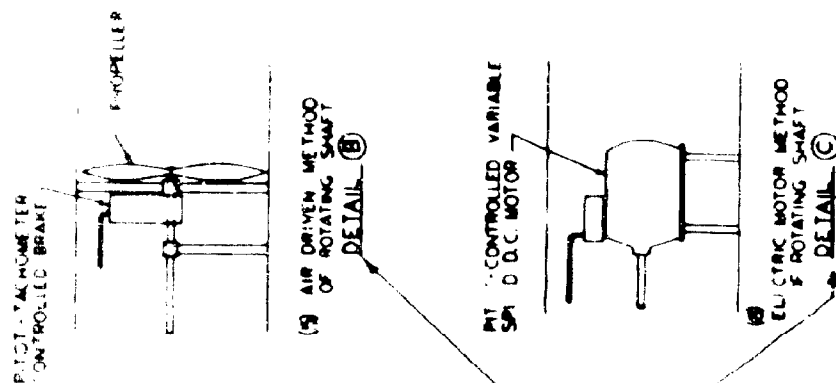
The test simulates loads applied to the air intake duct by the jet engine. The first of these loads is air turbulence in the duct within a few duct diameters of the intake which is most serious during ground runups. Another load is caused by vibration of the engine due primarily to the slight out-of-balance of the compressor and turbine rotating parts. This vibration is transmitted to the structure through the engine mounts. The third load is an acoustic load which in the duct consists mainly of compressor whine which propagates upstream against the air flow.

Structural failures of the intake duct due to the combination of loads described consist of fatigue cracking of the duct and supporting members near the intake end of the duct.

Nearly every jet aircraft has been plagued with fatigue failures of the intake duct requiring subsequent strengthening. It is desirable to structurally test the duct as early as possible in the development of a new aircraft. Normally, at the time the duct structure is ready for testing, the engine is either not yet available or at best, is available in limited quantities so that use of one or more engines for testing of the duct limits the engines available for other use and thereby delays the ultimate production scheduled for the aircraft. For these reasons it is considered desirable to simulate engine effects by test fixtures to permit early testing of the intake duct and associated structure.



14 DETAIL A OF  
SUCTION CHAMBER WALL



(2) TOP VIEW OF SUCTION CHAMBER

**FIGURE 12 ENGINE AIR INTAKE DUCT**

## Discussion

The test setup is shown in Figure 12, which uses the T38 aircraft as an example.

The air turbulence in the duct is created by attaching to the aft end of the duct, at the engine mating plane, a suction chamber from which air is evacuated by a suction source to provide an air flow in the duct corresponding to the air flow resulting from compressor suction during ground runup. Due to the sharply curved entry path of air into the duct when the duct is not moving through the air, turbulence is created which is most severe at approximately two to three duct diameters behind the intake. By providing the correct quantity of air flow by use of the suction chamber, nearly exact turbulence conditions will be simulated by the test setup. To prevent undesirable noise from propagating up the duct, the suction chamber has an inside surface which will absorb most of the sound in the chamber. A typical lining of the chamber and exhaust duct is shown in detail A (Figure 12(4)). Fiberglass or polyurethane can be used as an absorptive material. The chamber walls can be rolled aluminum plate or a suitable ducting metal. Rubber isolators and seals should be utilized where required.

Engine noise (compressor whine) is simulated in the test setup by a siren. A series of sirens can be installed if necessary to obtain the desirable engine compressor noise spectrum. The sound from the siren is collected by a transition section and ducted to the aft end of the vehicle duct where it is propagated upstream as if the actual engine was installed and running. The pressure wave enters the chamber as nearly parallel to the vehicle centerline as possible. One or more sirens can be installed in this manner depending on the test conditions.

Engine vibration is simulated by eccentric weights mounted on a rotating shaft. The mass and eccentricity of the weights are properly sized to provide the maximum vibration permitted by engine specifications. Since pre-test calibration of the vibration input will be required, the weights are used in pairs so that the location of the center of mass of the two weights can be varied by their relative angular position on the shaft. To simulate the correct dynamic properties of the engine, the longitudinal location of the weights and the bearings, as well as the size and stiffness of the shaft must correspond to the configuration of the actual engine.

The vibration forces caused by the rotating eccentric weights are transmitted through the shaft bearings and bearing supports to the structural members of the suction chamber and thence to the engine mounts from which the chamber is rigidly supported. To preserve the dynamic properties of the shaft, a flexible connection is provided at the point in the shaft where the actual engine shaft ends. Vibration of the suction chamber is similarly isolated from the exhaust duct by a flexible connection.

Two methods are available for driving the shaft. Detail B (Figure 12(5)) shows a propeller turbine which is spun by the air flow through the exhaust duct. Since there is no load on the shaft other than bearing friction, the rotational speed of the shaft is controlled by a band and drum type brake. It is necessary that shaft speed and air flow be in the correct proportions corresponding to variable engine power settings. Therefore, the braking force is set by a controller which measures air flow by means of a pitot tube and shaft rotation by means of a tachometer.

Detail C (Figure 12(6)) shows an alternate method of driving the shaft using a direct current variable speed electric motor. Again to provide the correct relationship between air flow and shaft speed, the motor speed is regulated by a controller which measures air flow by means of a pitot tube.

It is to be noted that the eccentric weights are located longitudinally on the shaft at the locations of the compressor and the turbine of the actual engine. By calibrating the weights, quite accurate simulation of vibration from these two sources can be achieved.

Another source of vibration from a jet engine may be the gear box, not located concentrically with the compressor and turbine shaft. This source has not been simulated since its effect is comparatively small on the forward portion of the duct where failures are encountered.

Other loads on the aircraft during ground runup such as the weight of the engine, rocking on the gear, thrust oscillation, or the environmental conditions of the incoming air mix are not considered significant to the fatigue failure of the duct and have not been simulated. These additional loads can be added simultaneously, however, using methods shown in other cases of this study.

The following technical data are included to illustrate the design conditions for the test fixtures:

Northrop Norair T-38 Engine (J-85)

- approximate weight 470 lbs.
- maximum allowable vibration (engine case displacement)
  - at forward end of compressor 0.006 inches
  - at aft end of compressor 0.005 inches
  - at turbine housing 0.005 inches
- air flow at 100 percent power 34,500 cfm (STP) duct diameter (at engine) 15.5 inches
- engine compressor noise spectrum given by manufacturer.

As noted in the following cases, all critical equipment and accessories should be protected from the sonic environment during calibration and test runs. The specimen shall be attached to the appropriate jig fixtures and reacted into the floor beams. The specimen or vehicle should be as complete as practicable in order to simulate the rigidity, the structural members, and the installation of various components and equipment. Pretest calibrations and checkouts will determine the amount of air to be displaced and the sound level at various areas along the vehicle.

#### AFTERBURNER TRANSIENTS AND MECHANICALLY TRANSMITTED THRUST OSCILLATIONS

##### Background

As part of the Air Force Structural Integrity Program, Convair, Fort Worth, Texas, was requested to perform an acoustic fatigue test during ground runup on the B-58 aircraft during afterburner operation.<sup>13</sup> The test was planned to show, on an accelerated basis, if any design details or structural areas possessed inadequate

service life due to sonic fatigue. During the progression of this test program a total of 579 failures were encountered, a small percentage of which would have caused mission abort.

### Problem Definition

It was determined during the course of this investigation that many of the in-wing structural failures were caused by a dynamic low frequency (less than 20 cps) cyclic shear in combination with a high frequency (greater than 100 cps) acoustic field occurring during afterburner operation. During a subsequent investigation of this phenomena<sup>14</sup> the low frequency shear was attributed to mechanically transmitted thrust oscillation or unsteady burning which contributed significantly to reinforcement of natural wing vibration modes. Mean stresses at some points reached values of 10,800 psi in wing spars due to mechanically transmitted thrust oscillations. Another phenomena occurring during the afterburner lightup period is that of afterburner transients. This is the transient vibratory motion caused by uneven engine operation during the transition period which occurs when engine power is advanced from military to maximum afterburner. Although occurring for only a very short time during the actual afterburner lightup period, it is believed that these transients are a contributing cause to many structural failures. It has been shown that the magnitude of the mean stresses caused by this increase in thrust are approximately twice the steady state afterburner stress levels. This would induce particular wing mean stresses on the order of 21,600 psi during the brief transition period prior to afterburner stabilization. This phenomenon will be described in further detail in the simulation method that follows.

### Simulation

Figure 13 and its discussion presents a means of applying the loads which occur during the afterburner transient condition. Means of simulating the occurrences during the transition period have been incorporated into the case discussion, i.e., afterburner transients, acoustic energy and thrust increase and can be accomplished as follows.

### Case History

#### Description

This case considers the principle causes of fatigue damage to the wing of a jet bomber, with the B-58 aircraft used as an example. The loadings involved are thrust variation caused by afterburner transient, mechanically transmitted thrust oscillation, engine vibration and acoustic energy from the engine exhaust. Thrust variation and thrust oscillation are simulated by a hydraulic cylinder applying forces to the engine mounts through a thrust harness. Rotational engine vibration is simulated by eccentric weights rotating at the location of the engines. Acoustic energy is supplied by the main low frequency siren bank of the RTD facility and portable auxiliary sirens, with the correct distribution pattern of sound pressure level obtained by using attenuating baffles or curtains. The overall test arrangement is shown in Figure 13.

#### Discussion

As shown graphically in Figure 14A afterburner transient loading consists of a pulse load of one or more peaks applied longitudinally to the engine mounts over a period of milliseconds. This pulse load is superimposed on the steady engine thrust, and is a phenomenon of afterburner ignition.



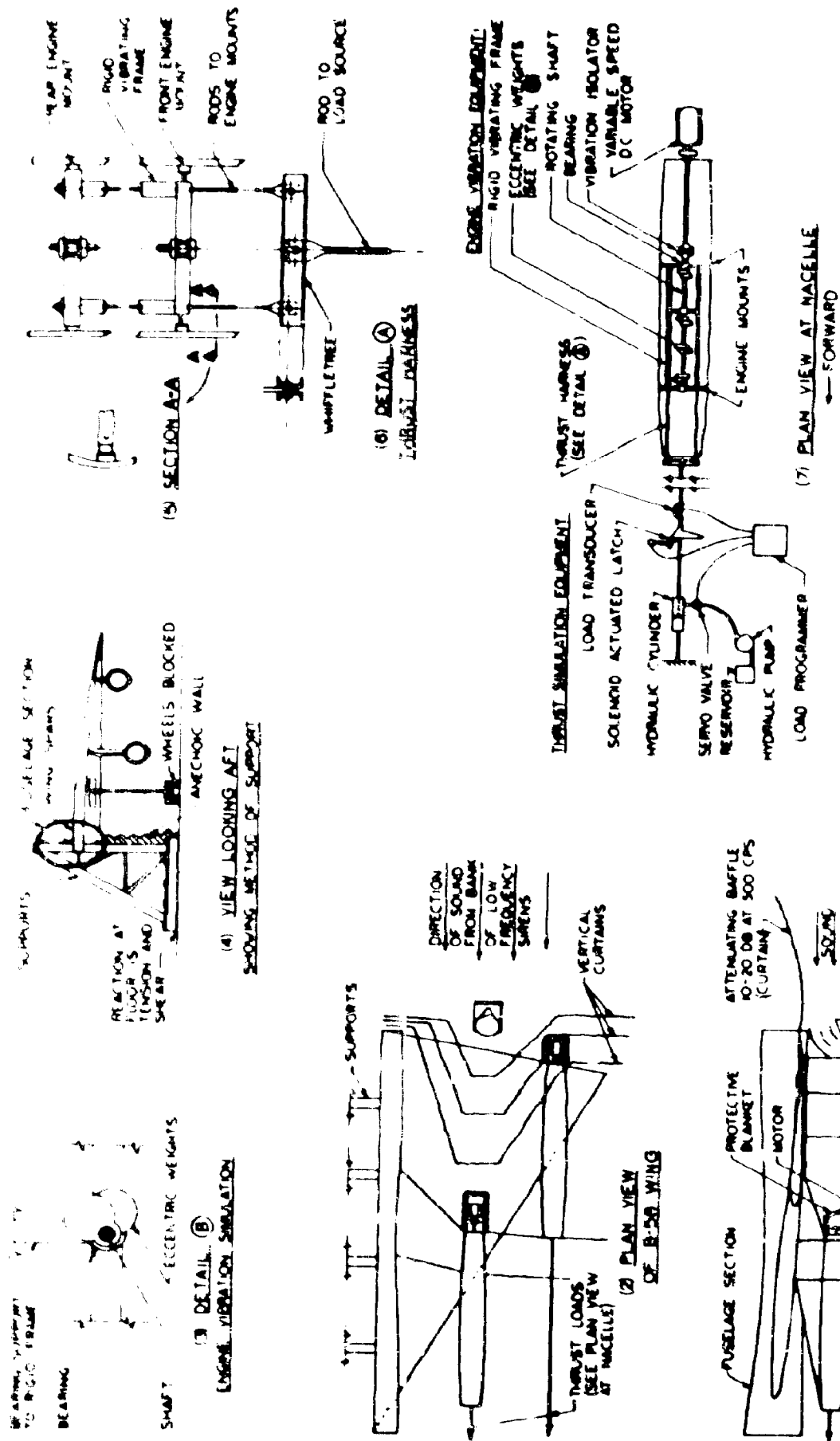


FIGURE 13 AFTERBURNER TRANSIENT AND MECHANICALLY TRANSMITTED THRUST OSCILLATION

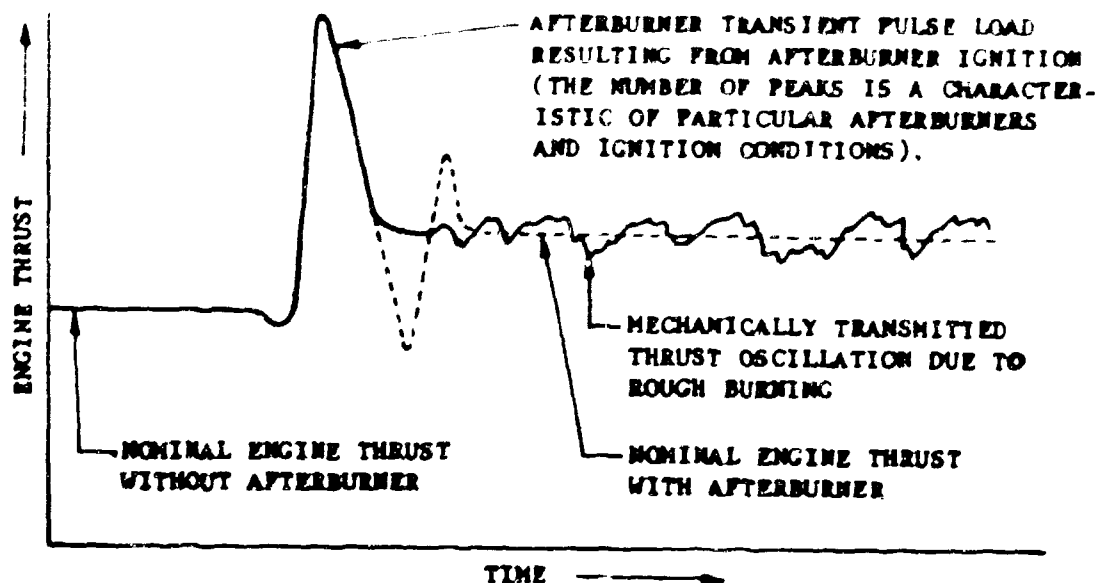
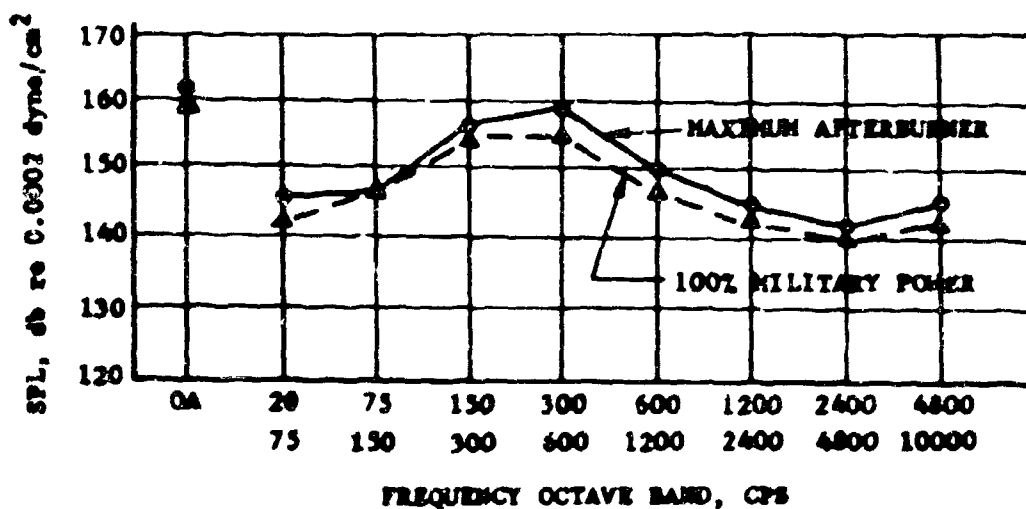


FIGURE 14a AFTERBURNER TRANSIENT AND MECHANICALLY TRANSMITTED THRUST OSCILLATION CURVE



B-56 ACOUSTIC NOISE MEASUREMENTS, AFT AREA OF LOWER SURFACE OF WING, ALL ENGINES OPERATING, GROUND STATIC TEST, 15.

FIGURE 14b ACOUSTIC LOADING SPECTRUM

Transient force situations involving a number of peaks is possible and should be investigated for the particular afterburner for which loading is to be simulated by test. The dynamic response associated with multiple peaks is almost proportional to the number of peaks involved, counting both the maximum and minimum peaks representing half cycles of the forcing function. There are also malfunctions which may occur at afterburner shutoff that lead to very high oscillatory forces, but since these do not represent the usual situation, these forces are not discussed further.

Mechanically transmitted thrust oscillation is produced by rough burning of the jet engine, in this case especially with the afterburner in operation as shown in Figure 14A. A condition of oscillating thrust is produced and mechanically transmitted by the engine mounting structure. The thrust oscillation produced by rough burning is a random frequency forcing function applied in the direction of the engine thrust. As this forcing function is transmitted through the engine and its mounting structure, the frequency spectrum is modified by the response of the mounting structure.

The resulting forcing function acting on the main wing structure produces a tendency toward rotation, causing torsion in the wing, and through coupling, vertical bending causing flexural stresses in the wing. Since the forcing function on the main wing structure is random in frequency, the wing tends to respond at its natural frequencies in torsion and flexure. This response results in low frequency cyclic shear stresses that contribute to wing spar fatigue failures.

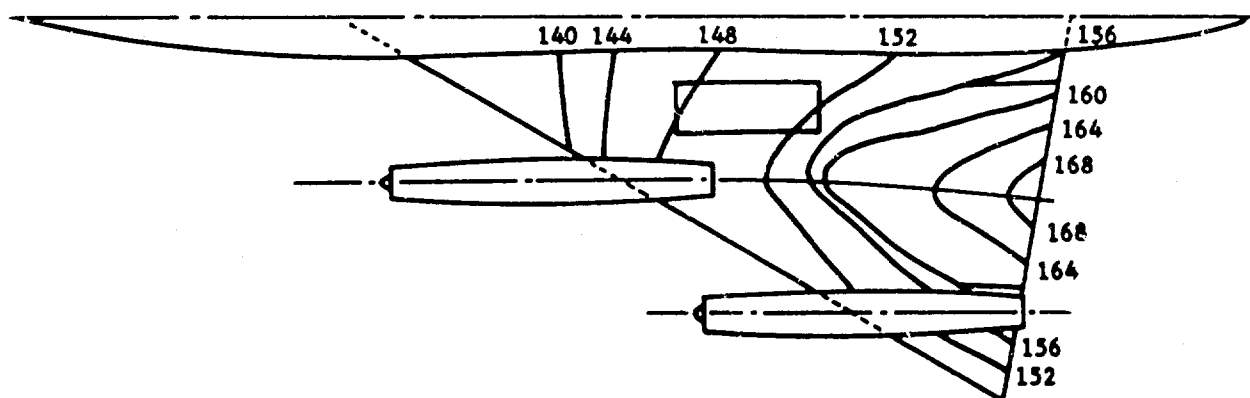
Vibration loads transverse to the longitudinal axis of the engine are caused by minor out of balance of the rotating parts of the engine.

Engine noise causes an acoustic environment on the lower surface of the wing. Because of the location of the engines, a predictable pattern of distribution of sound pressure occurs over the wing surface. The sound pressure level distribution over the wing of the B-58 aircraft is shown in Figure 15 and its spectrum in Figure 14B.

The test arrangement is shown in Figure 13 (1) and (2), which shows one wing of a B-58 aircraft. The equipment utilized is discussed in terms of the loading being simulated.

Steady engine thrust and the rapid variation in thrust resulting from the afterburner transient phenomena is provided by a hydraulic actuator and associated equipment and is transmitted to the engine mounts by a thrust harness as shown in Figure 13 (6) and (7). It is to be noted that in the example illustrated, all thrust is to be carried by the rear engine mounts. Therefore, as shown in Figure 13 (5) and (6), the connection between the rigid vibrating frame and the front engine mounts is designed to transmit transverse vibration forces but is flexible in the longitudinal direction to prevent application of thrust to these engine mounts.

Programming of the thrust loading is shown schematically in Figure 13 (7). Thrust loading is controlled by a load programmer which reads the load applied from a calibrated load transducer and controls the flow of hydraulic fluid into the hydraulic actuator through a pressure control servo valve. The response time of the hydraulic actuator permits the application of a pulse load over approximately 10 to 20 milliseconds. This time of application is lengthened by the response time of the thrust harness which carries the load to the engine mounts.



**NOTES:**

1. LEVELS IN DECIBELS re 0.0002 MICROBAR.
2. FOUR J-79-1 ENGINES OPERATING AT MAXIMUM REHEAT UNDER STATIC CONDITIONS.
3. REFERENCE 15, PAGE 17.

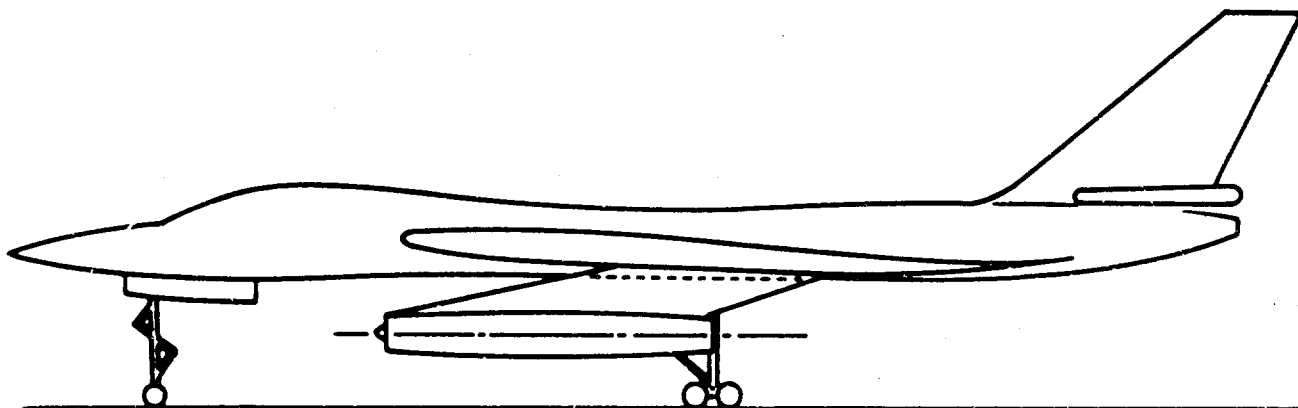


FIGURE 15 OVERALL SOUND PRESSURE LEVEL CONTOURS -B58 WING

For situations where the pulse load of afterburner transient must be applied more rapidly, the latch arrangement of Figure 13 (7) is inserted. By this arrangement, steady engine thrust is applied by the cylinder, after which the displacement of the harness is restrained by the latch so that no further load can be applied to the engine mounts. The pressure on the cylinder is then further increased. When the solenoid-actuated latch is released by the load programmer, the piston of the actuator is suddenly displaced which applies the additional pulse load through the harness to the engine mounts. The oscillation and decay of the load occurs relatively slowly and is provided by control of the hydraulic actuator through the load programmer. As the thrust load begins to stabilize at the value of thrust equal to nominal engine thrust with afterburner, the mechanically transmitted thrust oscillation loading begins, as discussed in a following section. The afterburner transient pulse load can then be repeated by reducing the load below steady engine thrust without afterburner so that the latch will reengage.

In order that the thrust load be applied equally to both engine mounts, it is important that the load be applied normal to the plane of the mounts. This is accomplished by locating the anchorage of the hydraulic cylinder sufficiently far from the engine mounts so that a slight eccentricity will cause minimum angular misalignment with the engine centerline. However, the length of the thrust loading harness should not be made excessive, as this would increase its time of response to the applied thrust loads. The supports must also be sufficiently rigid so as to permit minimum displacement due to the tendency of the thrust loads to rotate the wing in a horizontal plane. Blocking the main gear also assists in preventing this tendency to rotate. The whiffletree arrangement used in the thrust harness as shown in Figure 13(6), further tends to distribute the load equally to both engine mounts.

The mechanically transmitted thrust oscillation loading is simulated using the same equipment as that used to simulate the afterburner transient loading. The same hydraulic cylinder, shown in Figure 13(7), is used to provide the forcing function which simulates thrust oscillation due to rough burning of the engine.

As this cylinder completes the simulation of afterburner transient loading, the programmer, through control of the servo valve, causes the cylinder to apply a random frequency oscillation of force to the thrust harness and thence to the engine mounts. This thrust oscillation varies about the nominal value of thrust with afterburner as previously shown in Figure 14A. The duration of the thrust oscillation loading before application of the next cycle of afterburner transient pulse load will be determined by the mission profile of the vehicle.

Engine vibration is simulated by eccentric weights mounted on a rotating shaft shown in Figure 13(7). The mass and eccentricity of the weights are properly sized to provide the maximum vibration allowed by engine specifications. The weights are used in pairs which permits variation of the eccentricity of the combined center of mass by the relative rotation of the two weights as indicated in Figure 13(3). Multiple pairs of weights are located in the longitudinal area of the compressor and turbine of the engine to provide a rotating couple simulating dynamic unbalance. The location of the bearings, diameter of the shaft, etc., are made to correspond to the actual engine to simulate the correct dynamic properties.

The vibration forces caused by the rotating weights are transmitted through the shaft bearings and bearing supports to a rigid vibrating frame which is attached to the engine mounts. As shown in Figure 13(7), rotation of the shaft is provided by a variable speed direct current motor which must be protected from the acoustic load. A vibration isolator in the shaft prevents transmission of the vibration to the

motor and also preserves the dynamic properties of the shaft, which in the actual engine ends at the location of the isolator. In specific test conditions a gearbox arrangement may be utilized between the D.C. motor and shaft.

The acoustic load simulating engine noise is supplied by the main low frequency bank of sirens and auxiliary high frequency sirens as shown in Figure 13(1) and (2). The specimen is oriented with the area of highest Sound Pressure Level (SPL) toward the main bank of sirens to take advantage of attenuation with distance from the source to obtain decreasing SPL toward the forward portion of the wing. Since attenuation with distance will not alone provide the desired distribution of SPL over the wing surface, auxiliary sirens are used at the area of highest SPL to reinforce the main bank. To further control the distribution pattern of noise, attenuating curtains or baffles are placed vertically from the lower surface of the wing to the floor. The location of the curtains approximates the shape of the contours of equal SPL which are desired, as previously shown in Figure 15. If very light weight curtain material is found to be adequate, it can be supported by attachment directly to the lower wing surface with adhesive. However, if the adhesive or the weight of the curtain appreciably affects the response of the wing panels, then the curtains should be supported on rods from the floor. The curtain support method must be determined during calibration and checkout prior to the actual test program.

Since the SPL increases at the time the afterburner ignites, it is necessary to program the acoustic sources to simulate the increased SPL as the thrust loading mechanism simulates the thrust effect of afterburner ignition.

A sound-absorptive anechoic wall is required along the line of the supports under the centerline of the fuselage section as shown in Figure 13(4). This wall simulates the open area under the fuselage in actual engine operation on the ground, preventing sound reflection from the supports or the walls of the chamber beyond the supports. Additionally, the wall protects the supports from the effects of the acoustic energy.

Attenuation of the SPL toward the forward end of the wing could be accomplished by raising the forward end of the wing so that the area through which the sound energy is radiated increases as it progresses forward. However, this method would not provide the transverse attenuation required, so that curtains and auxiliary sirens would still be needed. In addition, raising the front of the wing would distort the effect of reflection from the floor which is present during actual ground runup as reflection from the runway.

It may be noted from Figure 13(1) that the sound energy from the main low frequency bank of sirens reaches the lower wing surface with essentially grazing incidence, while the sound from the high frequency auxiliary sirens is applied with a near-normal angle of incidence. Under actual acoustic loading from the engine there is essentially grazing incidence with a forward direction of propagation on the leading portion of the wing, so that the acoustic loading in this area is simulated reasonably well by the test arrangement. In the central and aft portion of the wing, the acoustic load due to the engine running varies from normal incidence near the engine to more nearly grazing incidence outward from the engine, with a direction of propagation away from the engine exhaust. Although the test arrangement simulates the coincidence angles and directions of propagation less faithfully in these areas the effect on panel response and the resulting fatigue failures is not expected to vary significantly from the actual acoustic loading of the engine exhaust. This is particularly true since the response in the fundamental mode is most important to fatigue damage and this in general is relatively independent of angle of incidence.

The response of the wing structure is significantly affected by the fuel in the wing tanks. During test, a non-combustible liquid, with approximately the same specific gravity should be in the tanks and the liquid level may be varied during test to approximate the actual fuel present during operation of the aircraft. Amsco 140, dyed red, or an equivalent may be substituted for JP-4 or JP-5 fuel.

Certain additional loads have not been illustrated for this case, but can be simultaneously applied. These include bending and torsion applied to the main gear simulating rocking of the aircraft during ground runup which would affect low frequency flexure and torsion in the wing. Vertical vibration loads on the gear, simulating the effect of runway roughness during taxi and takeoff, and the environmental effects on the wing from the engine exhaust such as heat can also be incorporated.

Although the design parameters for the loads must be established for each specific vehicle to be tested, the following technical data is included to illustrate the design conditions which were considered in developing the test methods. Much of the data regarding the B-58 aircraft's engines is contained in classified documents and is not reproduced here to prevent classification of this study. The information is available in "Model Specifications, YJ79GE-2 Turbojet Engine" and "YJ79GE-2 Engine Installation Manual," both classified Confidential.

- Weight of Test Specimen:

(Total weight of B-58 is approximately 160,000 pounds)

- Thrust of Engines:

Without Afterburner: Approximately 10,000 pounds

With Afterburner: Approximately 15,000 pounds

- Afterburner Transient:

The first pulse is applied over a period of milliseconds with each oscillation of decay occurring over tenths of seconds. The peak of the first pulse may approach twice the thrust with afterburner.

- Acoustic Loading Spectrum:

The acoustic loading spectrum for the aft end of the lower surface of the wing is shown in Figure 14B.

## PRIMARY STRUCTURAL QUALIFICATION

### Background

On any aerospace vehicle, proof testing of primary structure is a necessity in the early stage of development to prevent catastrophic failures during its operational status. Aerospace companies have established elaborate static fatigue test facilities to provide these qualifications. Of the larger order loads, those encountered during maneuver, steady air and ground-air-ground cycles are considered to be the most damaging to primary vehicle structure. The damage process occurring during these operations has caused, in many cases, complete loss of a lifting surface and missile stage failure with accompanying loss of life and total vehicle destruction.

## Problem Definition

In jet bomber type aircraft a jet noise gradient occurs over the wing surface as shown in Figure 15 for the B-58 aircraft, a typical weapons systems carrier. These large noise levels encountered during afterburner operation can couple with the fundamental vibratory modes of the vehicle itself and produce unwanted resonances that can be very damaging to primary structure. This is particularly true in the case of wing supported or integral mounted engines. A wing is shown in Figure 16 as an example but the method of static load attachment can be applicable to any part of the aircraft structure that encounters pressure variation and high acoustic loadings, i.e., vertical tail, fuselage, or missile skin.

## Simulation

Figure 16 and the following present a means of applying acoustic loads to a statically stressed wing. Means of providing in-flight pressure loads are presented which when programmed using a typical time-mission profile in conjunction with acoustic, static flexure, torsion and bending will structurally qualify a vehicle for service.

## Case History

### Description

The method of applying loads is applicable to any portion of a flight vehicle. A representative aircraft wing has been selected for illustration.

The following loads are simulated, as a basis for qualifying the primary structure of the vehicle.

- Loads causing flexure, torsion and shear in the flight vehicle are the result of maneuver, steady air loads, the ground-air-ground cycle and are applied in actual flight as pressures over an area of the vehicle which cause deflections of the primary structural members.
- Concentrated loads applied at the wheels in all three axes, which are transmitted by the gear to the primary structural members supporting the gear.
- The acoustic environment over the surface of the vehicle, the primary source of which is engine noise.

## Discussion

The test setup is shown in Figure 16(1), showing a representative aircraft wing. Test loads are applied to the gear by means of a dummy wheel by double-end hydraulic cylinders in the two horizontal directions and by a single-end cylinder vertically. The applied test load is sensed by calibrated load transducers which consist of a half-ring dynamometer in conjunction with a Schaevitz linear displacement coil. The closed loop linkage should be fabricated with aluminum flat-bars and short length cables around the pulleys. The linkage should be as long as practicable to eliminate component loads during specimen and gear deflections. The cables should be of a minimum length and prestretched prior to installation. A-frames and various floor supports can be fabricated to support the pulleys and cylinder-transducer combinations. As required all equipment should be protected by acoustic curtains to prevent failures in the sonic environment.



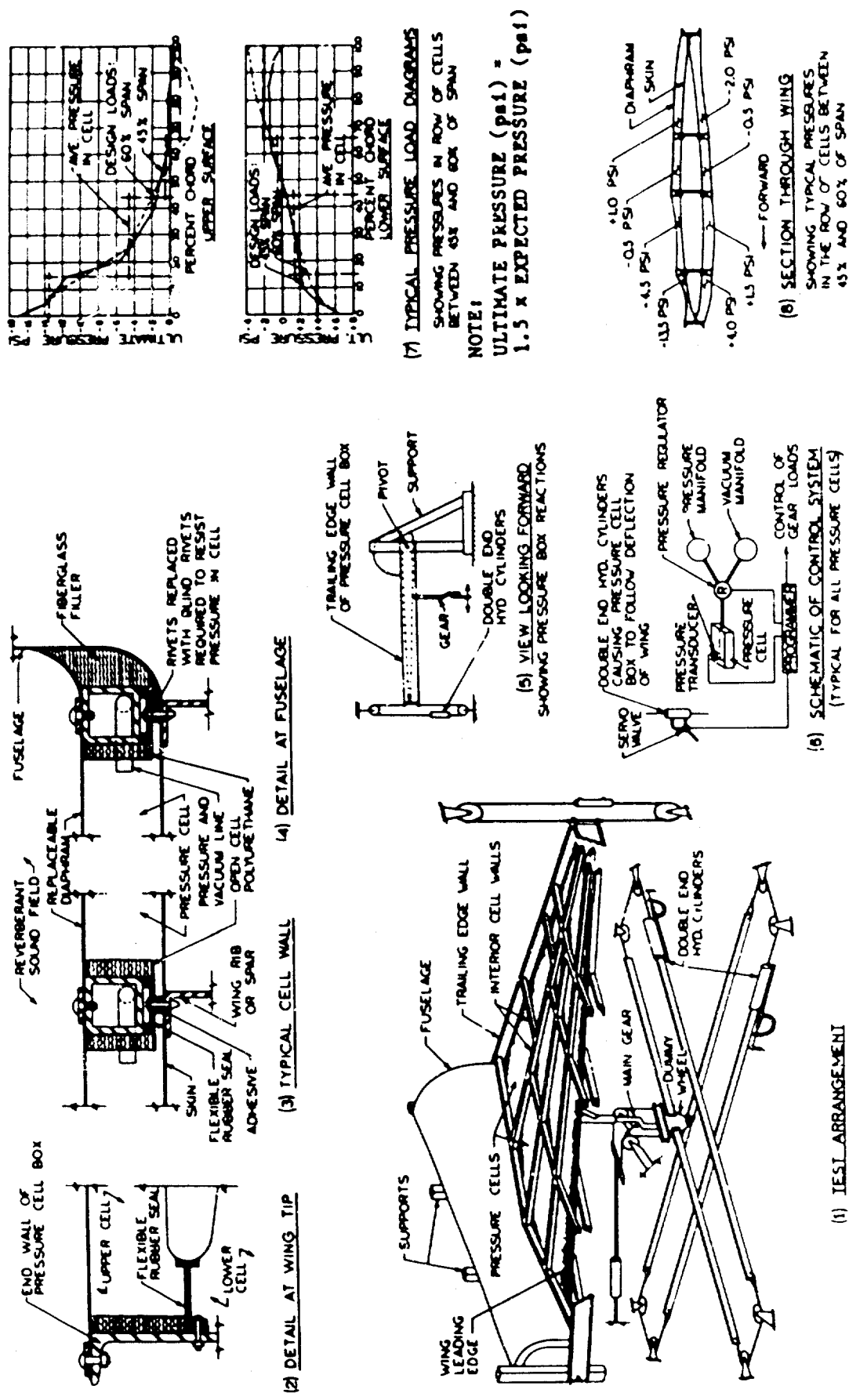


FIGURE 16 PRIMARY STRUCTURAL QUALIFICATION - PRESSURE CELL METHOD

Flexure, torsion and shear stresses are produced in the primary structural members by the application of the test loads. Test loads are simulated on the wing specimen by the application of differential pressures on the upper and lower surfaces of the wing simulating the in-flight pressures seen by these surfaces. Because the in-flight pressure varies over the surfaces, they are divided into cells on both the upper and lower surfaces of the wing. The pressure in each cell is made to be an average of the design load pressures over the surface enclosed by each cell. These loading conditions can be varied to approximate several design loads. A sample computation of average cell pressures for one pressure load condition is illustrated in Figure 16(7).

The design of the pressure cells is shown in Figure 16(3). The cell structure is isolated from the wing by flexible rubber seals cemented to the surface with adhesive, with bolts placed in rivet holes to hold down the cell wall to the skin to resist pressures in the cell. The rubber seal provides a separation between the different pressures in adjacent cells while still being flexible so as to have minimum effect on the response of the wing to vibration.

The pressure in a cell is contained by a replaceable diaphragm, which, although able to hold pressure, can simultaneously transmit acoustic energy. The pressure on the diaphragm is reacted at the cell walls which form a network of structural members which in turn react against the outside walls of the pressure cell box. The fuselage end of the outside walls reacts to the main supports through a pin connection. The assembly shall be adequate enough to enable the fixture to pivot easily during wing deflection and twisting. The outboard end of the fixture will be supported by a closed loop assembly which will enable the support to move up or down depending on the wing deflection direction. The double-ended cylinder in the closed loop circuit should be calibrated and programmed with the loading system during pretest setups and checkouts. Normally a dummy specimen is utilized during load calibrations to determine the deflections, clearances, safety circuits, and the lengths of the adapter to limit the stroke of the hydraulic actuators. Cable lengths and pulleys shall be held to a minimum and where possible flat bar linkage should be substituted. The design of the pressure cells is shown in Figure 16(2), (3) and (4). The details are self-explanatory and can vary to suit different specimen configurations. The test loads are controlled by the load programmer which shall sense any deviation in the required pressures and have a quick dump system if a malfunction should occur. Pressure transducers located in the critical pressure cells will serve as regulators and should be tied-in electronically to the programmer. Figure 16(6) shows a schematic of the control system. Both pressure and vacuum are available in manifolds with connections to a pressure regulator for each cell. Upon command from the programmer, the pressure regulators produce the desired pressure (or vacuum) condition in each cell, which is monitored by pressure transducers in each cell. As the differential pressures in the cells cause the wing to deflect, the programmer will also signal the double-end actuator assembly on the pressure cell support to follow the deflection of the wing. Minor relative movements between the cell box and the wing are permitted by the flexible rubber seals.

Several factors must be considered in a detail design of this loading system for a specific test article:

1. The design loading conditions to be simulated must be known, to determine the range of pressures or vacuum necessary in each cell, as illustrated by the typical load pressure diagrams in Figure 16(7), (8).
2. The layout of the cell walls is made so that the pressures in the cells will best simulate the variety of loading conditions. It is desirable to locate a cell wall at the point where the load changes from pressure to vacuum, although this point will vary for each loading condition.

3. Cell walls should be located over primary structural members wherever possible to minimize their effect on the response of skin panels to acoustic vibration.
4. The depth of the cells between the diaphragm and the vehicle skin should be held to a minimum to reduce the air flow required to obtain the desired pressure or vacuum.
5. The rubber seals at cell walls should be sufficiently flexible to have a minimum effect on vibration response, have sufficient strength to withstand pressure differentials between cells, and have adequate space for deflection to allow relative movement between the cell wall and the vehicle surface.
6. The overall rigidity of the cell box should be such that its deflection can be made to closely approximate the deflection of the wing, to minimize the relative movement between cell walls and vehicle surface.

The acoustic energy is provided by placing the test setup in the reverberant sound chamber of the RTD acoustic test facility. The sound energy striking the diaphragm of the pressure cells is transmitted by the diaphragm into the cell where it strikes the surface of the vehicle. To prevent reverberation within the cells, the cell walls are lined with a non-reflective material such as the open-cell polyurethane shown in Figure 16(3),(4). It is expected that under extended acoustic loading, the diaphragms will periodically fail, so provision for replacing the material is made in the method of attachment of the diaphragms to the cell walls.

Choice of a diaphragm material which will be relatively transparent to the acoustic energy and at the same time have sufficient strength to resist the required pressures is critical to the method shown. Mylar up to about 0.006 inch thickness has been found to be nearly transparent to acoustic energy and has adequate strength for limited pressures over small areas. Over a period of time, stretching of the mylar under load is to be expected. Greater strength is obtained with a rubber impregnated nylon fabric, but at the expense of poorer transmission of acoustic energy.

Even with a diaphragm material capable of transmitting all of the acoustic energy, a reflective surface would exist because of the different densities of the air inside and outside the pressure cells. For this reason, higher SPL's must be applied to the diaphragm than are desired on the surface of the vehicle within the cells. The SPL of the reverberant sound field should therefore be established to cause the maximum SPL desired in any cell. The SPL in other cells can then be varied by covering the diaphragm with varying thicknesses of sound absorptive material to approximate any desired distribution of SPL over the surface of the vehicle.

For simplicity of illustration, vibration loading has not been shown in Figure 16. However, when this type of loading is considered significant to the primary structural qualification of a vehicle, vibration can be introduced by mounting the supports on one, two, or three axis shakers.

In the case of a wing with pylons for engines or payload which see vibration loads, the pylons can extend from the pressure cell box and vibration loads can be applied at these points.

## STATIC FIRING OF MISSILE BOOSTER

### Background

To provide structural integrity a missile and/or upper stages must be statically fired and vibration levels measured at various points of the missile or stage, along with periodic checks for fatigue damage. This involves the costly process of many static firings to proof test the vehicle in its actual vibration environment. It would be desirable to test such a vehicle in the RTD sonic facility reproducing the expected vibration environment of static firing without actual engine operation. The capability of the facility seems ideally suited to this type of proof testing and could speed up overall development of any missile.

### Problem Definition

Acoustic noise levels at static firing of typical upper stage missiles have been measured at 148 db overall in the proximity of the electronic guidance compartment at the forward stage and 155 db overall in the engine area.<sup>16</sup> Vibration induced by rocket exhaust noise reaches significant proportions if structural resonances are excited. Peculiar to all cryogenic missiles is an additional 25 cps resonant vibration associated with pump action which has been measured at all points on the missile but is particularly strong at the engine mounting stations. Cryogenic fuels also present a peculiar problem and must be simulated due to their influence on material fatigue properties. The weight of the fuel itself, and its contribution to reduction in gross vehicle weight through burning and hence structural response, must also be taken into consideration for accurate reproduction of the static firing condition.

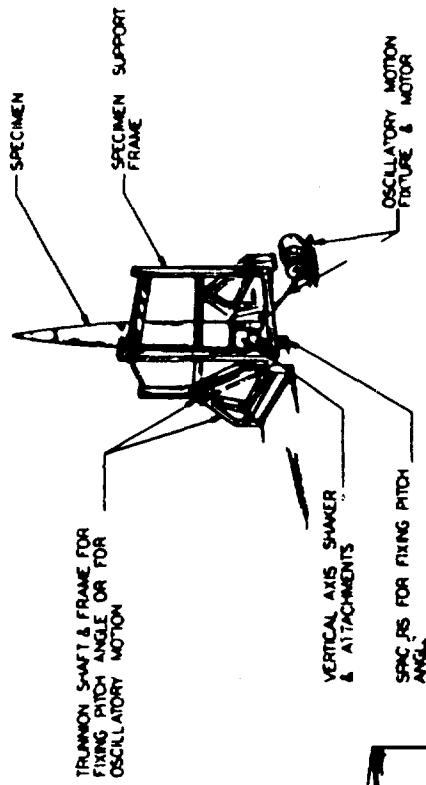
### Simulation

Simulation of the static firing of a missile and/or upper stages can be accomplished in the RTD sonic facility within the limitations of the large chamber vertical clearance. The vibrations produced from the pumping action can be reproduced by hydraulic cylinders placed at the engine mounts with dummy engines in place. The large siren bank can produce the desired gradient in acoustic levels over the height of the missile. Reinforcement may be accomplished at the missile base, as required, with the portable high frequency sirens placed near the engine mounts. This testing arrangement is shown in Figure 17 for a typical missile upper stage.

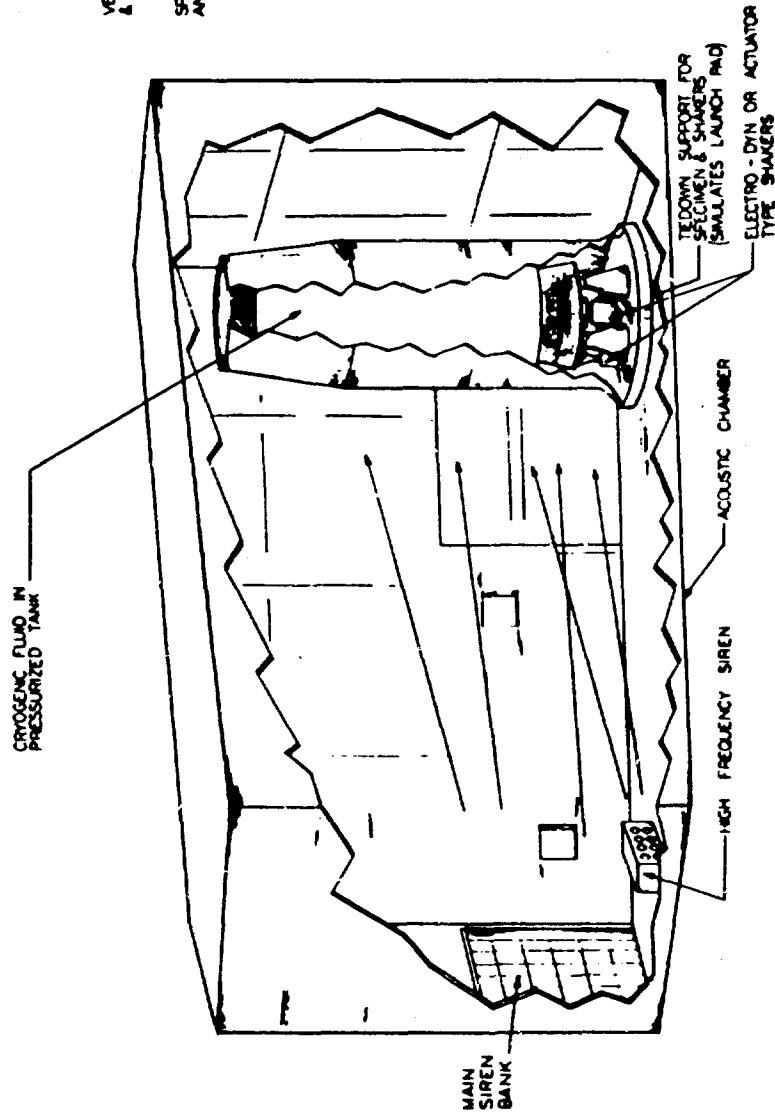
### Case History

#### Description

The acoustic load is caused by the engine exhaust, consisting of progressive wave, wide band (up to 8 octaves) random frequency sound. Because of the geometry of the blast deflector, the acoustic energy reaches the vehicle at an angle from one side, causing some gradient of SPL over the vehicle with some localized reflection from the blast deflector as shown in the following sketch:

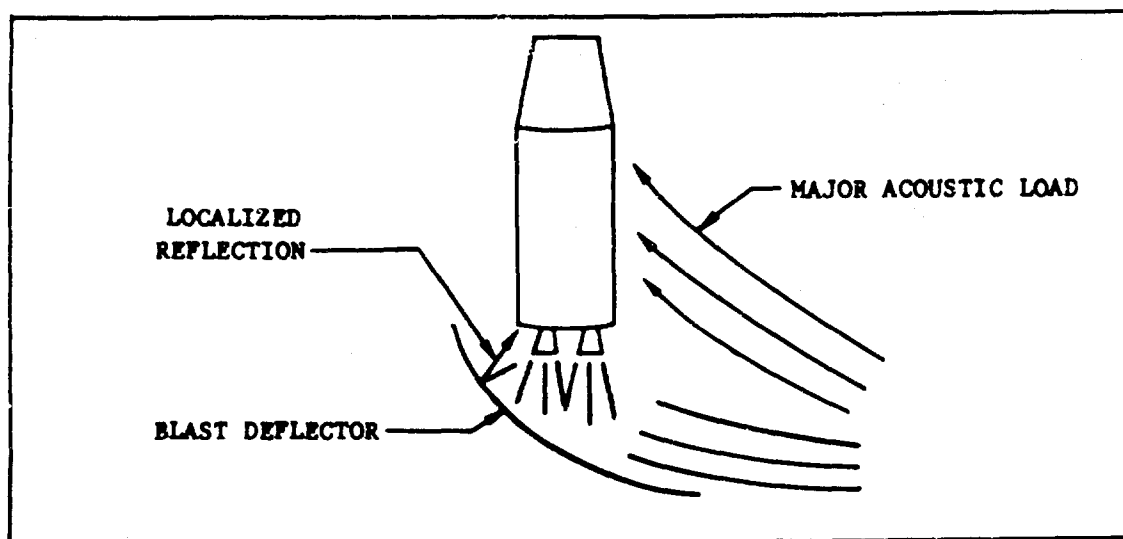


(2) ALTERNATE SETUP IN FACILITY



(1) STATIC FIRING OF MISSILE BOOSTER LAUNCH PAD  
TIEDOWN ATTACHMENT

FIGURE 17 STATIC FIRING OF MISSILE BOOSTER



Vibration exists from the operation of internal equipment such as fuel pumps. This vibration is random, from nearly zero up to approximately 1000 cps, and is applied to the engine frame on which the vibrating equipment is mounted. Low frequency chugging and high frequency screaming due to liquid rocket engine combustion instability is also a source of vibration.

Pressurized liquid fuel tanks result in hoop stresses in the tank walls of several thousand pounds per square inch.

Cryogenic fuels subject the walls of the fuel tanks to temperatures in the minus 200 to minus 400 degrees Fahrenheit range.

The weight of the fuel in the tanks is normally many times the weight of the empty structure. The weight of fuel decreases from its maximum to approximately zero during burning. The weight of upper stages and/or payloads may be simulated during static firing to obtain its effect on the response of the vehicle being tested.

No thrust load is applied to the vehicle proper because the tie downs cancel the engine thrust during static firing. Vibration effects of rough burning may be transmitted through the engine mounts, particularly during developmental firings of some vehicles.

#### Discussion

The acoustic load is provided by the main low-frequency siren bank of the RTD facility, supplemented with high frequency sirens as shown in Figure 17. The acoustic energy is provided as progressive wave, random frequency which simulates the engine exhaust during static firing.

The vibration of internal equipment is simulated by shakers acting on the engines mounting frame as shown in Figure 17(1). The shakers are programmed to provide random frequency vibration. The electro-dynamic exciters would be located at strategic points on the vehicle to induce the vibration spectrum. The exciters would shake in one axis and then be rotated to produce the required frequencies in another axis. In the first case the specimen could be tied down with its regular hold down bolts installed and the exciters and other test loads imposed on the vehicle. If the frequency spectra required a "floating" specimen two methods of suspension are available. The specimen can either be suspended from large size damping springs to make the natural frequency response as low as possible or utilize an air cylinder suspension system. The air cylinder system would be more feasible and economical. The setup is fairly simple and does not interfere with the acoustic energy flow pattern.

For certain size configurations, the specimen could be fastened to a large shake table and several shakers in parallel would supply the frequency input. All other simultaneous loads could also be applied as required including radiant heat. Normally one shaker could be utilized at the longitudinal centerline of the specimen as shown in Figure 17(2). An elastic cord or equivalent can be installed to remove the shaker table and specimen weight from the shaker armature or piston. A series of steel flexure plates can be installed to limit the travel of the specimen and also maintain the transverse motion during vibration. The oscillatory motion (if the test so requires) can be maintained by a simple motor and cam arm arrangement. The pitch angle of the specimen can be changed in this manner or can be held at some fixed angle other than vertical. The specimen fixture and frame work should be as simple as possible in order not to effect the sonic input.

The pressurization of the liquid fuel tanks is simulated using a pressurized gas source connected to the booster tank pressurization system. An inert gas, normally nitrogen, is used.

Several effects on the vehicle are caused by the fuel in the tanks. The primary effects are temperature, fluid pressure, weight, and the effect on the response of the tank wall due to the contact with the fuel.

The effect of temperature is significant to the fatigue of the tank structure for cryogenic fuels such as liquid oxygen and liquid hydrogen, whose temperatures range from minus 200 to minus 400 degrees Fahrenheit. Since the cryogenic fuels and oxidizers are hazardous materials, it is doubtful if they could be used within the facility. Inert liquid nitrogen, having a normal boiling point of minus 320 degrees Fahrenheit could be used to achieve low temperatures without the hazards of fire and explosion. Considerable difficulty is still present in handling liquid nitrogen, however, since insulation, pressure and considerable piping would be required.

The fluid pressure of the fuel on the walls of the tanks is a function of the depth and the density of the fuel. Any substitute liquid used in place of the normal fuel must have the same density if fluid pressures are to be accurately simulated.

The weight of the fuel in the tanks depends on the total volume and the density of the fuels. The weight should be reduced during the test simulating the reduction of fuel in the tanks as it is burned during static firing.

The vibration response of the walls of the tanks is affected by the presence of the fuels in contact with the inside surfaces. The effect of the liquid on vibration response may be a function of its bulk modulus, its viscosity, or a combination of properties. The use of a substitute liquid in place of the normal fuels must be analyzed in terms of the effect on response to vibration of the tank walls.

In view of the many effects of the fuel in the tanks which must be simulated during test, it is extremely doubtful if accurate simulation of all effects can be simultaneously provided when substitute liquids must be used to reduce hazards. The choice of a liquid to be used for any specific simulation must be based on consideration of the factors described, and decisions made as to which of the effects of the fuel are most important for accurate simulation in any specific test case.

## LARGE SCALE TURBULENCE

### Background

Attempts to simulate turbulence or any aerodynamic forcing function with acoustic energy is still in the realm of existing state of the art. However, it is possible that large scale turbulence can be reproduced with a certain degree of accuracy. Turbulence has always presented a problem to the design and test engineer in the areas of metal fatigue at regions of reattachment of aerodynamic flow around obstructions in the vehicle skin. This phenomena has caused numerous failures in many prototype vehicles and is difficult to predict on the full scale article. Cases have occurred where panels have actually been lost in flight due to progressive fatigue caused by turbulence. This presents itself as a difficult phenomena to simulate, but employment of an acoustic source should give a means of attempting this simulation for a velocity of Mach 1.3, which is the acoustic velocity.

### Problem Definition

High noise levels are produced by the turbulence in the reattachment area downstream from the obstruction. These high acoustic levels induce skin vibration resulting in fatigue failures of the affected panels. Stress levels of up to 28  $\mu$  inches/inch were recorded during dive brake extension aft of the speed brakes on the T-38, compared to 11  $\mu$  inches/inch before their employment. Typical flight/ground data for this aircraft is shown in Figure 18. The measured overall noise level was 154 db with speed brakes extended compared to 140 db during normal trimmed approach<sup>17</sup>.

Simulation created behind a speed brake, protrusion, or any change in structural curvature of an aerospace vehicle can be simulated as suggested in the following discussion and shown in Figure 19. Here a funneled progressive wave box is used in conjunction with a random sound source. The actuation of the speed brake mechanism can be accomplished without the presence of the brakes. This method can be used on any surface of the vehicle where a turbulent condition is anticipated.

### Case History

#### Description

This case is concerned with a method of simulating the effects of large scale turbulence, or pseudo-noise, using acoustic energy. The similarity of the forcing functions created by turbulence and acoustic energy suggests this simulation for testing purposes. Variables of the turbulence forcing function, which must be reproduced, are the direction and velocity of flow of the turbulence, the random frequency spectrum of the pressure variations over a surface, and the size of the areas affected by the random turbulent pressures as measured by their correlated areas.

In the method selected for this case, random frequency acoustic energy is supplied to the specimen as a progressive wave with the width of the correlated areas, established by wave guides or sound energy ducts, mounted on the surface to be tested. In the example used for illustration, the turbulence behind the open speed brakes of an aircraft is considered.



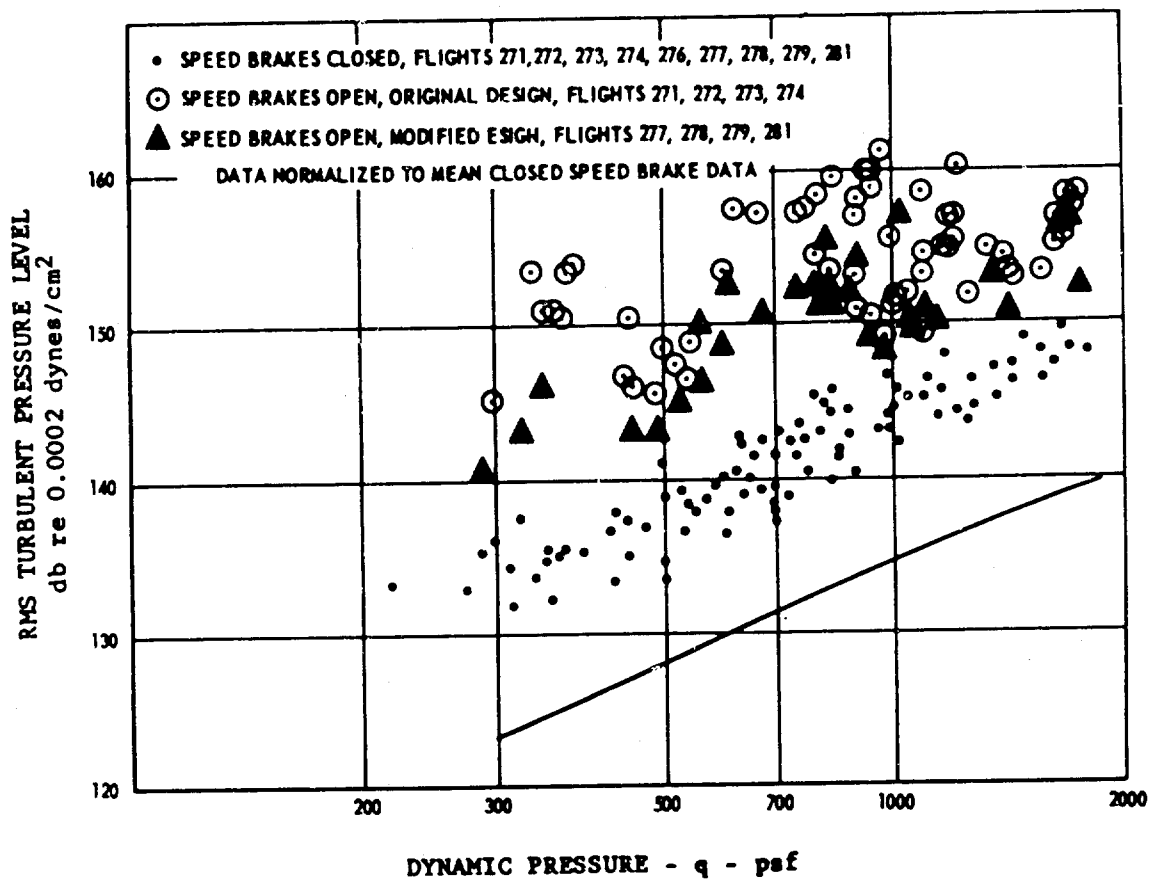
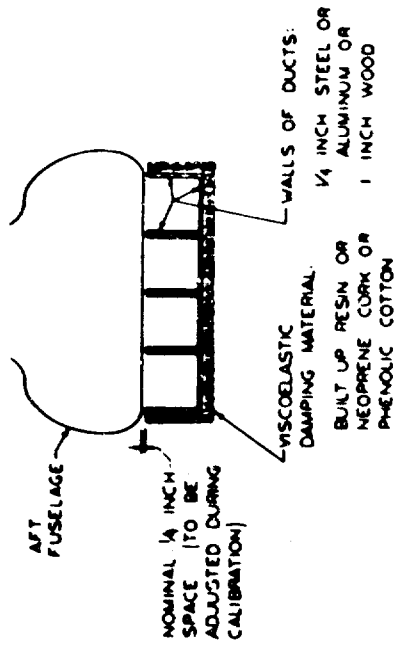
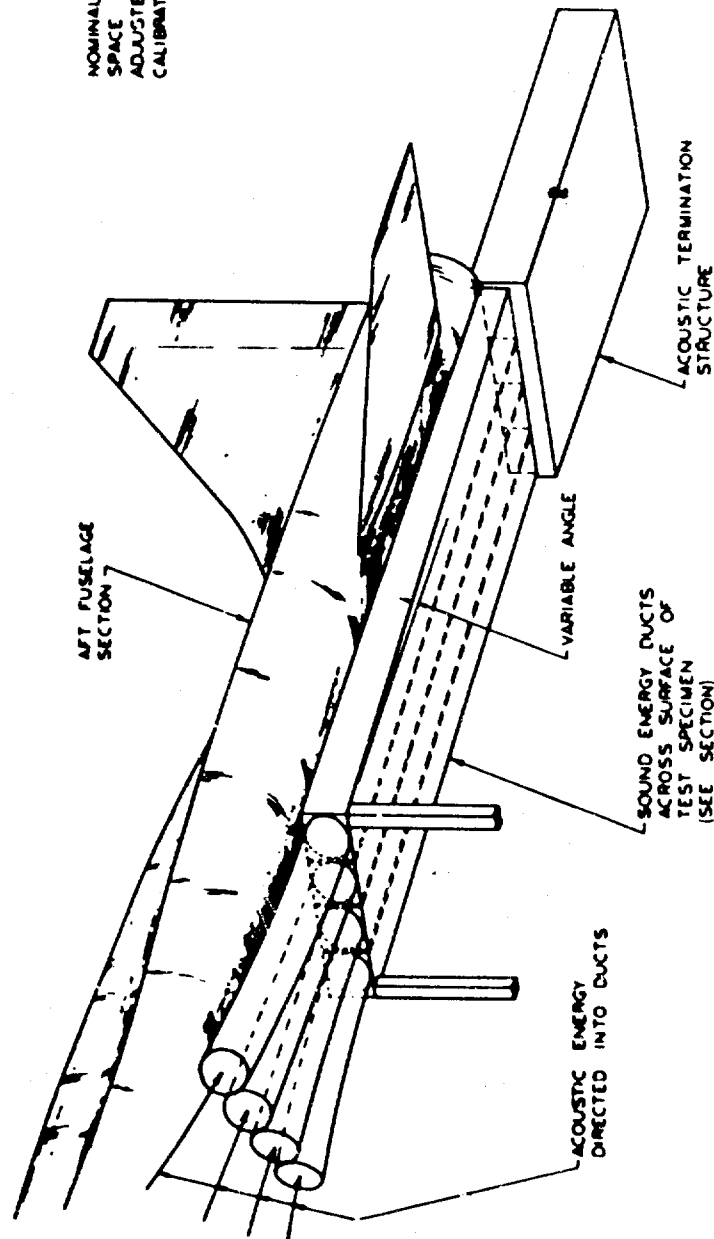


FIGURE 18 T-38A SPEED BRAKE MEASUREMENTS



(1) SECTION THROUGH  
SOUND ENERGY DUCTS



(2) BASIC TEST ARRANGEMENT

FIGURE 19 LARGE SCALE TURBULENCE

It may be desirable to compare the simulation of turbulence described with the alternative of producing the forcing function naturally by directing the appropriate air flow over the test specimen.

#### Discussion

Figure 20 illustrates the interruption of streamline air flow by an extended surface such as the speed brakes of an aircraft. Immediately aft of the speed brake is a region of turbulent air which travels with the vehicle. The shear between this dead air region and the free stream results in the generation of intense turbulent mixing. The width of this mixing region, and hence the typical size or scale of the individual eddies, increases approximately with distance aft of the projection.

For a detached or wake turbulent mixing flow, the eddies are convected past the aircraft surface at a mean velocity of approximately 0.5 times the free stream velocity. This convection velocity is less than the velocity for eddies in attached flow which is approximately 0.8 of the free stream velocity.

In each case, the intensity of the pressure fluctuations seen at any point on the aircraft surface are approximately equal to the fluctuating dynamic pressures of the turbulent eddies. Since the fluctuating turbulent velocities are much lower than the convection velocities, the rate of change of the pressures, when viewed by an observer moving with the mean velocity of the turbulent flow, is much less than the rate of change of pressure viewed by an observer fixed on the aircraft surface. Consequently, the pressure fluctuations observed at a point on the surface result from the variation of pressure with distance as measured in a co-ordinate system moving at the mean convection velocity. Hence, a typical frequency of the turbulent flow measured on the surface is given by the convection velocity divided by the typical scale of turbulence.

Since the eddies being formed are random in size, random sized areas of the aircraft surface tend to be dimpled in while the areas between the dimples tend to pop out. As the eddies and dimples they cause move aft, a rippling motion occurs in the surface. This effect on the surface is shown in Figure 21A.

Another separate deflection pattern may exist simultaneously in the surface due to the transmission of shock waves through the skin. As the initial upstream turbulence strikes the surface, the shock is propagated through wave action in the material at the preferred velocity for the material and its configuration. The preferred velocity differs for each frequency of the forcing function which initiates the shock.

The term "correlated area" is used to describe the area of a dimple in the surface. Since the eddies are nearly spherical, the area of the surface being dimpled is essentially circular, that is, the length and width of a dimple are correlated and are a function of the size of the balls of turbulence.

Test results show that the rms pressures decrease only slightly toward the aft end (on the order of 3 to 4 db in 10 to 15 feet), which is to be expected from the slight divergence of the zone of turbulent air.

In using acoustic energy to simulate the turbulent forcing function, three variables must be controlled. These are (1) the velocity and direction of propagation, (2) the frequency spectrum, and (3) the sizes of the correlated areas.

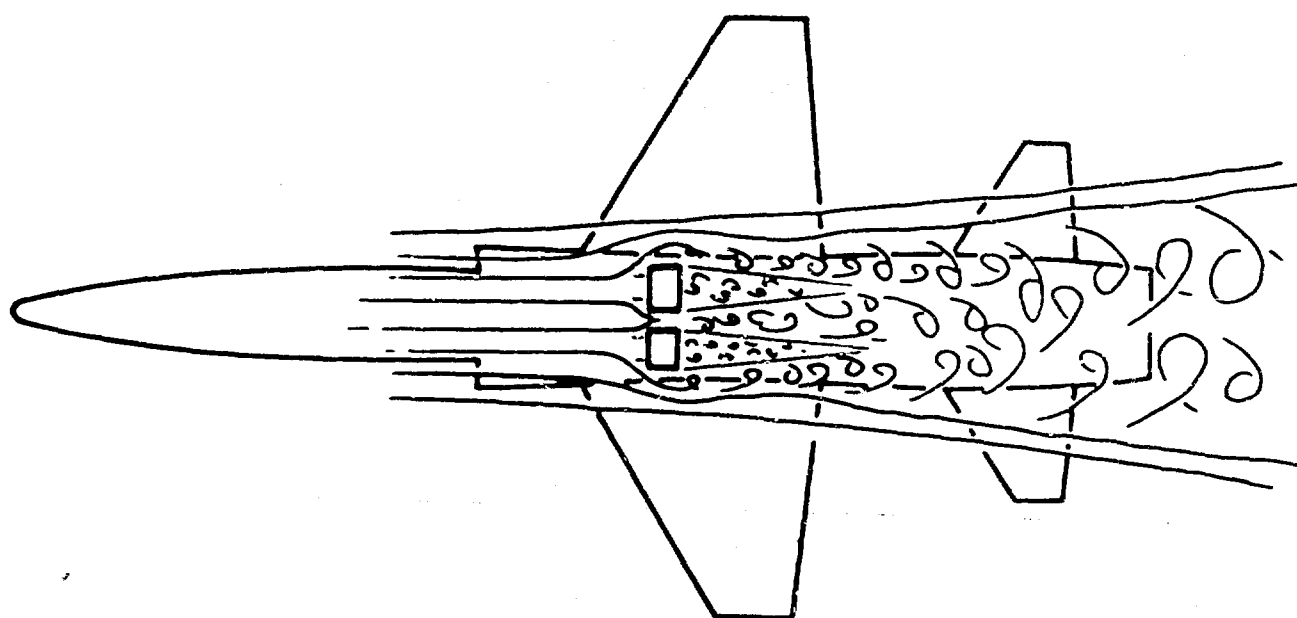
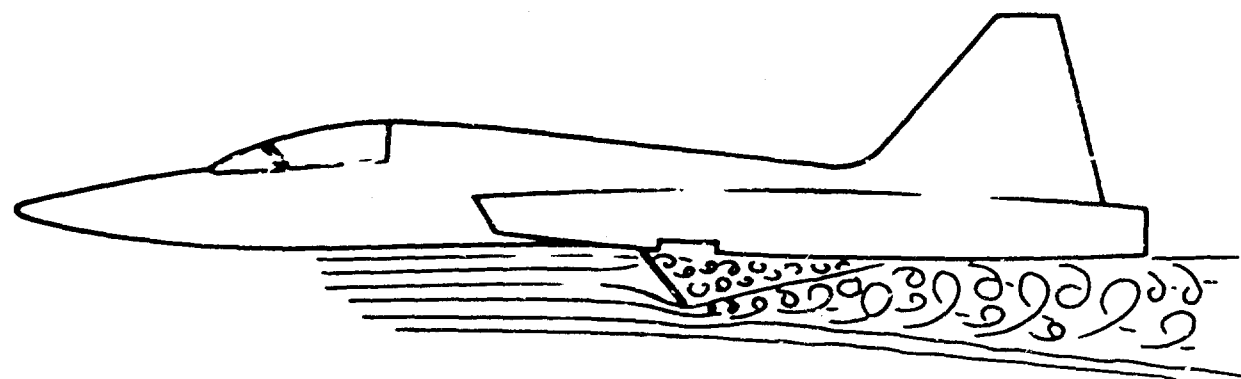
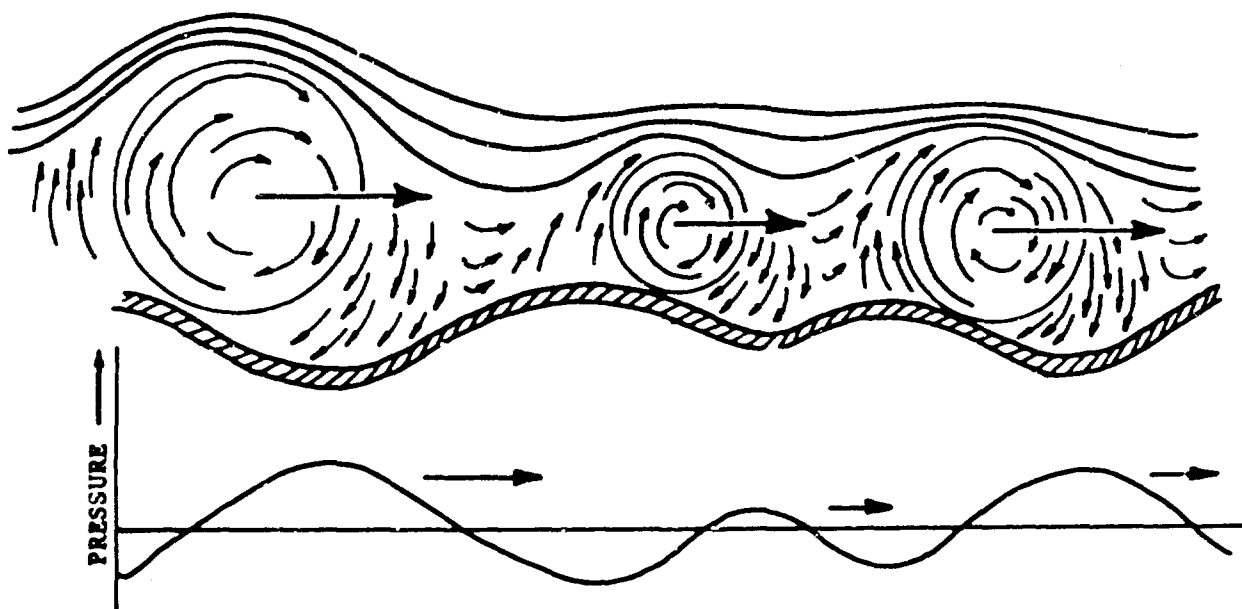
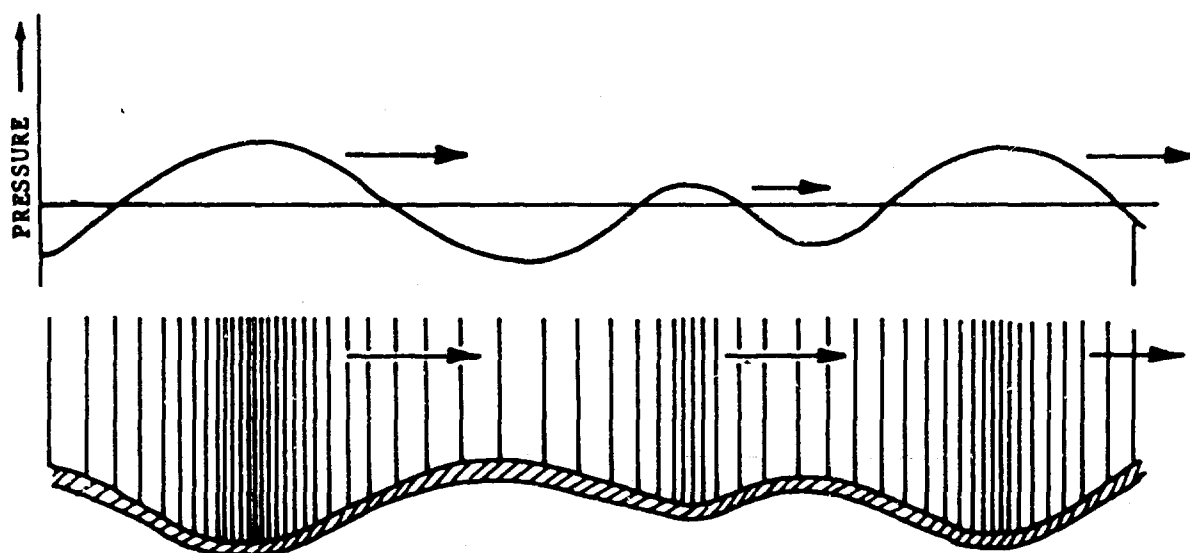


FIGURE 20    TURBULENCE BEHIND THE DIVE BRAKES OF  
AN AIRCRAFT IN FLIGHT



(a) INSTANTANEOUS DEFLECTION OF A SURFACE  
CAUSED BY RANDOM-SIZED, CONVECTED BALLS  
OF TURBULENCE



(b) INSTANTANEOUS DEFLECTION OF A SURFACE  
CAUSED BY RANDOM FREQUENCY PROGRESSIVE  
WAVE ACOUSTIC ENERGY

FIGURE 21 COMPARISON OF (a) TURBULENCE AND (b)  
ACOUSTIC FORCING FUNCTIONS

The test arrangement is shown in Figure 19(1) in which acoustic energy is released as a random frequency progressive wave across the section of fuselage aft of the speed brakes.

The direction of propagation is obtained by releasing the progressive wave in the aft direction from the location of the speed brakes. The velocity of propagation of the acoustic energy is the velocity of sound in air. This simulates the velocity of the turbulent flow over the surface at the speed of sound in air (approximately Mach 1.3) which is associated with a somewhat higher airspeed of the aircraft, (approximately Mach 2). To simulate turbulence at other than this one air speed, refinements to the basic test arrangement are required.

Two methods are suggested for increasing the velocity of propagation. As shown in Figure 22, it may be possible to direct the sound energy at an angle to the surface, so that the effective velocity over the surface is greater than the actual velocity of propagation in air. Problems with reflection from the surface and difficulties in providing the sound energy from an angle over large areas may offset the advantages of this method, particularly at the high incidence angles required to obtain significant increases in the velocity.

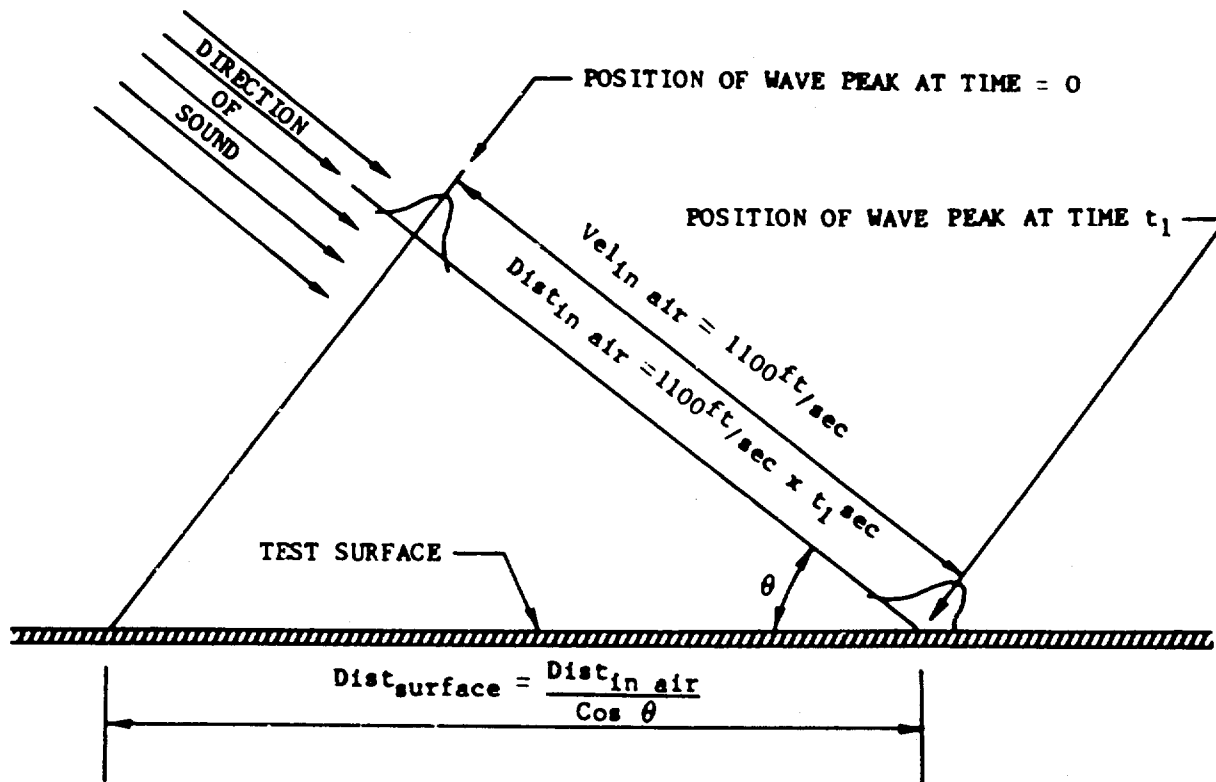
Another possible method involves using the basic test arrangement illustrated in Figure 19(1), but filling the ducts with a medium in which the velocity of sound propagation is greater than air. For example, the velocity of sound in hydrogen gas at normal pressure is almost four times the velocity of sound in air. However, a diaphragm capable of transmitting the acoustic energy would be required to contain the medium and prevent its displacement by the air flow from the sirens. Also, the SPL transmitted through the medium depends on its characteristic impedance which is lower for hydrogen than for air.

The frequency spectrum of the turbulent forcing function is obtained by programming the sirens as the source of acoustic energy to give random frequency sound over the required range. With several wide band sound sources available, one can be directed into each duct across the specimen. If discrete frequency sirens are available, or with relatively narrow band width available by modulation, it becomes necessary to duct the sound energy from several sirens into each duct across the specimen in order to obtain the necessary spectrum band width.

In either case, the spectrum will remain reasonably accurate as the sound energy moves downstream in the ducts because the high frequency portion of the spectrum will be attenuated more than the low frequency portion. As previously noted, the turbulent forcing function contains less high frequency energy as it progresses downstream.

When using the basic test arrangement, as shown in Figure 19, it will be necessary to determine the attenuation as the sound progresses down the duct. The cross sectional area of the duct can then be varied, perhaps made slightly convergent, as shown in Figure 19(1), to limit the attenuation.

The size of the correlated areas, i.e., the dimensions of the balls of turbulence, cannot be simulated precisely, but approximations are possible. By programming the frequency spectrum of the acoustic energy, the forcing function and its effect on the surface can be obtained as illustrated in Figures 21A and 21B, for the longitudinal direction. In the transverse direction, the width of the correlated area is established by the width of the duct. Since the widths of the eddies approximate their length, the same randomness in width is present under turbulent loading conditions. The best approximation of the random width is obtained by selecting an average width for the ducts, based on the average wave length of the forcing function, i.e., the average diameter of the balls of turbulence.



$$\text{Vel}_{\text{surface}} = \frac{\text{Dist}_{\text{surf}}}{t_1 \text{ sec}} = \frac{1100\text{ft/sec} \times t_1 \text{ sec}}{\cos \theta \times t_1 \text{ sec}} = \frac{\text{Vel}_{\text{in air}}}{\cos \theta}$$

**NOTE:** VELOCITY OF SOUND OVER THE SURFACE IS INVERSELY PROPORTIONAL TO THE COSINE OF THE INCIDENCE ANGLE.

INCIDENCE ANGLE $\theta$	RATIO: $\frac{\text{VELOCITY OVER SURFACE}}{\text{VELOCITY IN AIR}}$
$0^\circ$	1.0
$15^\circ$	1.03
$30^\circ$	1.15
$45^\circ$	1.41
$60^\circ$	2.00
$75^\circ$	3.90

FIGURE 22: INCREASING SOUND PROPAGATION VELOCITY OVER A SURFACE BY VARYING ANGLE OF INCIDENCE

The complete test arrangement is shown in Figure 19. The test requirements will determine the sound pressure level along the ducts and also the method of directing the energy into the ducts. The number of ducts along the specimen will depend on the required simulation, but for clarity only four ducts or channels are shown. The duct size will be determined analytically and may be modified after several calibration runs. The duct material should consist of aluminum plating or harborite plywood properly coated with the visco-elastic material as shown in Figure 19(2).

The gap between the ducts and the specimen will be determined during calibration runs and be consistent with the panel response amplitude of the specimen. The acoustic energy should be dissipated into a termination structure. A typical termination structure would consist of heavy wall construction material and filled with open cell polyurethane or an equivalent sound damping material. The termination is attached to the ducts with sufficient attachment fittings and properly sealed with neoprene gaskets. The vertical supports for the ducts and the termination structure will depend on the siren locations above the floor level. The structure must be adequate to support the ducts and termination structure as well as the specimen if the test setup warrants such a support. Individual supports may be constructed for the specimen depending on the configuration and size.

## SYSTEM VIBRATION TEST

### Background

This type of test can be more aptly called a "soak" test. The vibrational environment that any vehicle undergoes during its lifetime will, at most, require some nuisance repair and may actually produce malfunction damage. Therefore, it is necessary in any new aerospace vehicle or aircraft to proof test to provide the necessary background to prevent the so-called nuisance failures before production commences.

### Problem Definition

The significance of vibration induced damage has been shown to be a large part of the maintenance cost and "down-time" burden.<sup>18</sup> Grouping of this damage, of a secondary nature, can be shown to fall into three categories; namely, electrical and electronics, mechanical and engine. Approximately 180 such failures occurred during the testing of one aircraft sonically.<sup>13</sup> Electronic and electrical equipment malfunctions include such items as wire bundles, supporting brackets, terminal strips, broken clips and leads. Mechanical items requiring repair are clips and brackets for hydraulic and pneumatic lines, and broken lines at fittings. Fatigue failures also occurred in pneumatic line insulation, mounting flanges, gear doors, cables and pulleys. Engine vibration failures occur mainly at clips, fuel lines, pumps, fire detection systems, insulation blankets, and various small valves. This list does not include the sundry loose screws, bolts, and rivets that always accompany such a test.

Although the basis for producing these vibration failures is usually on an accelerated test basis, they nevertheless brought out the criteria necessary to prevent their reoccurrences in a later vehicle production stage.

### Simulation

Figure 23 and the accompanying writeup present a means of accelerated vibration testing. It must be remembered that all systems should be loaded and, if possible, in actual operating condition. These systems can then be monitored to record their proper working order and any malfunction detected and recorded.



- (3) EXAMPLES OF TYPICAL SYSTEMS TO BE TESTED IN A REVERBERANT ENVIRONMENT
1. STRUCTURAL
    - (A) EXTERNAL SUBSTRUCTURE
    - (B) PRIMARY SUBSTRUCTURE
    - (C) SECONDARY SUBSTRUCTURE
  2. MECHANICAL
    - (A) MECHANICAL COMPONENTS
    - (B) SUPPORTS
  3. HYDRAULIC, PNEUMATIC, FUEL
    - (A) MAJOR COMPONENTS
    - (B) PIPING & FITTINGS
    - (C) BRACKETS
  4. ELECTRICAL, ELECTRONIC
    - (A) MAJOR COMPONENTS
    - (B) WIRING BUNDLES & CIRCUITRY
    - (C) TERMINATIONS
    - (D) SUPPORT BRACKETS

NOTES:

1. THE COMBINED LOADS IN THIS QUALIFICATION ARE A GENERAL ACOUSTIC LOAD AND OPERATIONAL LOADS PECULIAR TO EACH SYSTEM.
2. COMPLETE VEHICLE TO BE PLACED IN A REVERBERANT SOUND FIELD IN THE LARGE TEST CHAMBER.
3. VEHICLE SYSTEMS TO BE OPERATED USING AUXILIARY POWER SUPPLIES WITH LOADS ON EACH SYSTEM.
4. ACOUSTIC ENERGY TO PROVIDE BROAD BAND RANDOM EXCITATION INCLUDING THE HIGHER FREQUENCIES.
5. VEHICLE SURFACES SUBJECT TO LOWER SPL IN SERVICE TO BE COVERED WITH ACOUSTIC BLANKETING.

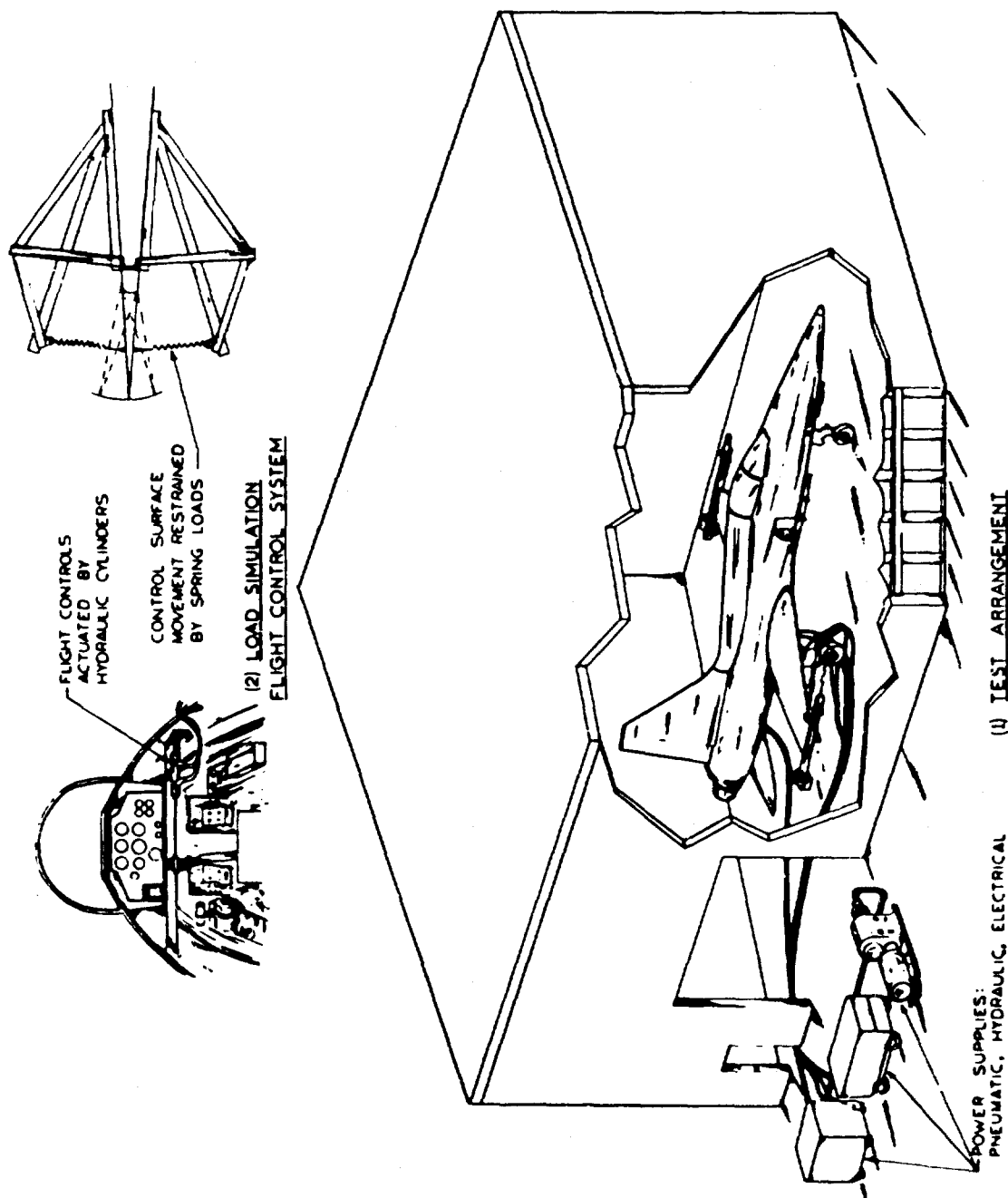


FIGURE 23 VEHICLE SYSTEMS VIBRATION TEST IN A REVERBERANT SOUND FIELD

## Case History

### Description

This case features a means of qualifying a complete vehicle with special emphasis on the installed operational systems of the vehicle. The loading consists of broad band random frequency reverberant acoustic excitation in combination with the operational loads peculiar to each operational system. The vehicle is placed in the reverberant sound field of the large RTD acoustic chamber while vehicle systems are operated using auxiliary power supplies with loads imposed on each system.

### Discussion

During its service life, a vehicle may be exposed to acoustic excitation from two major sources. The first of these is the noise from the power plant and the second is the pseudo-noise resulting from aerodynamic turbulence. The characteristics of this acoustic excitation vary widely during operation of the vehicle. The engine noise is normally most severe during ground operation while the pseudo-noise caused by turbulence becomes more severe as speed increases. When the total service life environment is considered, the acoustic loading from both engine noise and turbulence exhibits broad band random frequency spectra, hence producing variable sound pressure levels up to the maximum conditions, with variable directivity and distribution patterns of the acoustic energy over the vehicle.

Typical functions performed by systems in a flight vehicle include flight control, propulsion, communication, navigation, life support, instrumentation, and many more. These systems, classified by the functions they perform, utilize several methods of operation, i.e., electrical power, hydraulic pressure, mechanical linkages, etc.

The loads on the vehicle's systems can readily be defined by consideration of the power used in the method of operation. The vehicle's systems can then be considered in terms of operational classifications to include structural systems, mechanical systems, hydraulic, pneumatic, and fuel systems, and electrical and electronic systems.

The test arrangement is shown in Figure 23 (1). The complete vehicle, with its operational systems installed, is placed in the large scale acoustic chamber.

It is presumed that major components have previously been qualified with regard to design requirements including vibration, acoustic and operational loads. The purpose of the test shown in this case is to qualify the total installation. While relatively few failures are to be expected in the previously qualified components, the majority of failures are expected in methods of attachment, electrical terminations, joints in fluid pressure lines and other secondary equipment items which are not normally incorporated into component testing. The dynamic response of these items depends on the complex relative motions of supports and is influenced by the manner in which they are installed.

To cover the wide range of variables in the acoustic loading during the vehicle's service life, the load imposed during test is an acoustic "soak" using the main low frequency bank of sirens and portable high frequency sirens. The sirens are programmed to provide broad band random excitation in a reverberant chamber.

The systems of the vehicle are in operational status with imposed loads representative of the service loads on each system. The source of power for most systems comes from the engine gear box. Since it is not desirable to operate the engine within the facility, auxiliary power sources can be used.

Figure 23(2) illustrates a means of operating a portion of the flight control system using a hydraulic cylinder to move the control stick. The load is applied by a spring arrangement which restrains the motion of a control surface. Stresses are thereby caused in the mechanical linkages between the control stick and the control surface while hydraulic or electrical systems involved in moving the control surface are subjected to their operational loads. Similar loadings are applied to other systems by appropriate means.

All jig fixtures and supports should be as simple as possible in order to prevent change in panel responses. Dummy stores on the pylons and wing tips can be readily utilized depending on test requirements. Appropriate safety circuits and indicator lights can be installed to denote failures or malfunction in particular critical systems. Restraint of the aircraft should be accomplished by chocks at the landing gears.

## COMPONENT TEST

### Background

Any vehicle which will be subjected to a combined loads environment will encounter, during some time in its life, periods of severe acoustic environment in particular structural locations. These parts are in many cases the control surfaces of aircraft, highly stressed components which could fail causing vehicle destruction. Any component of this type which will in service encounter an acoustic environment is usually tested in a siren or jet noise facility and a final "beefed up" configuration chosen. Many times the selected configuration will subsequently fail in service. It is then proof tested on the vehicle until a fail safe design is approved. In many cases this involves a very costly testing program with accompanying delays in vehicle delivery. The best possible solution to this testing problem is the application of as many service loads as possible. In many cases this will require acoustic, dynamic, static and heat simulation on one test article. Many times actual service failures cannot be duplicated in a simulated test environment. The reason for this lack of correlation can usually be traced to unwittingly omitting one of the many influencing stress parameters which occurred during service operation in the component test program. This will lead to erroneous evidence resulting in structurally weak designs and additional testing requirements.

The proposed test arrangement described in the following is an attempt to reproduce these combined loads on small test articles and obtain a more realistic representation of the actual in-service conditions.

### Case History

#### Description

A test fixture is proposed as shown in Figure 24 to permit full scale testing of components under combinations of loadings. It can be used for proof testing of components to determine if the required resistance to the design environment has been achieved. However, the fixture may be of greater value for experimental research into the fatigue relationships existing when acoustic loading is combined with other forcing functions, and for the empirical development of design parameters where the design must be based on a combination of loads.

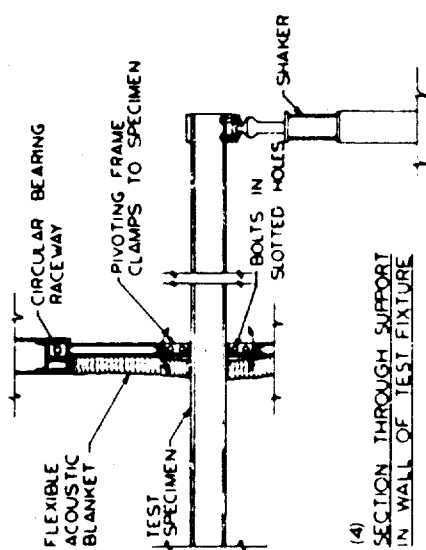
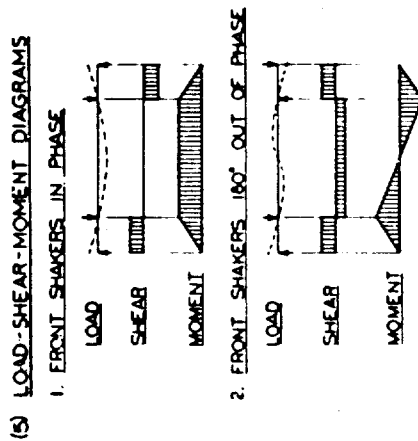
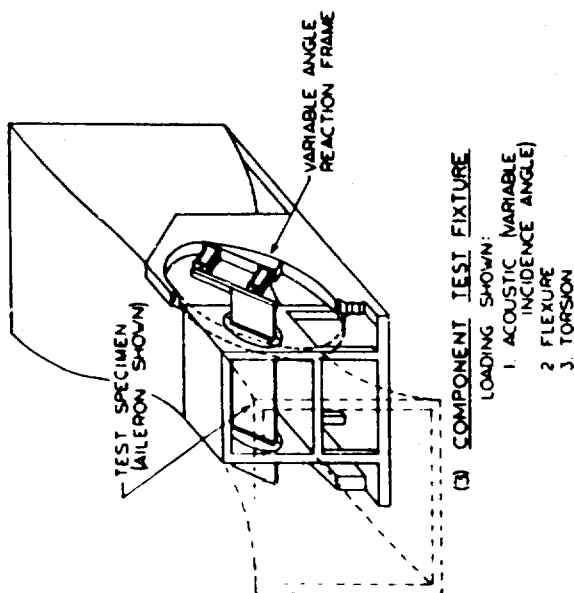
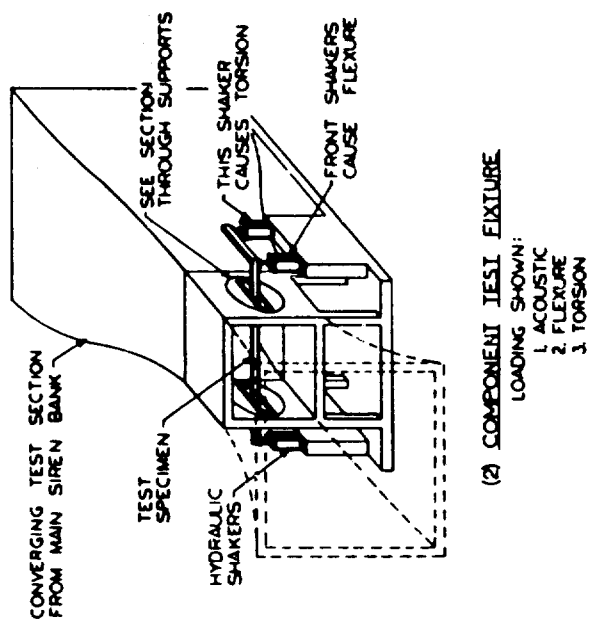
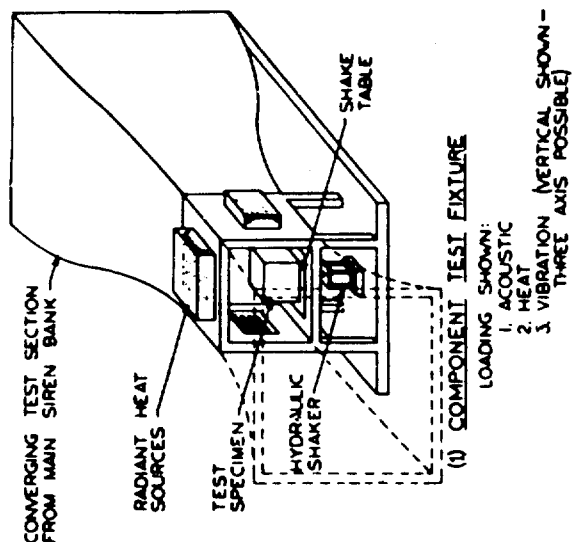


FIGURE 24 COMPONENT TEST

A variety of specimens can be tested, including structural sections, structural assemblies such as skin panels, doors, etc., mechanical components such as pumps, valves, hinges, actuators, etc., and avionic "black box" electronic packages.

The following loads can be simulated:

- Acoustic; High SPL, random or discrete frequency normal, grazing or variable incidence, progressive wave or reverberant environment.
- Static or rapidly cycled static loadings can be simulated to produce flexure, torsion and shear in structural specimens.
- Dynamic loadings are simulated by applying vibration and shock to the specimen.
- Heating of the specimen during dynamic conditions can also be provided.
- Within the limits of the RTD acoustic facility, certain environmental conditions such as humidity, salt spray, etc., can be provided.

#### Discussion

The component test fixture is shown installed in the RTD facility in Figure 24.

A converging test section is shown leading from the main bank of sirens which permits increased sound pressure levels at the lower frequencies by concentrating the sound energy over a smaller area. Although not shown, it would be possible to adapt the test section to introduce sound energy from the high frequency bank of sirens to increase the available frequency range, although the limitations due to finite amplitude distortion would limit the availability of high frequency sound energy in the smaller test section.

Either discrete or random frequency sound energy can be provided by selection and programming of the sirens used. The orientation of the test specimens permits variation of the angle of incidence from grazing to normal or at any angle in between. The orientation of the specimen is permitted by the circular bearing raceway within which the specimen is clamped, as shown in the section through support in wall of test fixtures, Figure 24(4).

With the end of the test chamber open as shown, the specimen is subjected to a progressive wave. A reverberant environment can be created by closing the end of the chamber with an irregular reflective surface and providing slotted openings to relieve air pressure from the sirens.

As shown in Figure 24(1), a specimen can be subjected to vibration by mounting it on a shake table in the bottom of the chamber. For simplicity, only one hydraulic shaker is illustrated, producing vertical vibration. By the addition of two shakers in the horizontal plane, three axis vibration can be provided.

Test specimens to be subjected to flexure, torsion or shear are mounted in supports in the side walls of the test fixture, as shown in Figure 24(3). The specimen is clamped between two channels as shown in the detail of the support. Bolts

attaching the channels to the end supports ride in slotted holes to provide for clamping specimens of varying thickness. The space between the clamping channels which is not occupied by the specimen must be blocked off. The entire frame in which the specimen is clamped is mounted on pins which permit the slope of the specimen to change as it is flexed by the action of the hydraulic shakers. The pins should be designed to take all the shear loads.

The specimen is subjected to torsion by the action of the rear shaker. The rear support in the wall of the fixture is allowed to rotate since the support is mounted in a circular bearing raceway, while the far support is locked to prevent this rotation.

Load, shear, and moment diagrams for a specimen subjected to flexure are shown in Figure 24(5) for two conditions, one with the flexure shakers operating in phase, and two with these shakers moving the specimen in opposite directions. These shakers could also be programmed to provide a random pattern of shear and moment.

The specimen can be subjected to thermal gradients simultaneously with the other loadings by mounting radiant heat sources such as quartz lamps on the test fixture as shown in Figure 24(1). In addition to an opening provided in the top of the fixture, the openings in the side walls and shaker table bottom can be adapted to a heat source when they are not used as supports for the specimen.

Because of the high acoustic loading present, the test equipment mounted around the test chamber must be enclosed and adequately protected from the acoustic environment.

Substantial reactions will result from the action of the hydraulic cylinders, or vibration shakers. It is desirable that the supports for the cylinders be both massive with high inertia and be capable of spreading the reactions from the cylinder over the floor area and to the columns supporting the floor. A continuous support under the entire test fixture serves these requirements, and has the added advantage of permitting the entire fixture to be moved in and out of the large test chamber as a unit with a minimum of set-up time.

The converging test section horn can be fabricated from aluminum plate or harbo-rite (veneer plywood). For either material the total outside surface should be coated with a damping visco-elastic material such as Neoprene cork or Chenolic cotton. The bolted connection between the horn and test specimen fixture should be properly designed and sealed with Neoprene rubber or an equivalent gasket.

The test fixture shall be designed to withstand the imposed loading conditions plus the high acoustic energy. Magnesium should be utilized where possible to reduce the weight. Continuous welds shall be employed at all critical joints on materials such as steel or magnesium. Bolted connections must be properly designed with sufficient edge distances to eliminate premature failures at these points. In all cases, vital accessories such as loading cylinders, radiant heat banks, hydraulic shakers, hoses and electrical conduits should be protected against the acoustic energy by visco-elastic coatings, acoustic shielding curtains or solid panel walls, etc.

Two hydraulic cylinders can be actuated simultaneously to cycle the bending load on the specimen. The cylinders should be programmed through a load programmer and controlled by a hydraulic pressure control servovalve (such as a Morg valve). The system cycling rate could then be varied from approximately 2 to 150 cps depending on the load magnitude and specimen deflections. For vibratory loads and a random sweep phase, hydraulic or electro-dynamic shaker units can be interchanged on the test fixture - the setup would depend on the load spectra and test specifications.

The test fixtures, cylinders and shakers shall be properly reacted into the floor beams or a suitable A-frame reaction jig constructed to route the loads into the floor beams. Specimen deflections, actuator stroke, clearances, proper load magnitudes, safety devices and other miscellaneous requirements can be determined by previous calibrations and calculations. Trial runs should be initiated prior to operating the acoustic portion of the test setup.

Stress-strain data shall be acquired by properly located strain gages (axial, shear, and rosettes) and failures can be normally determined by the installation of crack detection wire (one or two mils thick). The radiant heat source should be quartz lamps installed in proper holders with a reflective shield to suit the particular test setup. The testing requirements will determine the number of lamp banks required and their location in respect to the specimen. The lamp holding fixtures should be adequately designed to withstand the acoustic environment and also the vibration inputs. The outside surfaces of the holders should be coated or covered with an acoustic damping material. Failures of the quartz lamps should present no problems as they are easily replaced with spares during inspection periods.

#### ALTERNATE TEST METHODS AND COMMENTS ON TEST PROCEDURES

Throughout the text, various test setups have been described and elaborated on with no considerations for alternate methods. New test techniques and highly accurate electronic equipment are constantly changing the test methods in order to maintain the state of the art. If the discussed test methods do not appear feasible or suitable for a particular test specimen configuration, new ideas and designs can be incorporated as well as standby setups such as a centrifuge or sled. A complete acceleration sled (approximately 45 feet long) could be installed in the acoustic chamber and short duration runs at high accelerations on special equipment could be accomplished. Because of the short time duration during acceleration and deceleration, the test requirements would have to justify this particular test method.

Various centrifuge designs have been established for testing components and large scale specimens and this method should be given some thought during test setup studies. Small centrifuge tables, specimens and cages suspended on revolving counter-balanced arms, and housed specimens riding on a circular track are several of the test configurations available for the RTD facility. All methods are rather costly and extensive to set up but could meet the requirements of certain test specifications. Northrop Norair Report No. NOR-60-291, (AF Contract 33(616)-6679) describes a typical centrifuge facility which could be modified to suit the particular needs at RTD. The counter-balanced revolving arm is perhaps the simplest method for producing the various dynamic and inertia loads on a specimen at constant acceleration, but the design would have to eliminate a failure which would tend to damage the RTD acoustic chamber or sirens. Hydraulic and electrical power requirements are easily adapted to the centrifuge by means of swivel joints and slip rings. Electric shakers can also be attached to the arm as well as a radiant heat source. The specimen can be rotated without too much difficulty to produce g-loads and accelerations along the various axes.

Large capacity fatigue test machines could be installed in the acoustic chamber with a four or five foot long specimen. Either full scale coupons or sample coupons can be programmed into the test machines and an automatic random fatigue spectrum setup on electronic controllers. Here again the test machine and automatic programmers would have to be protected from the sonic environment.

All cables used as tension linkage should be as short as possible and double clamped to insure the safety of personnel and specimen. All cables shall be pre-stretched prior to installation.

All loading applicators, cable, whiffletrees, pressure bags, pressure supports, rotary weights, etc., shall be designed to withstand the design loads coupled with a safety factor to compensate for fatigue within the sonic environment. Major supports and A-frames should be self-contained or reacted into the facility floor beams.

Minor failures of the pressure cell diaphragms will probably occur. (See section IV, page 48. Spare items should be available and the design such that the replacement will not delay test runs for long periods of time.

Prior to running any tests, all test loads applied must first be calibrated with the specimen intact or with a dummy setup. In the case of a programmed fatigue or static load this calibration will enable the loads to be programmed accurately with considerations for specimen deflections. Where possible, all loads should be applied simultaneously or as programmed according to the test plan.

All extraneous equipment and accessories not pertinent to the specimen should be located outside the chamber or protected inside the chamber by acoustic blankets in order to prevent failures of these items.

Electronic load programmers are available that will automatically apply the test loads in the proper sequence and also within close accuracy (1% to 3%). These programmers should be located outside the facility and shall be equipped with their own power supplies. All electrical lines shall be properly shielded and grounded to eliminate drift and inaccuracies. Servo valves and load transducers shall be as close to the loading actuators as practicable. The load reading link (or transducer) should be close to the specimen load point in order to compensate for deflections and load linkage discrepancies. The load links may be removed after calibration but it would be best to have the links in the system at all times in order to recalibrate with a minimum of changes.

Strain gages should be installed at all critical locations and recorded strains can be programmed into an oscillograph or on magnetic tape. Crack detection wire (ex., Formvar Annealed Copper Wire, 1 and 2 mils in diameter) should be installed as required. The wire is easily cemented to the specimen surface by Duco cement or its equivalent. The lead wires should be routed into a failure detection panel with an appropriate scanning mechanism to scan all circuits about every 60 seconds.

For ordinary service, 3000 to 5000 psi hydraulic flow benches will be sufficient with flows up to 30 gallons per minute. Special hydraulic supplies and servo valves will be required for the electro-hydraulic shakers. The specimens should have special safety circuits installed in order to dump the hydraulic pressure in case of a malfunction or excessive specimen deflections. Normally, micro-switch arms suspended at the correct locations (obtained during specimen calibrations) around the specimen will quickly dump the hydraulic fluid in case of a malfunction. Various other safety devices can also be incorporated as required.

Induction heating methods can be employed to provide localized high magnitude thermal environment. Induction heating installations are costly and the design of the coils around or about the specimen are rather extensive. Coils must be located close to the specimen surface and generally would interfere with the acoustic energy penetration and the specimen deflections. Where possible, the induction heating system should be utilized during test programs on components or sub-assemblies. The quartz lamp method is perhaps the best heating method available and should be utilized whenever possible.



## V CONCLUSIONS

The interactions between static and dynamic loads have not been considered previously as a major element in design and analysis. The initial studies in fatigue, probability of failure, and combined loads presented here show this is a fallacious approach. Adequate substantiation through failure cases and presentation of new data in fatigue and probability of failure show the importance of combined loads when static loads are accompanied by the dynamic and/or high intensity acoustic loads.

The different structural metals act differently under random loading. The fatigue performance of these materials is less than standard practice in structural analysis admits. There is great variability in the performance of different materials, by a factor of 2:1 between steel and aluminum, for example. Further variability is brought about by the different fatigue techniques, some of which are quite inappropriate for high dynamic and acoustic loads.

The mission load history and load sequencing alter the fatigue damage significantly and have led to the conclusion that particular combinations of loads occurring in the early life must be so simulated. Other combinations occurring in sequence during later stages of the life must be simulated in their order of occurrence. A very large positive or negative load alters the cumulative damage fraction over the range from less than 1.0 to approximately 7 as a result of residual stresses induced by the high loads.

A theory of acoustic fatigue by Dr. S. R. Valluri forms a part of this study (RTD-TDR-63-4021, Supplement 1). The theory is based on crack growth and loss in residual strength which it implies. The influence of design mean stress on time to failure is considerable, decreasing the effective crack length and increasing the probability of failure. Reductions in strength which follow from fatigue damage are more significant than reductions in stiffness in the material. The engineering theory presented proposes an important solution to the nucleation problem explaining the mechanism, exposing the influencing parameters, and providing an estimate of the cycles involved. A further substantiation from recent data is presented for the Griffith-Irwin theory. A column analogy has been drawn.

Seven combined loads cases are presented to show appropriate means of simulation in the RTD sonic test facility. New and unique test arrangements are shown and described in detail for each case. Other failures due to combined loading are presented in detail to further substantiate the importance of the problem.

The many various types of dynamic, acoustic, and aerodynamic loads may not presently receive satisfactory emphasis in design and analysis which places a much higher requirement on test accuracy.

Important new developments in fatigue theory are presented and the conclusion drawn that fatigue lies at the heart of these dynamic qualifications. While the present requirements are for test solutions to the overall problem, many important aspects of the engineering theory of fatigue must be solved in order to arrive at engineering methods that allow analytical solutions. Fatigue damage due to random loading is one of the reasons for the existence of combined load failures.

One of the major connotations of the investigations is the potential use of the reliability approach to structural design as opposed to the present arbitrary design

criteria route. Since the loads and the material performance are probabilistic events, a parameter of value would be the probability of failure at several key points throughout the vehicle in order to provide a fundamental new look at the structural performance. Radical progress in engineering design and mission capability has outrun the arbitrary design criteria developed partially on a cut-and-try basis, including vibration contributions from each of a series of vehicles in an evolutionary chain. The analytical development presented here regarding fatigue, if substantiated by further study, also militates against the old approach.

## VI RECOMMENDATIONS

Of the many combined loads cases presented in this contract; primary structural qualification would be the testing arrangement most desirable as an initial effort in the RTD sonic facility. It describes a unique solution to an age-old problem of reliability testing, yet should be relatively inexpensive to set up and maintain.

Investigation should also be made into the possible extension to the existing facility for handling cryogenic fuels and high temperature equipment. These will be highly desirable during the present state of the art for the production of space temperature differentials which play such an important role in accelerating the fatigue process of high strength materials.

Incorporation of some means of obtaining high acceleration loads would also increase the capability of accurate load simulation.

During the course of some vehicle reliability testing it may become mandatory to operate the propulsion plant as the only solution for production of some loadings. It would therefore be highly desirable if some means of directing or exhausting the waste products from the test chamber were incorporated into the overall facility.

Many of the aerodynamic and static loads can be faithfully reproduced by large air flow and/or suction. Provision should be made to have such a system available for the simulation of these phenomena.

## REFERENCES

1. Jordon, G. H., and McLeod, N. J., Structural Dynamic Experiences of the X-15 Airplane, NASA TN-D-1158, March 1962.
2. Lansing, W., Mueller, W. H., Malakoff, J. L., and Mantus, M., Dynamic Loads During Nose Tow Catapulting, ASME Paper Nr. 60-AV-49, June 1960.
3. Barton, M. V. and NASA Research Advisory Committee on Missile and Space Vehicle Structures, Important Research Problems in Missile and Spacecraft Structural Dynamics, NASA TN-D-1296, 1961.
4. Freudenthal, A. M. and Heller, R. A., On Stress Interaction in Fatigue and a Cumulative Damage Rule, Journal of the Aerospace Sciences, July 1959.
5. Valluri, S. R., A Unified Engineering Theory of High Stress Level Fatigue, Guggenheim Aeronautical Laboratory, California Institute of Technology, April 1961.
6. Schijve, J., The Estimation of the Fatigue Performance of Aircraft Structures, NLR Report MP-212, National Aeronautical Research Institute, Amsterdam, June 1962.
7. Christensen, R. H. and Denke, P. H., Crack Strength and Crack Propagation Characteristics of High Strength Metals, ASD-TR-61-207, January 1962.
8. Burbank and Strause, Heat Transfer to Surfaces and Protuberances in a Supersonic Turbulent Boundary Layer, NACA RML58E01a, July 1958.
9. Bouton, I., Structural Design Criteria from Statistical Flight Data, WADD-TR-60-497, March 1961.
10. Gray, C. L., Feasibility of Using Structural Models for Acoustic Fatigue Studies, ASD-TR-61-547, November 1961.
11. Schjelderup, H. C., and Gale, A. E., Aspects of the Response of Structures Subject to Sonic Fatigue, WADD-TR-61-187, July 1961.
12. Grabow, F. A., T-38 Sonic Fatigue Test Results and Sonic Fatigue Life Evaluation, NOR 60-308, Northrop Norair, Hawthorne, California.
13. Anderson, J. D. and Hillis, Jr., B. H., Ten Hour Maximum Afterburner Power Ground Sonic Fatigue Test of B58A, FZS-4-212, General Dynamics, Fort Worth, Texas, May 1960.
14. Nevius, H. E. and Hillis, Jr., B. H., Strain Measurements of Internal Wing Structure During Static Ground Engine Runs of B58A, FZS-4-224, General Dynamics, Fort Worth, Texas, December 1962.
15. Calvit, H. H., and Hillis, Jr. B. H., Ground Static External Surface Noise Measurements B58 Airplane No. 4, FZS-4-199, General Dynamics, Fort Worth Texas, August 1959.

16. Eldred, K., Roberts, W. H., and White, R., Structural Vibrations in Space Vehicles, ASD-TR-61-62, March 1962.
17. Blake, E. B., and Barrett, J. O., T-38 Sonic Environment Test Results, NOR-60-304, Northrop Norair, Hawthorne, California, February 1961.
18. Bingman, R. N., Resonant Fatigue Failures Associated with Noise, SAE Paper 164B, April 1960.

**APPENDIX A**

**LIMITING PHENOMENA FOR  
FATIGUE CRACK FAILURES**

## APPENDIX A

### LIMITING PHENOMENA FOR FATIGUE CRACK FAILURES

#### INTRODUCTION

A survey of the recent literature concerning fatigue crack theory leads to the belief that there is need for synthesis and clarification of the principle phenomena involved in order to eliminate areas of confusion, and to take proper advantage of applicable fundamental concepts.

It is proposed that the limiting phenomena of fatigue crack failure can be adequately defined in terms of the Griffith crack theory, the average net cross-section stress, and the elastic and plastic properties of the material. When viewed in terms of these simple concepts, many serious errors in assumptions can be prevented, the seeming direct dependence of critical crack length on specimen width can be reduced and areas requiring additional study can be more accurately determined.

#### GRIFFITH CRACK THEORY

Griffith proposed a theory of critical crack length for catastrophic propagation in an elastic material based upon experiments made with glass. Orowan proposed modifications to include materials having both elastic and plastic properties. Irwin and his associates have written extensively on brittle fracture based upon the modified Griffith Theory<sup>1</sup>. The modified form of the Griffith equation can be expressed as

$$l_c = \frac{2pE}{\pi\sigma^2} \quad (3)$$

where the term  $p$  includes both surface energy and the energy of plastic deformation,  $l_c$  is the critical crack length,  $\sigma$  the imposed stress level, and  $E$  the modulus of elasticity. If  $p$  can be determined, the crack length critical for catastrophic propagation can be computed for any stress level.

#### ELASTIC-PLASTIC CONSIDERATIONS

It is convenient to separate the Griffith equation into two parts  $\sigma^2/2E - p/\pi l_c$  where  $\sigma^2/2E$  represents the stored elastic energy and  $p/\pi l_c$  contains the elastic-plastic and dimensional material variables. The quantity  $\pi l_c$  was originally part of the energy term as derived by Griffith in his work dealing with glass whose critical crack length was in the order of  $10^{-3}$  cm. Placing the term  $l_c$  with the work term  $p$  indicates that  $p$  and  $l_c$  are both variables, being to some extent a function of the load history. In Griffith's original work the terms  $\pi l_c$  were obtained by relating the shape of an elliptical crack to previously published solutions for stress and strains around such a crack.<sup>1</sup> The strain energy resulting from cracking was thus expressed in terms of the crack length  $l_c$ , an entirely consistent approach to the problem for materials with crack lengths in the order of magnitude of those found in glass. However, for cracks of the length discussed here it is considered appropriate to place some weight on Saint-Venants principle thus assuming that the stress field at the end of a long crack is partially independent of the crack length. Actually the  $\pi$  term is of little significance for long cracks, but has been retained to utilize work of previous investigations.

The work term  $p$  has been shown indirectly by Yusuff<sup>2</sup> to vary with the processing for a given aluminum alloy. For example, 2024-T3 was found to have a  $p$  of 1330 in-lbs/in<sup>2</sup> as compared to 855 in-lbs/in<sup>2</sup> for 2024-T36. Reference (3) found "Subtle difference in fracture strengths of fatigue cracked metal panels as a function of the environment used to generate the crack". It can be assumed that modification of loading history will show some variance in the work factor  $p$ . Variance in the work factor  $p$  would result in a compensating variance of the critical crack length  $l_c$ . This assumption is possible if the stored energy can be assumed, at least partially, to be independent of the length  $l_c$ . While changes in critical crack length are obvious in the case of 2024-T3 and 2024-T36, it is not as obvious that changes in load history affecting  $p$  in a material such as 2024-T3 could also result in changes in critical crack lengths.

In essence, the critical energy level at a given stress is in part independent of crack length, and dependent on loading history. Variance in test procedures can be expected to yield diverse results in terms of critical crack, stress relationships. It is, therefore, essential to fully explore the relationship between  $p$  and the fundamental variables of load history.

### NET STRESS

Specimens of different width, when subjected to the same gross area stress  $\sigma_g$  will have dissimilar net stress for the same crack length. The net stress crack length relationship is dependent upon the relationship between the crack length  $l$  and the specimen width  $B$ .

$$\text{NET STRESS} = \sigma_n = \sigma_g \frac{B}{B-l} \quad (4)$$

The critical crack phenomena is principally dependent on the stress environment and is thus dependent on  $\sigma_n$ . Study of crack growth phenomena for sheets of various widths in terms of  $\sigma_g$  will yield different values of critical crack length  $l_c$  for the same gross stress, whereas study of the relationship of  $l_c$  to  $\sigma_n$  will show the uniqueness of the critical crack stress environment relationship for similar load histories.

It is also possible to explain a considerable portion of the observed plastic zone phenomena at the head of a crack by the stress environment around the crack defined by the net stress. By assuming a more or less consistent elastic stress concentration  $K_t$  dependent upon the shape of the crack front, the observed increase in size of the plastic enclave with increasing crack length can be seen to result in part from the increased intensity of the stress environment as indicated in Figure 25.

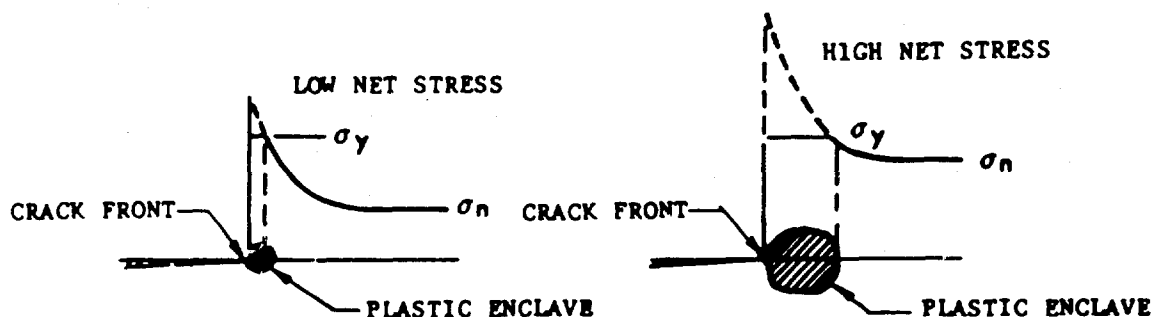


FIGURE 25 STRESS ENVIRONMENT

The recent work of Weibull<sup>4</sup> reporting the observed constant rate of growth of fatigue cracks in a constant stress environment substantiates to some extent the dependence of the crack growth rate on the stress environment. The normally observed relationship of increased rate of crack growth with increased crack length is to considerable extent dependent on increased net stress.

#### THE COMBINED PHENOMENA

The three principle limiting concepts can now be combined to form a unified theory of controlling fatigue crack phenomena. The model for the theory presented is well established in its application to another stability problem, the column, where the elastic column stability relationships are expressed by the well-known Euler equation.

The Euler equation without modification is valid only to the extent that the column remains elastic. The combined column theory can be shown diagrammatically in the form of Figure 26. A similar approach to crack stability phenomena will result in Figure 27.

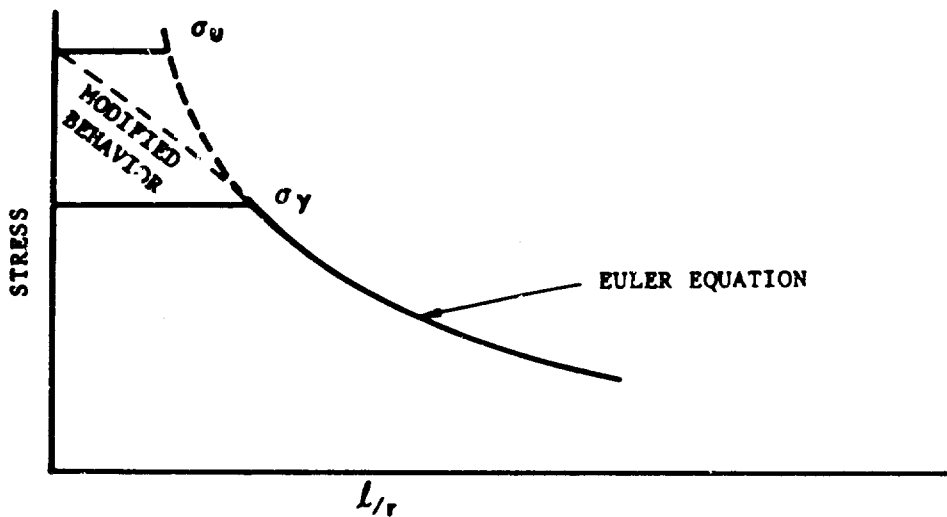


FIGURE 26 COLUMN THEORY

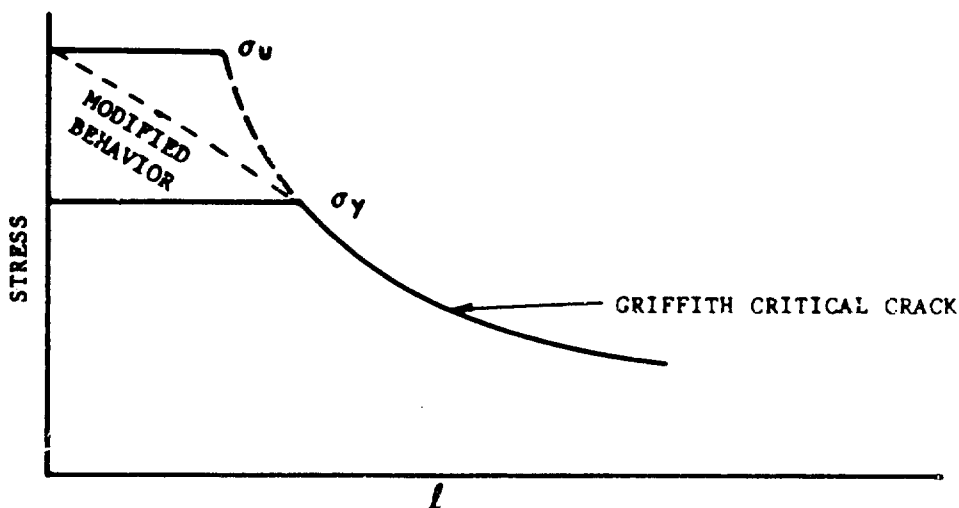


FIGURE 27 CRACK THEORY



The basic difference between the Figures 26 and 27 is the dependence of  $\sigma$  on  $l$  in Figure 27, a difficulty not inherent in the relationship between  $\sigma$  and  $l/r$  in Figure 26. However, net stress curves can be developed as shown in Figure 28 for sheets of different widths  $B$ , where the intercept on the stress axis denotes the gross stress  $\sigma_g$ , and the curves represent the crack length, net stress relationship for the widths  $B_1, B_2, B_3$ , etc. The curves are obtained by computing net stress for increments of crack length using the relationship  $\sigma_n = \sigma_g \frac{B}{B-l}$ .

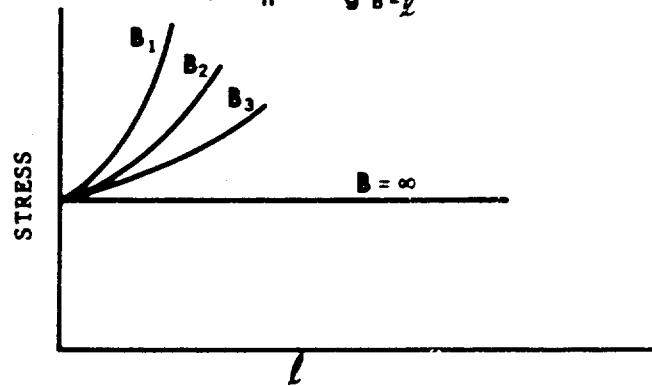


FIGURE 28 NET STRESS

Superposition of Figure 28 on Figure 27 results in diagrammatic presentation of the limiting phenomena of critical crack theory, Figure 29.

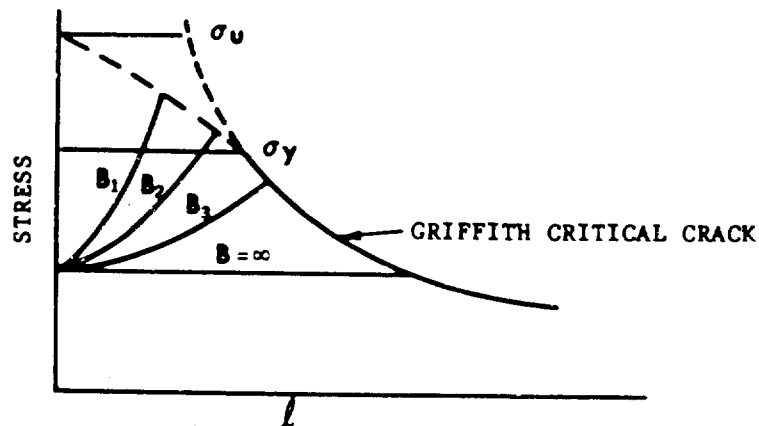


FIGURE 29 CRITICAL CRACK THEORY

The intersection of the net stress curves of Figure 28, with the controlling crack phenomena curves of Figure 27, will yield the crack lengths critical for catastrophic propagation. When a net stress curve indicates stress above the yield stress, modified behavior can be expected. It can be seen that small test specimens will normally fail in the "modified region" and thus do not respond directly to the Griffith crack theory. Any attempt to develop residual strength theory based on crack growth theory and S-N curves developed from small test coupons should recognize these limitations.

## APPLICATION OF THEORY TO TEST DATA

Reference 3, Figures 128 and 129, provides test data for critical crack length, gross stress relationships for 2024-T3 and 7075-T6 aluminum. The developed critical crack, gross stress relationships presented in Reference 3 were obtained from Reference 5, Figures 3, 4 based on "170 tests of 2024-T3 and 7075-T6 clad aluminum alloys". Unfortunately neither Reference 2 nor 5 defined the test procedure.

The recent paper of Yusuff<sup>2</sup> provides values of  $p$  for calculations of critical crack lengths. Considering the curves of Figures 128, 129 of Reference 3 as representative of the data plotted, the intercept of these curves with values of  $\sigma_{gross}$  and  $l_c$  were determined and plotted along with critical crack length curves and net stress curves to yield Figures 30 and 31. It can be seen that good agreement with the proposed control phenomena is obtained.

Figures 32 and 33 show similar plots of critical crack, gross stress relationships for data presented in Reference 2. These data were obtained by applying cyclic loads to specimens containing transverse saw cuts until failure occurred under the cyclic load.

The deviation of crack lengths in the lower stress region, especially in 2024-T3, can be seen. The  $p$  values presented in Reference 2 were determined at stresses near 60,000 psi where the plots of gross stress, crack length for 10 inch and 30 inch specimens are not significantly different. Deviation of the crack lengths obtained for 2024-T3 in Reference 2 from the  $p$  values computed is considered to be a function of the continued loading history during cyclic loading to failure. A need for more complete understanding of the effect of the rate of static load application and load history on critical crack phenomena is indicated.

## CONCLUSIONS

1. Critical crack length theory, net stress, and the elastic-plastic properties of a given material are control phenomena for critical crack lengths.
2. The aluminum alloy 7075-T6 conforms to the proposed control phenomena.
3. The aluminum alloy 2024-T3 conforms to the proposed control phenomena for some load histories. Since 2024-T3 is easily strain hardened, variance in load history will result in variance of the observed critical crack lengths.
4. Additional study of the relationship between load history, rate of loading, and plastic work  $p$  is needed.
5. Use of the proposed concepts result in greatly simplified forms of data presentation in a form easily understood by engineers.

## RECOMMENDATIONS

The region marked "modified elastic behavior" on Figure 27 requires additional study. Effort should be directed towards determination of  $p$  values for more materials and the effects of strain hardening and temperature on this variable. It is suggested that strain hardening at the crack tip will result in changes in  $p$ , resulting in changes in critical crack lengths from that of virgin material.

Concentration of research effort on the dependence of the work factor  $p$  on the variables of loading and temperature should prove a rewarding approach to the critical crack length problem.

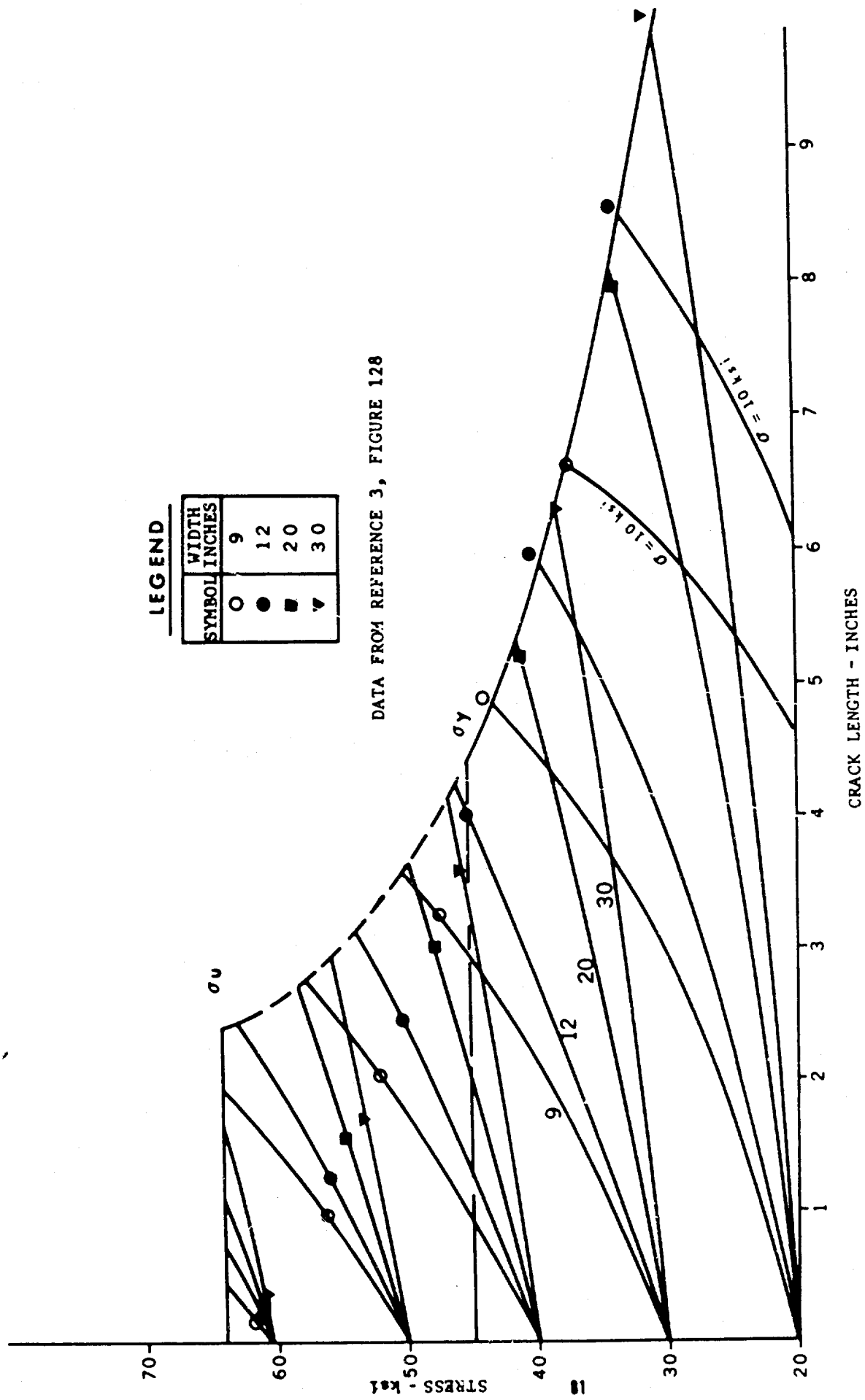
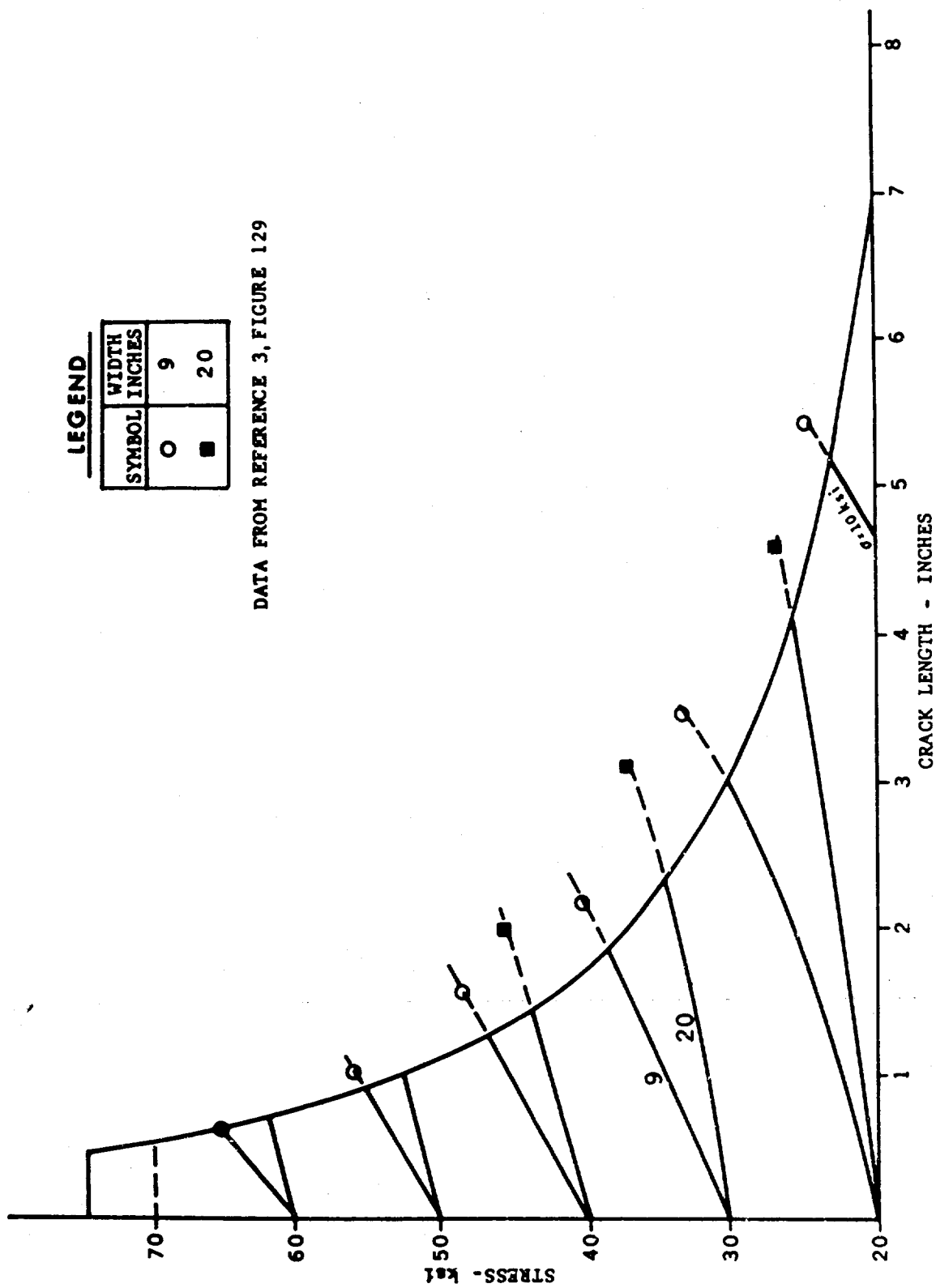


FIGURE 30 FATIGUE CRACK STABILITY CURVE - 2024-T3 ALUMINUM

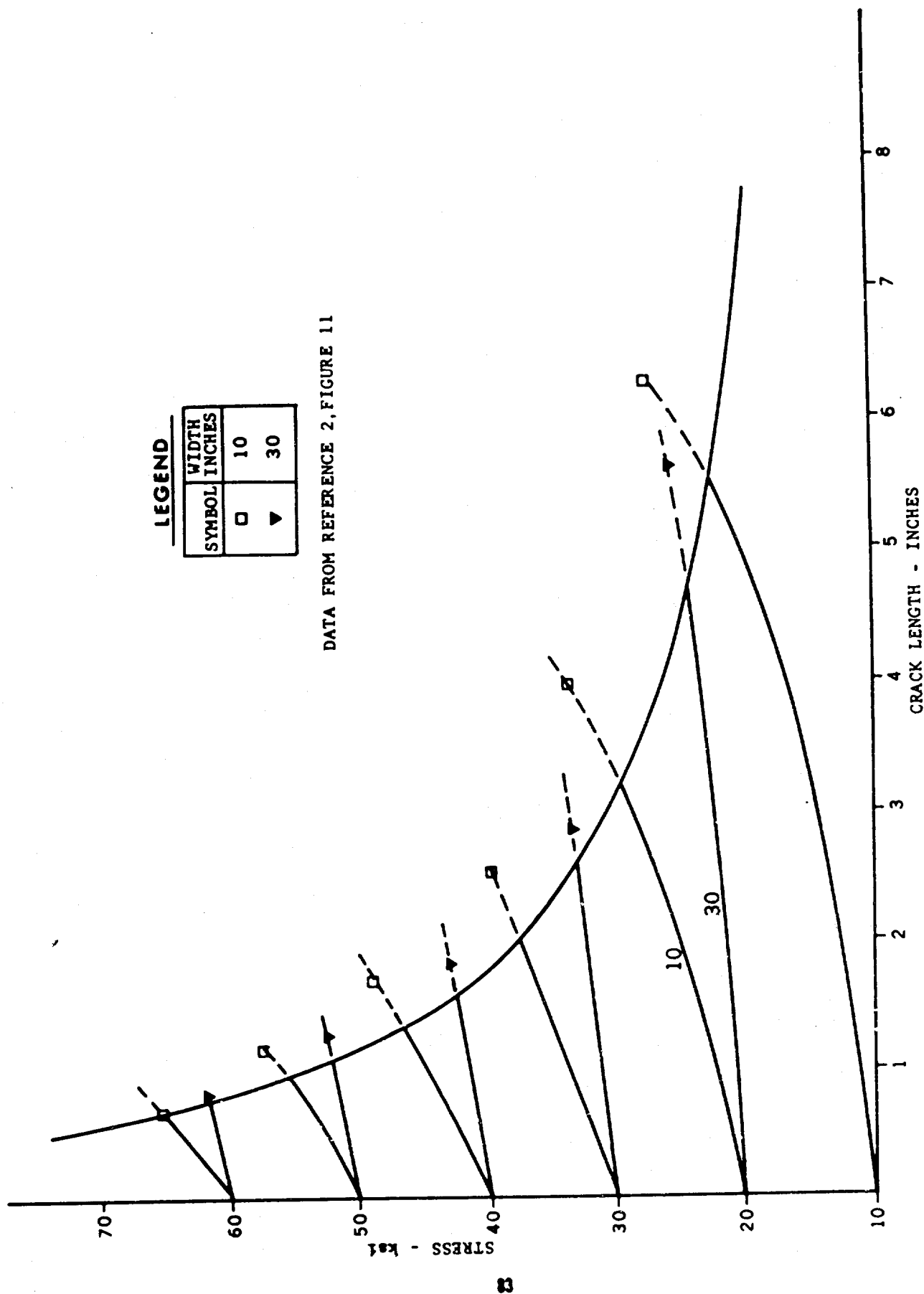


**LEGEND**

SYMBOL	WIDTH INCHES
○	9
■	20

DATA FROM REFERENCE 3, FIGURE 129

FIGURE 31 FATIGUE CRACK STABILITY CURVE - 7075-T6 ALUMINUM



DATA FROM REFERENCE 2, FIGURE 11

FIGURE 32 FATIGUE CRACK STABILITY CURVE - 7075-T6 AND DTD 687 ALUMINUM



#### REFERENCES

1. Spretnak, J. W., A Summary of the Theory of Fracture in Metals, Report #157 - Defense Metals Information Center, Battelle Memorial Institute, Columbus 1, Ohio.
2. Yusuff, S., Fracture Phenomena in Metal Plates, Aircraft Engineering, May 1962.
3. Christiansen, R. H. and Denke, P. H., Crack Strength and Crack Propagation Characteristics of High Strength Metals, ASD-TR-61-207, JANUARY 1962.
4. Weibull, W., Size Effects on Fatigue Crack, Initiation and Propagation in Aluminum Sheet Specimens Subjected to Stresses of Nearly Constant Amplitude, FFA Report 86, Stockholm, 1960.
5. Crichlow, W. J., The Ultimate Strength of Damaged Structure, ICAF-AGARD Symposium on Full-Scale Aircraft Fatigue Testing, Amsterdam, Netherlands, 9-11 June 1959.

**APPENDIX B**

**EFFECTS OF LIQUID LOADING**



## EFFECTS OF LIQUID LOADING

An estimate of the effect of liquid loading on the vibration of a typical panel in its fundamental mode in a large cylindrical tank can be obtained by examining the effect of liquid loading on a piston mounted in an infinite wall as shown in Figure 34.

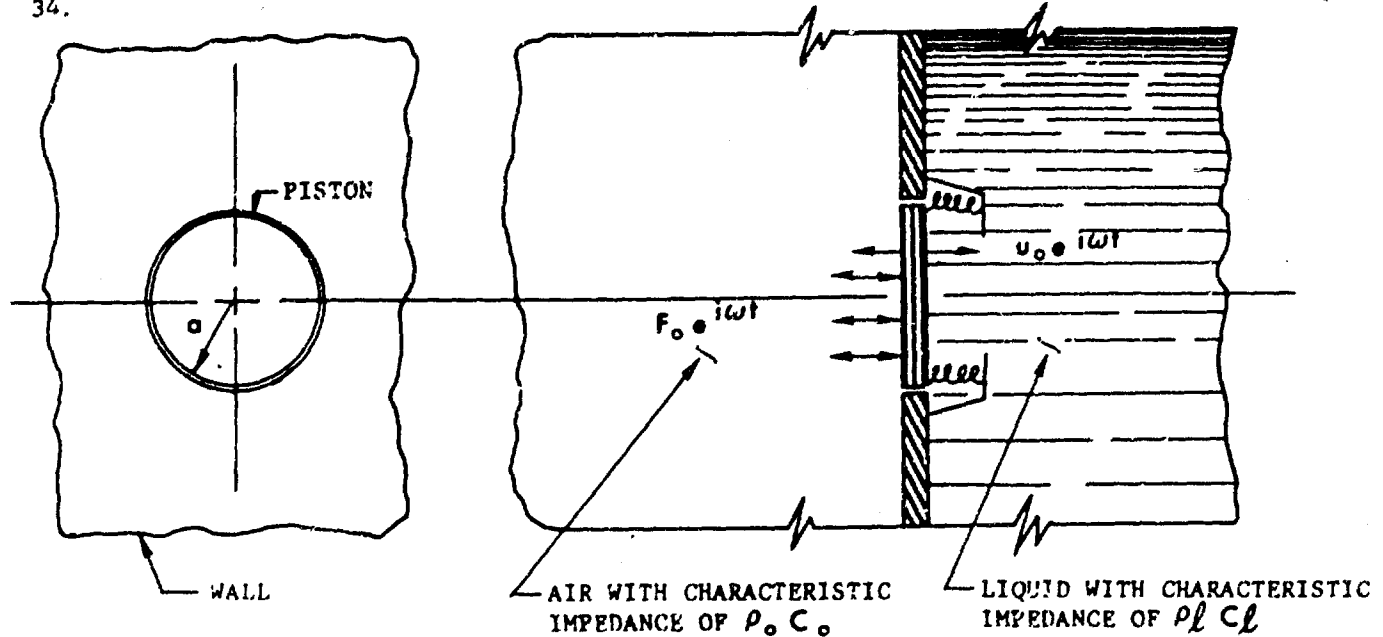


FIGURE 34 LIQUID LOADING ON A PISTON IN AN INFINITE WALL

Consider a piston of radius  $a$  and mass  $m_p$  mounted in the plane of an infinite wall, and supported by the wall through a spring of stiffness  $k_p$  and equivalent viscous damping  $r_p$ . Let the piston be driven by a normally incident acoustic wave with pressure  $p = p_0 e^{i\omega t}$ .

The reaction of the liquid on the piston can be described by the impedance  $Z_l$  seen by a piston radiating sound into an infinite medium. This impedance, as derived in References 1, 2 and 3, is given by

$$Z = \frac{F}{u_0 e^{i\omega t}} = \pi a^2 \rho c \left( 1 - \frac{J_1(2ka)}{ka} \right) + \frac{i\omega \rho \pi}{2k^3} K_1(2ka)$$

where

$$J_1(\beta) = \frac{\beta}{2} \left[ 1 - \frac{\beta^2}{2 \cdot 2^2} + \frac{\beta^4}{2 \cdot 4 \cdot 6 \cdot 2^2} - \dots \right]$$

$$K_1(\beta) = \frac{2}{\pi} \left[ \frac{\beta^3}{3} - \frac{\beta^5}{3^2 \cdot 5} + \frac{\beta^7}{3^2 \cdot 5^2 \cdot 7} - \dots \right]$$

$$k = \omega / c$$

(5)

$C$  = velocity of sound, and

$\omega = 2\pi f$  = frequency in radian/sec.

The first term behaves like a resistance of  $\pi a^2 \rho c$  when  $ka > 2$ . The second term represents an inertia load which approaches zero at  $ka \gg 1$  and  $8\rho a^3/3$  when  $ka \ll 1$ . This latter limit represents the mass of fluid in a cylinder of base area equal to the piston area  $\pi a^2$  with a height of  $8a/3\pi$ .

In general, for the panels of interest, the fundamental mode occurs at a frequency where the acoustic wavelength is large relative to the panel dimensions. Hence, for this illustration we can concentrate on the region where the circumference of the piston is less than a wavelength, or equivalently,  $ka < 1$ . Here, equation (5) can be simplified to give, approximately

$$Z = \pi a^2 \rho C \frac{(ka)^2}{2} + \frac{i\omega \rho 8a^3}{3} \quad (6)$$

With this simplification, the terms in Figure 35 become

$$r_o = \pi a^2 \rho_o C_o \frac{(k_o a)^2}{2} \quad (7)$$

$$m_o = \frac{8\rho_o a^3}{3}$$

$$m_p = \pi a^2 \rho_p t_p$$

where  $t$  is the thickness of the piston.

$$1/k_p = 1/m_p \omega_1^2$$

where  $\omega_1$  is the natural frequency calculated for the unloaded piston.

$$r_p = m_p \omega_1 / Q_1$$

the equivalent viscous damping coefficient for the unloaded panel, where  $Q_1$  is the amplification factor for the unloaded panel.

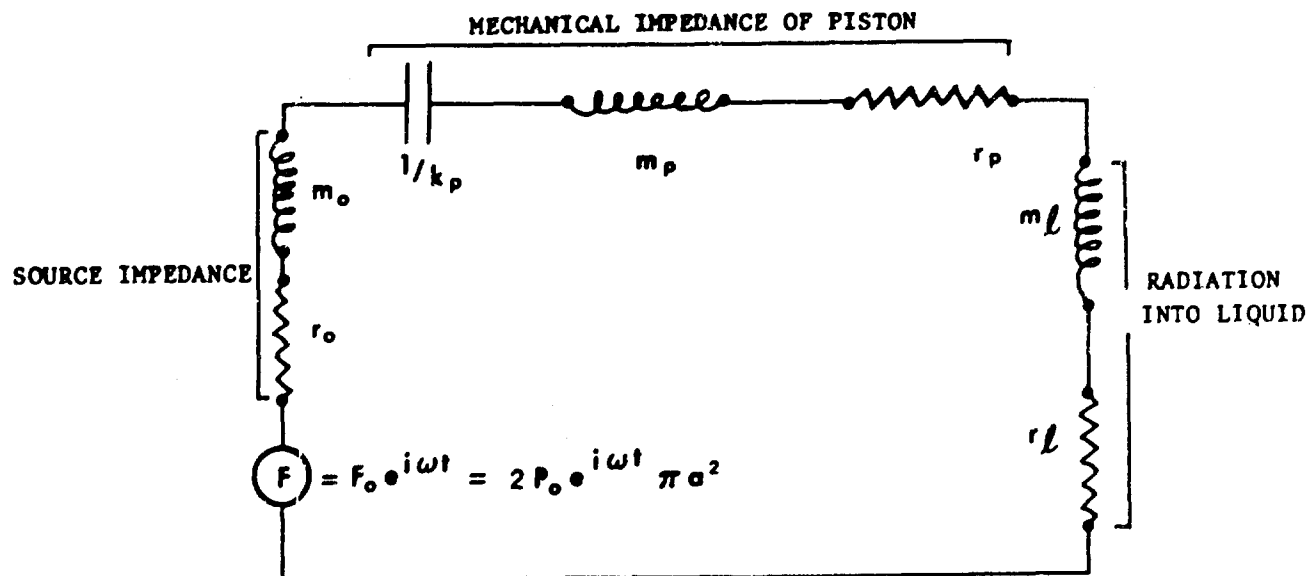
$$= m_p \omega_1 \eta_1$$

where  $\eta_1$  is the loss factor for the unloaded panel.

$$m_l = \frac{8\rho_l a^3}{3}$$

$$r_l = \pi a^2 \rho_l C_l \frac{(k_l a)^2}{2}$$

# COMPLETE EQUIVALENT CIRCUIT



## SIMPLIFIED CIRCUIT

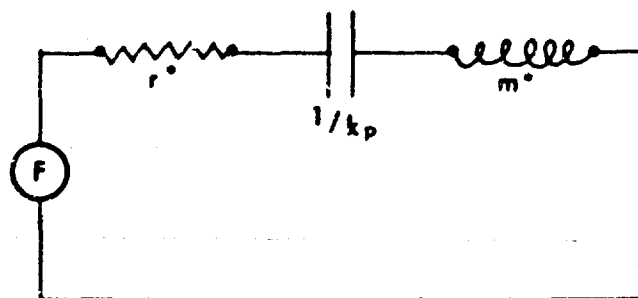


FIGURE 35 EQUIVALENT CIRCUIT OF PISTON IN INFINITE WALL

With these definitions, the effect of loading on the dynamics of the panel can be directly seen in  $m^*$  and  $r^*$ . Here;

$$\begin{aligned} m^* &= \pi a^2 \left[ \frac{8a}{3\pi} (\rho_o + \rho_l) + t_p \rho_p \right] \\ &= m_p \left[ 1 + \frac{8a}{3\pi t_p} \left( \frac{\rho_o + \rho_l}{\rho_p} \right) \right] \end{aligned} \quad (8)$$

$$\begin{aligned} r^* &= \frac{\pi a^4 \omega^2}{2} \left( \frac{\rho_o}{C_o} + \frac{\rho_l}{C_l} \right) + r_p \\ &= m_p \omega_1 \left[ \frac{a^2 \omega^2}{2 t_p \omega_1 \rho_p} \left( \frac{\rho_o}{C_o} + \frac{\rho_l}{C_l} \right) + \eta_1 \right] \end{aligned} \quad (9)$$

The ratio of the loaded natural frequency  $\omega^*$  to  $\omega_1$  is

$$\frac{\omega^*}{\omega_1} = \left( \frac{m^*}{m_p} \right)^{-1/2} = \left[ 1 + \frac{8a}{3\pi t_p} \left( \frac{\rho_o + \rho_l}{\rho_p} \right) \right]^{-1/2} \quad (10)$$

$$\eta^* = \frac{r^*}{m^* \omega^*} = \left[ 1 + \frac{8a}{3\pi t_p} \frac{\rho_o + \rho_l}{\rho_p} \right]^{-1/2} \left[ \frac{a^2 \omega^2}{2 t_p \omega_1 \rho_p} \left( \frac{\rho_o}{C_o} + \frac{\rho_l}{C_l} \right) + \eta_1 \right] \quad (11)$$

For a square panel of side "a" at resonance ( $\omega = \omega^*$ )

$$\eta^* = \left[ 1 + \frac{8a}{3\pi t_p} \left( \frac{\rho_o + \rho_l}{\rho_p} \right) \right]^{-1/2} \left[ \frac{\pi^2 C_p}{2.9 \rho_p} \left( \frac{\rho_o}{C_o} + \frac{\rho_l}{C_l} \right) + \eta_1 \right]$$

where  $C_p = \sqrt{E/\rho_p}$

The above derivation is applicable only under the following restrictions; (1) that areas adjacent to the vibrating panel (piston) approach the condition of infinite impedance and (2) that only the first mode is excited, since higher modes produce cancellation effects.

**References:**

1. Crandall, "Theory of Vibrating Systems and Sound," Van Nostrand Co., page 143.
2. Rayleigh, "The Theory of Sound", Dover Publications, page 162.
3. Morse, "Vibration and Sound," McGraw-Hill, page 332.

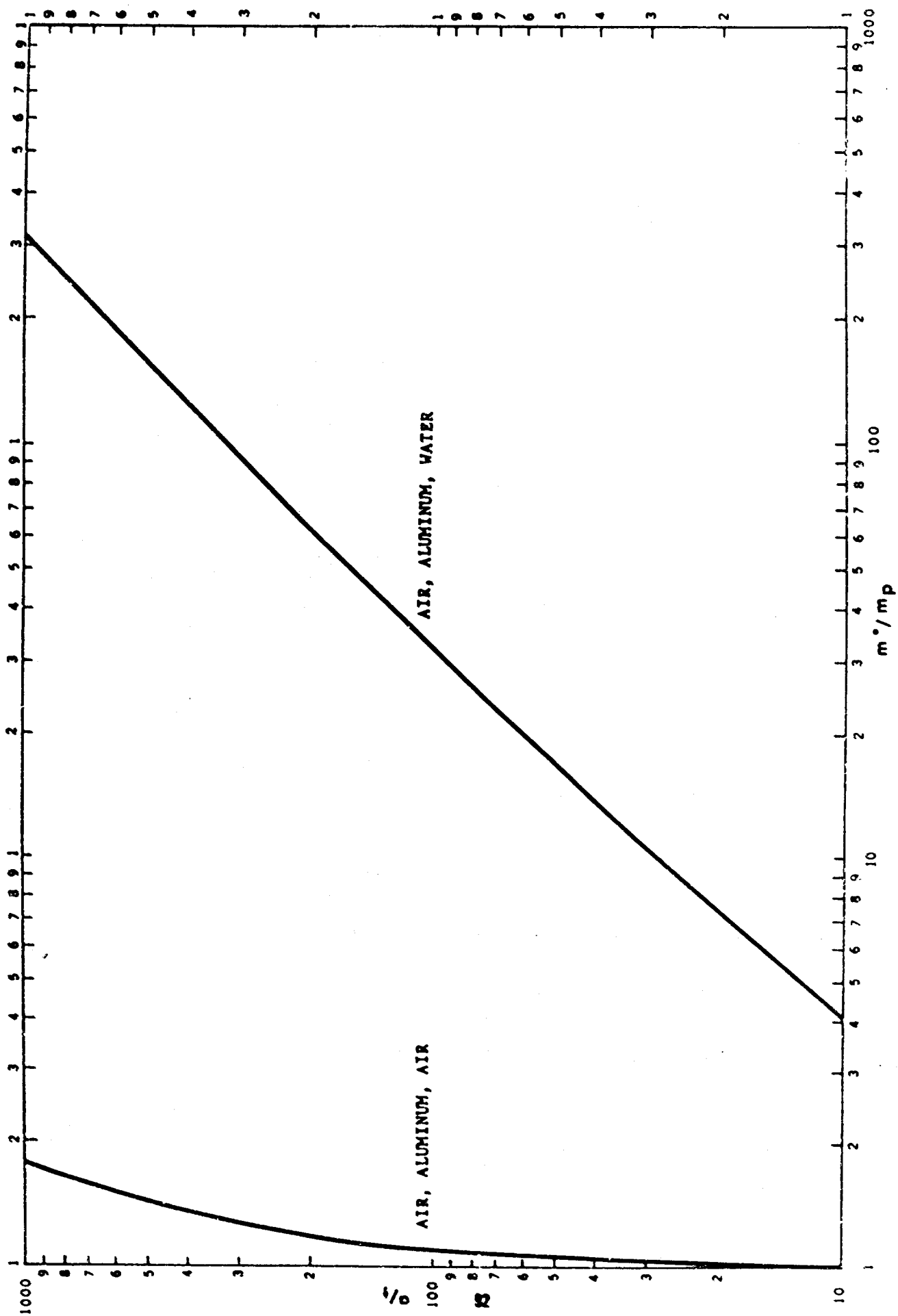


FIGURE 36 RADIUS TO THICKNESS RATIO VERSUS RATIO OF EQUIVALENT SYSTEM MASS TO MASS OF PISTON

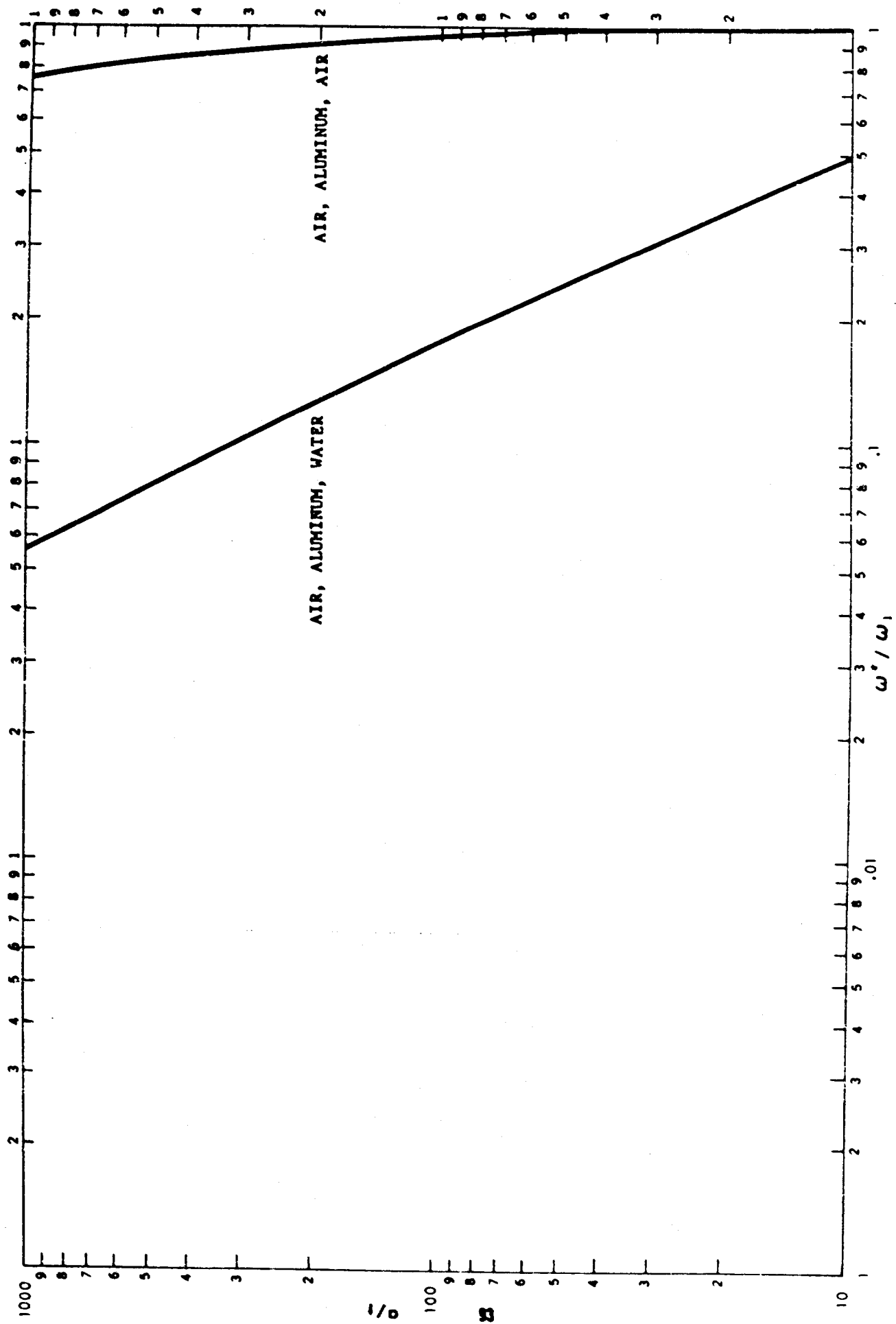


FIGURE 37 RADIUS TO THICKNESS RATIO VERSUS RATIO OF LOADED NATURAL FREQUENCY OF EQUIVALENT SYSTEM TO UNLOADED NATURAL FREQUENCY OF PISTON

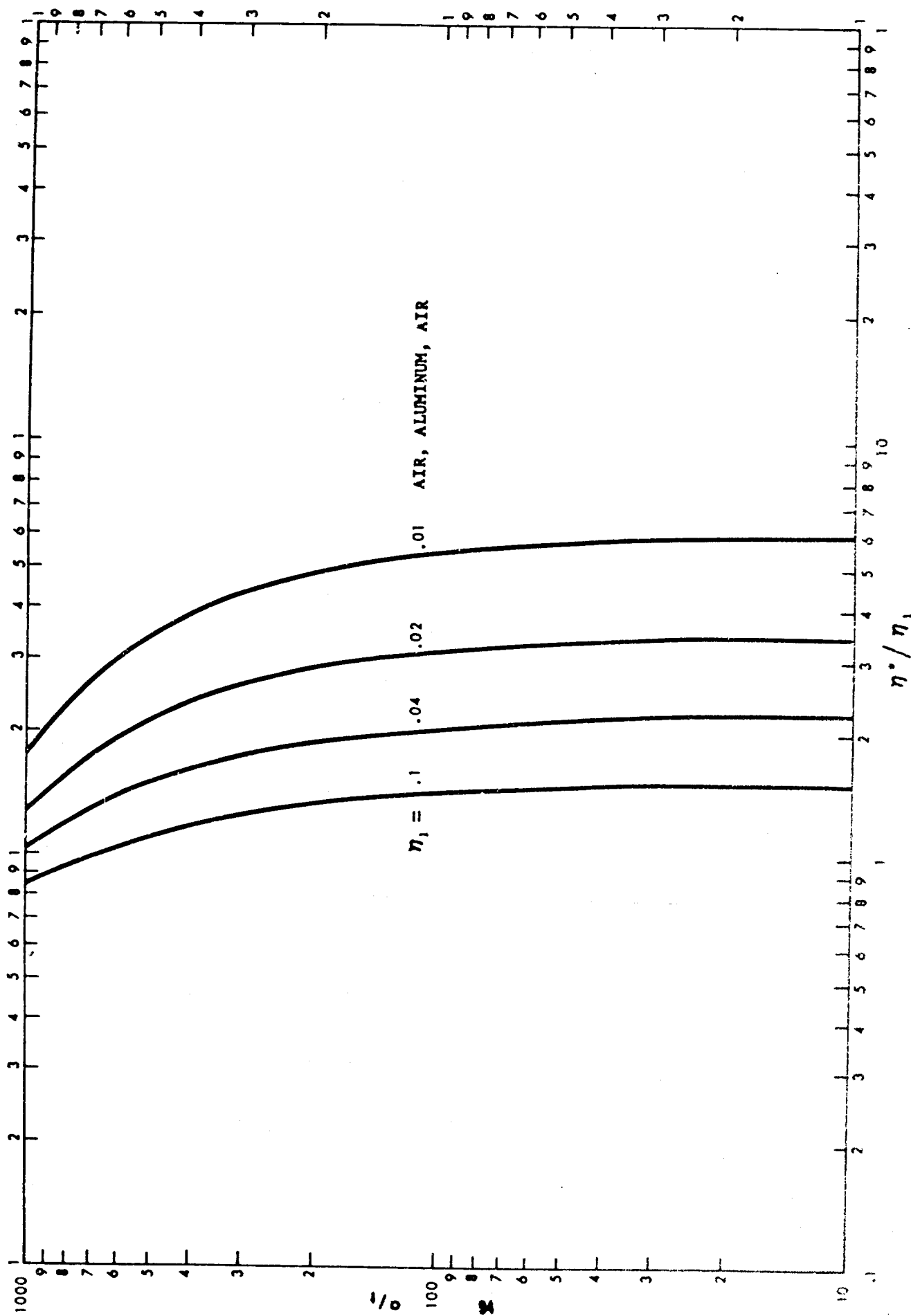


FIGURE 38 RADIUS TO THICKNESS RATIO VERSUS ACOUSTIC EFFICIENCY RATIO OF LOADED EQUIVALENT SYSTEM TO UNLOADED PISTON



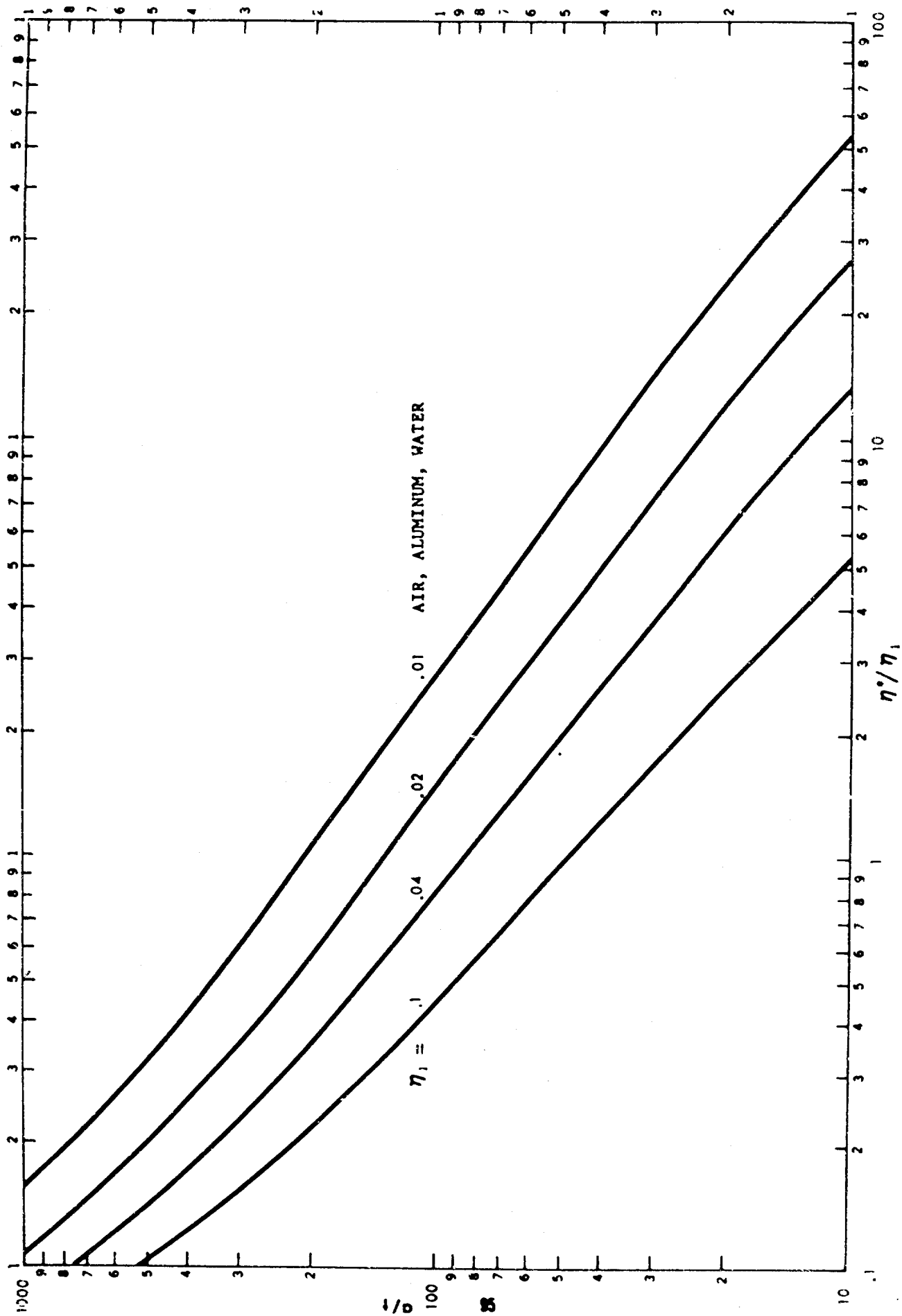


FIGURE 39 RADIUS TO THICKNESS RATIO VERSUS ACOUSTIC EFFICIENCY RATIO OF LOADED EQUIVALENT SYSTEM TO UNLOADED PISTON

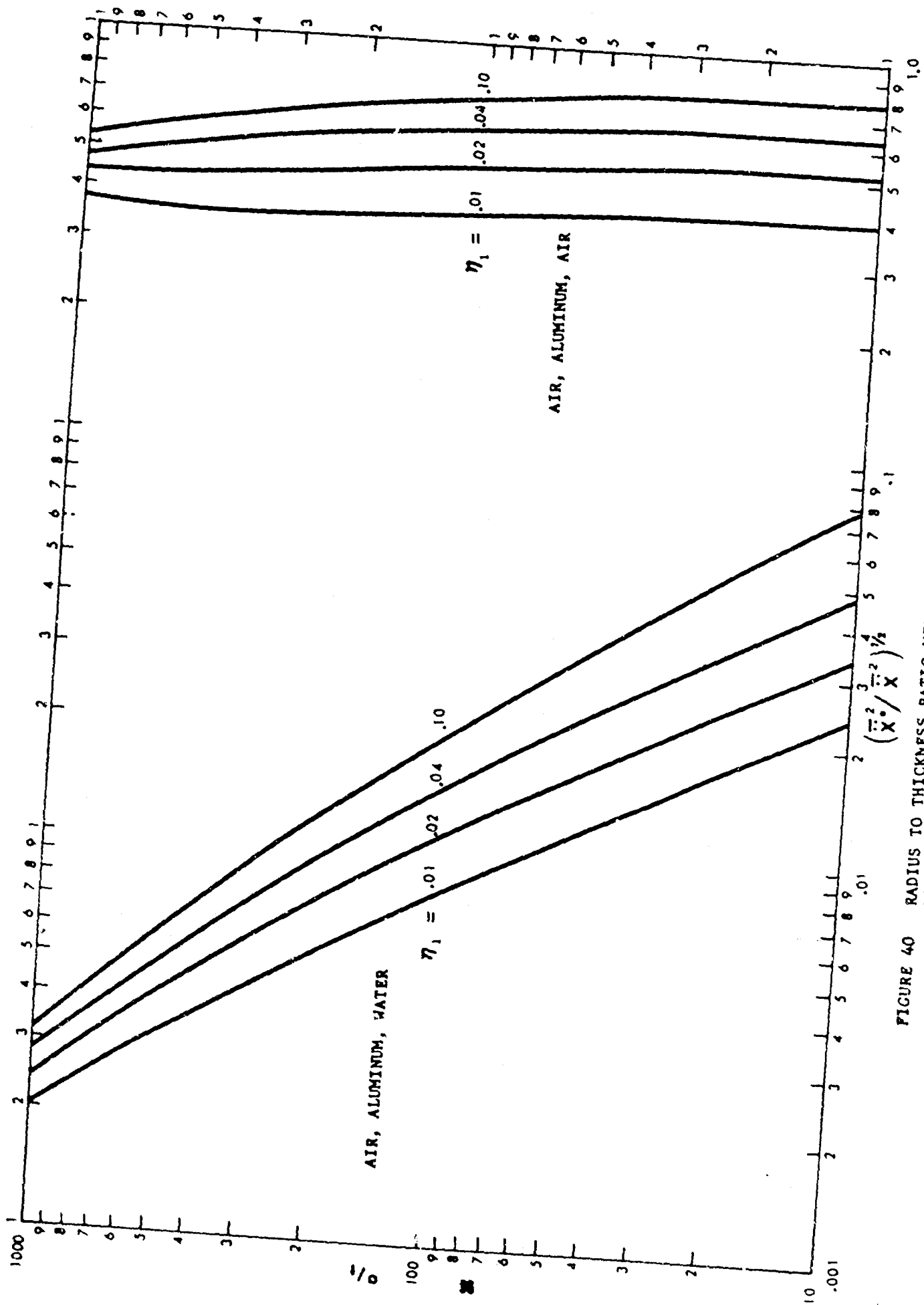


FIGURE 40 RADIUS TO THICKNESS RATIO VERSUS RATIO OF MEAN SQUARES OF EQUIVALENT LOADED SYSTEM TO UNLOADED SYSTEM

## APPENDIX C

### PROBABILITY DENSITY FUNCTION OF THE SUM OF TWO RAYLEIGH VARIABLES

# PROBABILITY DENSITY FUNCTION OF THE SUM OF TWO RAYLEIGH VARIABLES

Assume  $X$  and  $Y$  are independently distributed Rayleigh random variables with probability density functions respectively:

$$g(x) = \begin{cases} \frac{x}{\nu^2} \cdot e^{-\frac{1}{2}\left(\frac{x}{\nu}\right)^2} & , x \geq 0, \nu > 0 \\ 0 & , \text{otherwise} \end{cases}$$

$$f(y) = \begin{cases} \frac{y}{\mu^2} \cdot e^{-\frac{1}{2}\left(\frac{y}{\mu}\right)^2} & , y \geq 0, \mu > 0 \\ 0 & , \text{otherwise} \end{cases}$$

where  $\nu \neq \mu$  to preserve generality.

Since  $X$  and  $Y$  are independent, their joint p.d.f. can be written as

$$P(X, Y) = g(X) \cdot f(Y)$$

Make the transformation:  $Z = X + Y, W = X$ .

The Jacobian is

$$J = \begin{vmatrix} \frac{dW}{dX} & \frac{dW}{dY} \\ \frac{dZ}{dX} & \frac{dZ}{dY} \end{vmatrix} = 1 ,$$

so that the transformation is one-to-one and it follows that

$$p(x, y) = g(w) f(z-w) = p(z, w).$$

Then, since  $0 \leq w < \infty$ ,

$$\begin{aligned} p(z) &= \int_0^{\infty} g(w) f(z-w) dw \\ &= \int_0^z \left[ \frac{w}{\nu^2} e^{-\frac{1}{2} \left( \frac{w}{\nu} \right)^2} \right] \left[ \frac{(z-w)}{\mu^2} e^{-\frac{1}{2} \left( \frac{z-w}{\mu} \right)^2} \right] dw \\ &= e^{-\frac{1}{2} \left( \frac{z}{\alpha} \right)^2} \int_0^z \frac{w(z-w)}{\nu^2 \mu^2} e^{-\frac{1}{2} \frac{\alpha^2}{\nu^2 \mu^2} \left( w - \frac{\nu^2 z}{\alpha^2} \right)^2} dw \end{aligned}$$

after completing the square on  $w$  and setting  $\nu^2 + \mu^2 = \alpha^2$ .

Make the transformation:

$$t = \frac{\alpha}{\nu \mu} \left( w - \frac{\nu^2 z}{\alpha^2} \right)$$

so that

$$w = \frac{\nu \mu}{\alpha} t + \frac{\nu^2 z}{\alpha^2}$$

and

$$dw = \frac{\nu \mu}{\alpha} dt.$$

Then, after some algebra

$$p(Z) = \frac{1}{\alpha^2} e^{-\frac{1}{2}\left(\frac{Z}{\alpha}\right)^2} \int_{-\frac{\nu}{\mu\alpha}Z}^{\frac{\mu}{\nu\alpha}Z} \left[ \left( \frac{\mu^2 - \nu^2}{\alpha^2} \right) Z t - \frac{\mu\nu}{\alpha} t^2 + \frac{\mu\nu}{\alpha^3} Z^2 \right] e^{-\frac{1}{2}t^2} dt$$

$$= \frac{1}{\alpha^2} e^{-\frac{1}{2}\left(\frac{Z}{\alpha}\right)^2} \left\{ I_1(Z) - I_2(Z) + I_3(Z) \right\},$$

where

$$I_1(Z) = \left( \frac{\mu^2 - \nu^2}{\alpha^2} \right) Z \int_{-\frac{\nu}{\mu\alpha}Z}^{\frac{\mu}{\nu\alpha}Z} t e^{-\frac{1}{2}t^2} dt,$$

$$I_2(Z) = \frac{\mu\nu}{\alpha} \int_{-\frac{\nu}{\mu\alpha}Z}^{\frac{\mu}{\nu\alpha}Z} t^2 e^{-\frac{1}{2}t^2} dt,$$

$$I_3(Z) = \frac{\mu\nu}{\alpha^3} Z^2 \int_{-\frac{\nu}{\mu\alpha}Z}^{\frac{\mu}{\nu\alpha}Z} e^{-\frac{1}{2}t^2} dt.$$

Let

$$\frac{\mu}{\alpha \nu} = \gamma \quad , \quad \frac{\nu}{\mu \alpha} = \beta .$$

Immediately,

$$I_1(Z) = \left( \frac{\mu^2 \nu^2}{\alpha^2} \right) Z \left[ e^{-\frac{1}{2}(\beta Z)^2} - e^{-\frac{1}{2}(\gamma Z)^2} \right]$$

and

$$I_3(Z) = \frac{\mu \nu}{\alpha^3} Z^2 \left[ \Phi(\gamma Z) + \Phi(\beta Z) - 1 \right] (2\pi)^{\frac{1}{2}}$$

where

$$\Phi(W) = \frac{1}{\sqrt{2\pi}} \int_{-\infty}^W e^{-\frac{1}{2}t^2} dt = \text{standardized}$$

Normal probability integral. Values of  $\Phi(W)$  are available in tables of the standardized normal distribution.

The evaluation of  $I_2(Z)$  is somewhat more complicated.

Consider

$$I_2(Z) = \frac{\mu \nu}{\alpha} \int_{-\beta Z}^{\gamma Z} t^2 e^{-\frac{1}{2}t^2} dt .$$

Note that

$$\frac{d^2}{dt^2} \left[ e^{-\frac{1}{2}t^2} \right] = t^2 e^{-\frac{1}{2}t^2} - e^{-\frac{1}{2}t^2}$$

Thus

$$\begin{aligned}
 I_2(Z) &= \frac{\mu \nu}{\alpha} \int_{-\beta Z}^{\gamma Z} \left\{ \frac{d^2}{dt^2} \left[ e^{-\frac{1}{2}t^2} \right] + e^{-\frac{1}{2}t^2} \right\} dt \\
 &= \frac{\mu \nu}{\alpha} \left[ \frac{d}{dt} \left( e^{-\frac{1}{2}t^2} \right) \right]_{-\beta Z}^{\gamma Z} + \frac{\sqrt{2\pi}}{\sqrt{2\pi}} \int_{-\beta Z}^{\gamma Z} e^{-\frac{1}{2}t^2} dt \\
 &= \frac{\mu \nu}{\alpha} \left\{ \left[ t e^{-\frac{1}{2}t^2} \right]_{-\beta Z}^{\gamma Z} + \sqrt{2\pi} \left[ \Phi(\gamma Z) + \Phi(\beta Z) - 1 \right] \right\} \\
 &= \frac{\mu \nu}{\alpha} \left\{ \sqrt{2\pi} \left[ \Phi(\gamma Z) + \Phi(\beta Z) - 1 \right] - \beta Z e^{-\frac{1}{2}(\beta Z)^2} - \gamma Z e^{-\frac{1}{2}(\gamma Z)^2} \right\}
 \end{aligned}$$

Referring to the definition of  $p(Z)$  in terms of the  $I(Z)$ 's, collecting terms and simplifying, there results, finally,

$$\begin{aligned}
 p(Z) &= \frac{e^{-\frac{1}{2}\left(\frac{Z}{\alpha}\right)^2}}{\alpha^4} \left\{ \mu^2 Z e^{-\frac{1}{2}(\beta Z)^2} + \nu^2 Z e^{-\frac{1}{2}(\gamma Z)^2} \right. \\
 &\quad \left. + \sqrt{2\pi} \gamma (Z^2 - \alpha^2) \left[ \Phi(\beta Z) + \Phi(\gamma Z) - 1 \right] \right\},
 \end{aligned}$$

where

$$Z \geq 0.$$